Accepted Manuscript

Design and synthesis of aminothiazole based Hepatitis B Virus (HBV) capsid inhibitors

Ting Pan, Yanchao Ding, Liyang Wu, Liting Liang, Xin He, Qianwen Li, Chuan Bai, Hui Zhang

PII: S0223-5234(19)30058-3

DOI: https://doi.org/10.1016/j.ejmech.2019.01.059

Reference: EJMECH 11066

To appear in: *European Journal of Medicinal Chemistry*

Received Date: 30 September 2018

Revised Date: 30 December 2018

Accepted Date: 18 January 2019

Please cite this article as: T. Pan, Y. Ding, L. Wu, L. Liang, X. He, Q. Li, C. Bai, H. Zhang, Design and synthesis of aminothiazole based Hepatitis B Virus (HBV) capsid inhibitors, *European Journal of Medicinal Chemistry* (2019), doi: https://doi.org/10.1016/j.ejmech.2019.01.059.

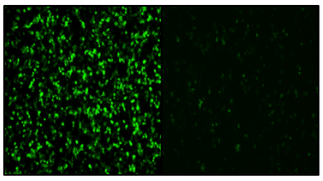

HTS in cells

High-throughput screening

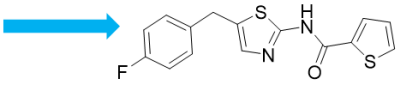

IC_{50}=6.15 μM
CC_{50}>50 μM

Scaffold hopping and SAR

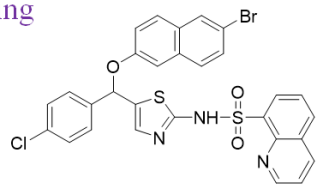

IC_{50}=0.18 μM
CC_{50}>50 μM

Design and Synthesis of Aminothiazole Based Hepatitis B Virus (HBV) Capsid Inhibitors

Ting Pan[†,‡,#], *Yanchao Ding*[†,‡,#], *Liyang Wu*[†,‡,#], *Liting Liang*[†,‡], *Xin He*[†,‡], *Qianwen Li*[†,‡], *Chuan Bai* [†,‡,*]，*and Hui Zhang* [†,‡,*]

[†] Institute of Human Virology,

[‡] Key Laboratory of Tropical Disease Control of Ministry of Education,

Guangdong Engineering Research Center for Antimicrobial Agent and Immunotechnology

Zhongshan School of Medicine,

Sun Yat-sen University,

Guangzhou, Guangdong, China, 510080

* To whom correspondence should be addressed:

Sun Yat-sen University

74 Zhongshan 2nd Road

Guangzhou 510080, China

Phone: +86-20-8733-2588

Fax: +86-20-8733-2588

Dr. Chuan Bai or Dr. Hui Zhang

Email: baichuan@mail.sysu.edu.cn or zhangh92@mail.sysu.edu.cn

# These authors contributed equally to this work.

Abstract

The capsid assembly is an essential step for Hepatitis B Virus (HBV) life cycle and is an important target for anti-HBV drug development. In this report, we identified a hit compound with aminothiazole structure by the high throughput screening (HTS) which inhibited the interaction of HBV capsid protein within the cells. The structure hopping and SAR studies of the hit compound afforded compound **79** with potent anti-HBV replication activity and good basic drug-like properties. The working mechanism studies showed that compound **79** could bind to the similar binding site of known HBV capsid inhibitor with heteroaryldihydropyrimidine (HAP) scaffold, through similar hydrophobic interactions but with a different hydrogen bond. This compound exerted potent inhibitory effect upon HBV production, either in cell culture or in mice with no obvious acute toxicity. We propose that further development of this compound could lead to novel potent anti-HBV inhibitors that target HBV capsid assembly.

Introduction

HBV has been a severe public health threat because it has infected approximate 257 million people worldwide in 2017[1]. The progression of HBV infection is highly correlated with cirrhosis and hepatocellular carcinoma. However, the currently available therapeutics including IFN-α and nucleot(s)ides have not been able to afford satisfying effects in clinical practice because of the high cost, severe side effects, or the development of viral drug resistance[2-4]. Moreover, neither IFN-α nor nucleot(s)ides could eradicate HBV infection because of the stable covalently-closed circular DNA (cccDNA) of HBV. Therefore, further development of new anti-HBV drugs targeting other vital process in the viral life cycle has been an urgent requirement [5, 6]. The HBV capsid assembly is one of the key steps for HBV replication and plays important roles in stabilizing cccDNA. Previous studies showed that blocking HBV capsid assembly led to effective inhibition of HBV replication and impaired the cccDNA stability [7-14]. Since the first HBV capsid assembly inhibitor BisANS was discovered [15], many HBV capsid assembly inhibitors with different scaffolds have been studied [16-21]. Among these HBV capsid inhibitors, the compounds with heteroaryldihydropyrimidine (HAP) structure including Bay 41-4109[10], GLS4 [22, 23], and NVR-010–001-E2 [24] showed potent anti-HBV activity *in vitro* and *in vivo*, and their binding models and working mechanisms against HBV capsid assembly have been elucidated [22, 25, 26].

Most of the HBV capsid inhibitors were first discovered with the HTS system in which the expressed capsid proteins assembled in a non-cellular environment [10, 27, 28]. Therefore, this HTS system may not be able to investigate some important factors involved in capsid assembly in the cellular environment. To overcome this problem, we developed a capsid-GFP assay by using capsid protein fused with GFP fragments that was expressed in 293T cells. This screening method was designed to be more correlated with the real conditions that was required for HBV capsid assembly in viral replication and therefore, could identify hit compounds more efficiently and accurately. With our HTS system, we

identified a hit compound targeting HBV capsid assembly. Based on the hit compound, we discovered a new potent HBV capsid assembly inhibitor (**79**) and it was able to inhibit HBV replication inhibitor *in vivo* and *in vitro*. The aminothiazole structure of this active compound may have hydrogen bond interactions with Ser121 of HBV capsid protein. Our discoveries afforded a new scaffold for the development of new HBV capsid assembly inhibitor and shed light on the design of more potent structure.

Results

Section 1. High throughput screening of HBV capsid inhibitors

To explore new HBV capsid inhibitors, we performed a cell-based high-throughput screening by using a bimolecular fluorescence complementation (BiFC) assay to determine the binding states of HBV capsid proteins in 293T cells. In brief, we first constructed plasmids of two nonfluorescent fragments of VFP (Venus fluorescent protein) fused with HBV capsid protein, which were HBVcAg-VFP-N1-154 (HBc-VN) and HBVcAg-VFP-C155-239 (HBc-VC). These two fragments could reconstitute the fluorophore only when the HBV capsid proteins get close enough during the assembly of HBV capsids. The HBc-VN and HBc-VC plasmids were co-transfected into 293T cells and the cells were treated with a commercial drug-like chemical library composed of 40155 compounds at 50 μM (Figure 1A). After duplicated screening, 439 hit compounds were identified and they were further screened by anti-HBV replication assay in which the amount of HBV DNA was quantified by qPCR after the treatment. 125 compounds showed activity to inhibit HBV replication at 50 μM and 9 hits at 5 μM in HepG2.2.15 cells (Figure 1B). Because one the hit compound (Figure 1B) showed low cytotoxicity (CC_{50}>500μM, Figure 1C) and high potency (IC_{50}= 6.15 μM in anti-HBV replication assay, Figure 1D), we chose it for further studies.

Section 2. SAR of hit compound and the structure hopping

We first conducted the structure-activity relationship (SAR) studies of the hit compound, with the synthesis methods showed in scheme 1 [29-31].

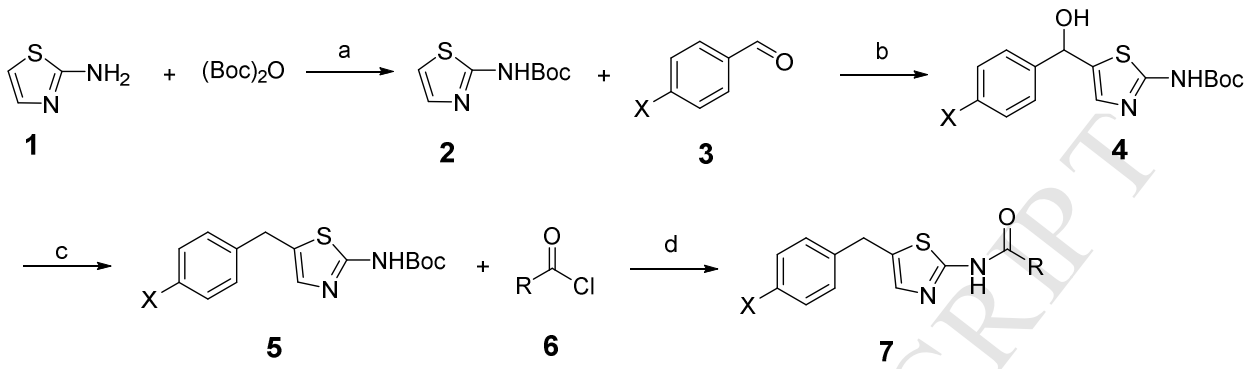

Scheme 1. The syntheses of derivatives of hit compound (**22).** Reagents and conditions: (a) THF, rt; (b) *n*-BuLi, THF, -78℃; (c) Et_3SiH, TFA, DCM, rt; (d) Pyridine, DCM, rt.

In the SAR studies for this project, the compounds were first tested in the Capsid-GFP assay (CGA in Tables) and in the cytotoxicity assay. Only when the tested compound was active in Capsid-GFP assay at 50μM concentration and also showed no obvious cytotoxicity (CC_{50}>50 μM), it would be tested in HBV replication assay.

First, the alky-, aromatic or hetero cyclic modifications on the amide group (**14-20,** Table 1) did not afford better activity in Capsid-GFP assay. Replacement of *p*-fluorobenzene of the hit compound with *p*-chlorobenzene (**21**) afforded improvement on the anti-HBV replication activity (IC_{50} from 6.15 μM to 3.62 μM). Therefore, in the further SAR studies, we focused on *o*-chlorobenzene as the substitution group.

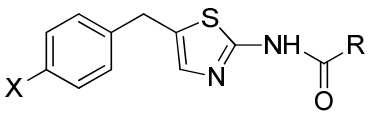

Table1. The SAR studies of the hit compound

Compd. No.	X	R	CGA (%)[a]	CC_{50}[b]	IC_{50}[c]	clog P[d]
14	-F	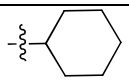	N	>50μM	/	4.26
15	-F	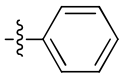	0.60	N	/	3.76
16	-F	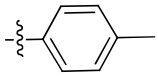	0.53	N	/	4.10
17	-F	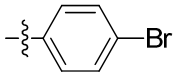	N	>50μM	/	4.52
18	-F	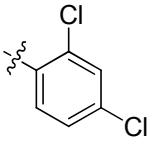	N	>50μM	/	5.07
19	-F	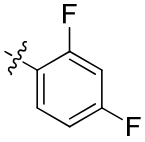	N	N	/	4.04
20	-F	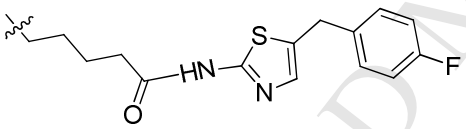	N	>50μM	/	5.93
21	-Cl	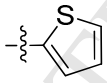	0.59	>50μM	3.62μM	4.34
22	-Br	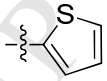	N	>50μM	/	4.45
23	-Br	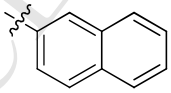	N	>50μM	/	5.54

a: CGA, Capsid-GFP Assay. The percentage of inhibition with compounds at 50μM concentration in Capsid-GFP assay. N: test result did not show activity.

b: CC_{50} (μM), median (50%) cytotoxic concentration; N: CC_{50} value lower than 5μM and too toxic for further test.

c: IC_{50} (μM), half maximal (50%) inhibitory concentration to inhibit of HBV replication. This test was performed only when capsid-GFP assay showed positive result and on obvious cytotoxicity was observed (CC_{50}>50μM).

d: clogP was calculated by LigandScout 4.1

These results prompted us to design compounds by referring with the successful HAP structure. After we compared the structures of hit compound with NVR-010-001-E2 (Scheme 2), we noticed that our hit compound possessed two hydrophobic groups: benzene (green) and thiophene (blue), which were similar with the ethyl (green) and thiazole groups (blue) in NVR-010-001-E2. The previous working mechanism studies of NVR-010-001-E2 already elucidated that these two groups had strong hydrophobic or aromatic interactions with the hydrophobic pockets of HBV capsid protein, and thus they were important for its activity [24]. Moreover, HAP structure had the halogenated benzene ring (cyan) which bound with the third hydrophobic pocket in HBV capsid protein. However, our hit compound lack of the third hydrophobic group. The docking studies also showed that the hit compound could bind in the same site as NVR-010-001-E2, but it was lack of a hydrophobic group to bind with the hydrophobic cavity that was occupied by the halogenated benzene of NVR-010-001-E2 (Figure S1.). Thus, we proposed that the methylene group on hit compound could be substituted with a hydrophobic group (cyan) to afford the necessary hydrophobic interaction (Scheme 2).

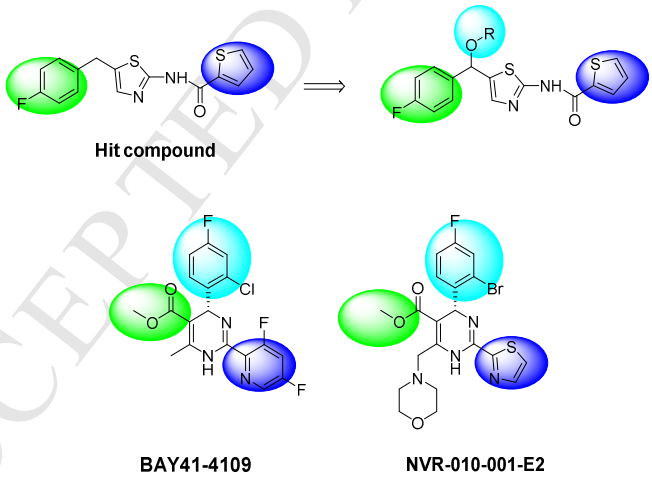

Scheme 2. The design and structure hopping of hit compound. The hit compound has two hydrophobic groups (green and blue). Our design added one more hydrophobic group (cyan) enlightened by the capsid inhibitors in clinical trials with HAP structure (BAY41-4109 and NVR-010-001-E2).

Section 2. SAR studies of the compounds with the third hydrophobic groups

According to the analysis on the possible binding model of the hit compound described above, we designed and synthesized its derivatives with the methods described in scheme 3.

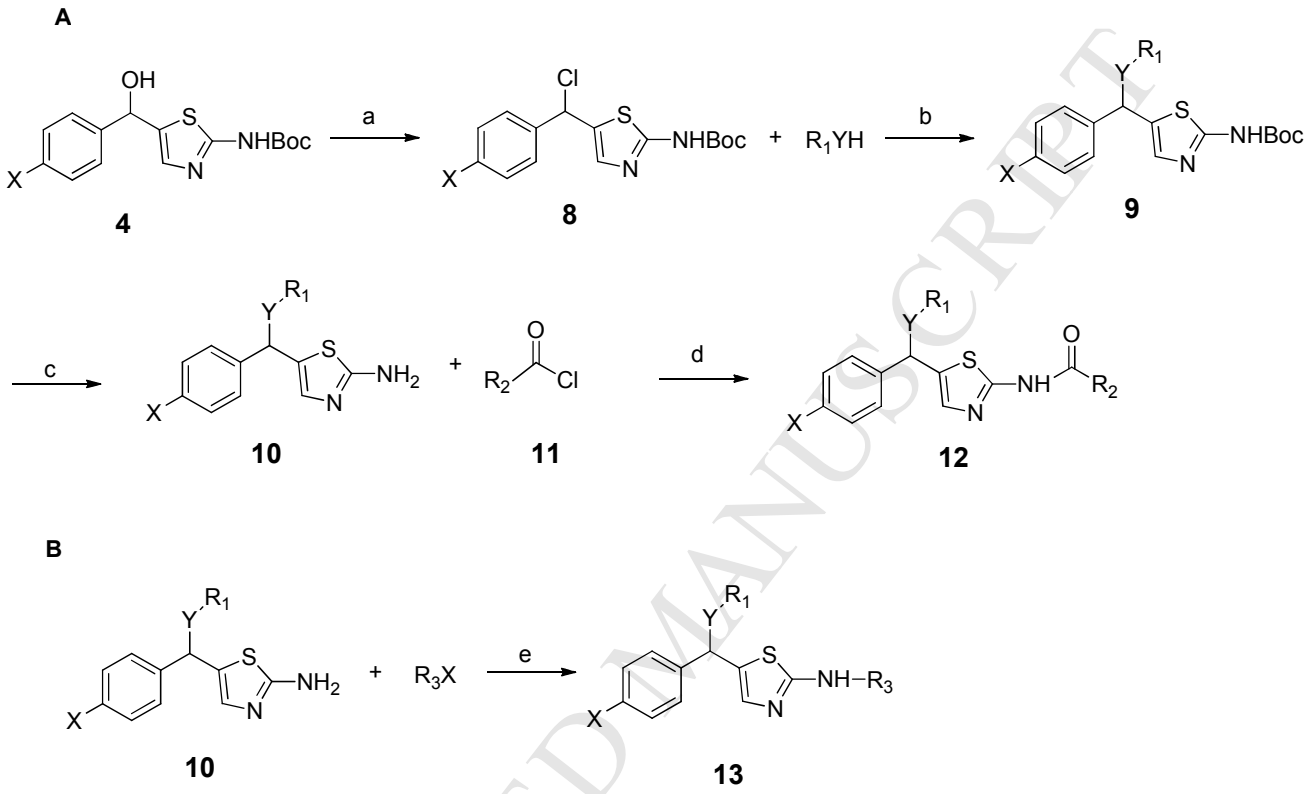

Scheme 3. The syntheses of compounds with three hydrophobic groups. Reagents and conditions: (a) $SOCl_2$, DCM, Reflux; (b) K_2CO_3, DCM, Reflux; (c) TFA, DCM, rt; (d) Pyridine, DCM, rt; (e) Cs_2CO_3, DMF, rt.

To explore the chemical diversity in the third hydrophobic groups on the methylene group, we synthesized the intermediates with chloro-subtituted methylene group (compound **8,** Scheme 3A) to conveniently construct an ether link to install the third hydrophobic groups (compound **9**, Scheme 3A). With the *p*-chloride substitution on benzene ring and with Boc groups in the amide position, different hydrophobic or aromatic rings were installed (**24-33,** Table 2). Among these tested compounds, the α-bromide-naphthalene groups (**31**) afforded good activities both in Capsid-GFP assay and anti-HBV

141 replication test. Next, we optimized compound **31** by replacing the Boc group with thiophene group and
142 found this modification (**33)** afforded good activity in Capsid-GFP assay (CGA) but its cell toxicity was
143 too high (CC_{50}<5μM) to test its anti-HBV replication activity. It was also interesting that other aromatic
144 groups tested in our studies (**34-41**) did not affect the activity in Capsid-GFP assay but led to the loss of
145 activity to inhibit HBV replication. These data indicated that the size of the aromatic groups may not be
146 important to interrupt the assembly of capsid protein, but the *p*-chloride benzene was important to
147 inhibit HBV replication in cells. The SAR studies in this series of compounds afforded support on our
148 hypothesis that the third hydrophobic groups could be a good position for further design.

149

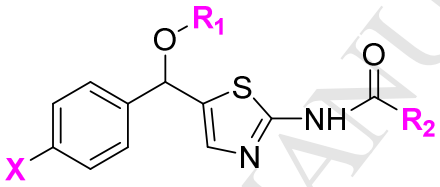

150

151 **Table 2. The SAR studies of the compounds with the third hydrophobic groups**

Compd No.	X	R_1	R_2	CGA (%)[a]	CC_{50}	IC_{50}	clogP
24	-Cl	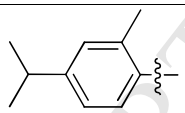	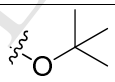	N	>50μM	/	7.50
25	-Cl	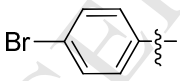	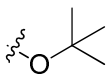	N	>50μM	/	6.83
26	-Cl	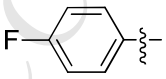	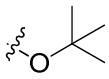	N	>50μM	/	6.20
27	-Cl	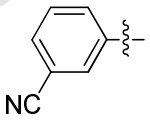	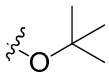	N	>50μM	/	5.94
28	-Cl	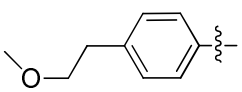	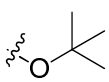	N	>50μM	/	6.25

Compd No.	X	R_1	R_2	CGA (%)[a]	CC_{50}	IC_{50}	clogP
29	-Cl	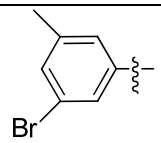	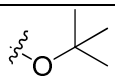	N	>50μM	/	7.13
30	-Cl	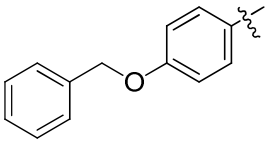	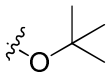	N	>50μM	/	7.36
31	-Cl	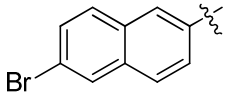	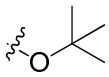	0.55	>50μM	2.27μM	7.00
32	-Cl	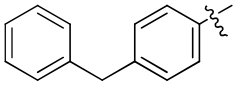	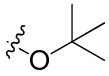	N	>50μM	/	7.52
33	-Cl	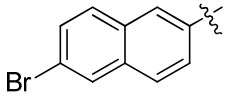	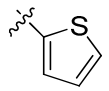	0.47	N	/	7.71
34	H	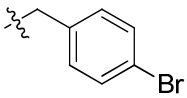	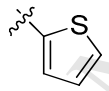	0.64	N	/	5.76
35	H	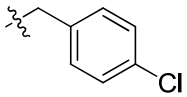	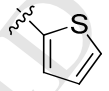	0.59	N	/	5.65
36	H	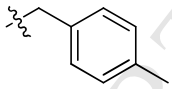	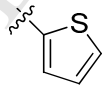	0.64	N	/	5.31
37	H	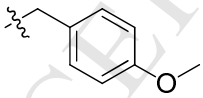	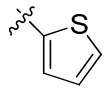	0.64	N	/	5.01
38	H	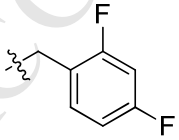	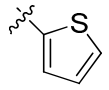	0.26	N	/	5.28
39	H	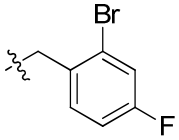	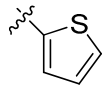	0.27	N	/	5.90

Compd No.	X	R_1	R_2	CGA (%)[a]	CC_{50}	IC_{50}	clogP
40	H	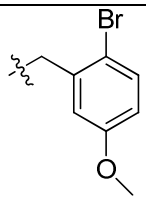	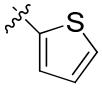	0.45	N	/	5.77
41	H	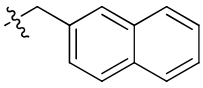	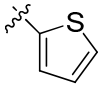	0.47	N	/	6.16

152 **Section 3. The SAR studies at thiophene group and its linker**

153 Based on the results of section 2, we first tested whether it would afford better activity to replace the
154 amide group with alky-substituted amine groups. The Capsid-GFP assay showed that this type of
155 modification totally abolished the activity to inhibit HBV replication (**42-48**, Table 3). It indicated that
156 the aromatic ring or/and the amide structure were necessary for the activity, which fit our hypothesis
157 that the large hydrophobic or aromatic groups were required in this position.

158 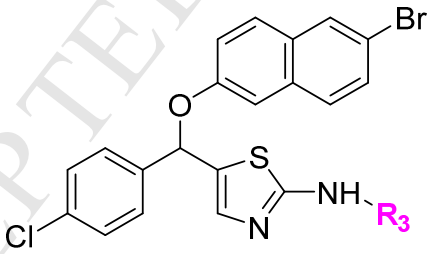

159 **Table 3. The SAR studies of alkyl-substituted amine**

Compd. No.	R_3	CGA (%)[a]	CC_{50}	IC_{50}	clogP
42	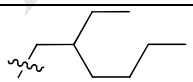	0.55	N	/	9.26
43	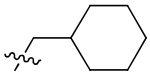	0.61	N	/	8.62
44	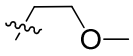	0.37	N	/	6.69

45	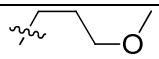	0.38	N	/	7.08
46	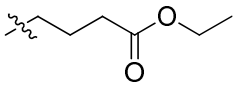	0.35	N	/	7.39
47	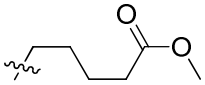	0.40	N	/	7.39
48	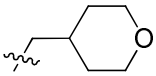	0.43	N	/	7.47

We then synthesized amide structure with alky or aromatic ring substitutions (Table 4). First, the small alkyl groups, such as cyclopropane (**49**) and neo-butyl (**51**), could maintain the activity in Capsid-GFP assay but did not afford any activity in HBV replication assay. The similar results were observed in the compounds with substitution groups (**52**-**54**) with hetero atoms. Second, among the compounds with substituted benzene ring (**55**), or benzene rings with electron donating groups (**56**, **57**) or electron withdrawing groups (**57**-**63**), most of them were active in Capsid-GFP assay. Among these compounds, only compounds **57** and **61** showed potent anti-HBV replication activity but they had a too high LogP value for good DMPK properties. Therefore, we tried to install heterocycles (**64**-**65**) or carbohydrate precursor (**66**) in this position. However, these structures did not afford higher anti-HBV replication activity. Meanwhile, based on compound **57**, we studied the effects of different linkage atoms. It turned out that the compound with nitrogen atoms (**67**) was still active in both assays, although less active than compound **57.** However, the sulfur atom (**68**) led to the loss of the activity to inhibit HBV replication.

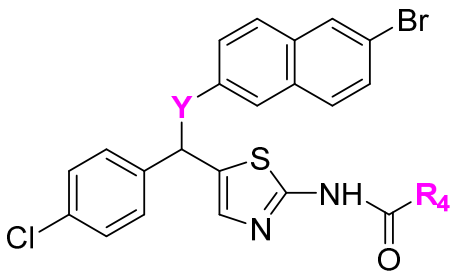

Table 4. The SAR studies of alkyl- or aromatic-substituted amide

Compd. No.	Y	R_4	CGA (%)[a]	CC_{50}	IC_{50}	clogP
49	-O		0.67	N	/	6.92
50	-O	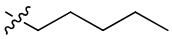	N	>50μM	/	8.15
51	-O		0.47	N	/	7.62
52	-O	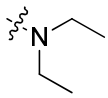	0.67	N	/	7.51
53	-O	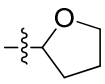	0.35	N	/	6.75
54	-O	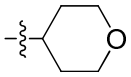	0.66	N	/	7.00
55	-O	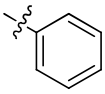	0.58	N	/	7.65
56	-O	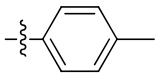	0.71	N	/	7.96
57	-O	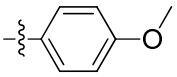	0.54	>50μM	1.45μM	7.66
58	-O	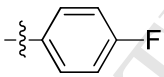	0.50	N	/	7.79
59	-O	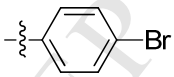	N	>50μM	/	8.42
60	-O	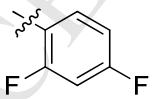	0.51	N	/	7.93
61	-O	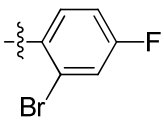	0.65	>50μM	3.55μM	8.55
62	-O	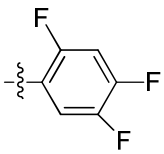	0.44	N	/	8.07

Compd. No.	Y	R_4	CGA (%)[a]	CC_{50}	IC_{50}	clogP
63	-O	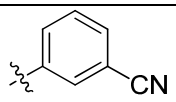	0.70	>50μM	/	7.53
64	-O	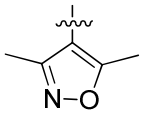	0.64	N	/	7.26
65	-O	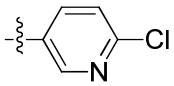	0.45	N	/	7.70
66	-O	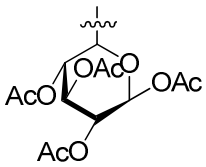	0.40	N	/	5.37
67	-NH	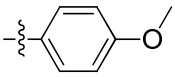	0.69	>50μ M	6.85μM	6.93
68	-S	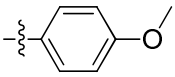	0.49	N	/	7.61

To further optimize compound **57**, we then tested if sulfonamide bond would better than amide (Table 5). Compound **69** showed that the sulfonamide bond would not decrease the activity in Capsid-GFP assay, but it was inactivity in anti-HBV test. We then synthesized derivatives with benzene (**70**) or substituted benzene rings (**71**-**74**). It turned out that only compound **70** afforded good activity in both Capsid-GFP assay and anti-HBV replication assay. We next try to install larger hydrophobic groups (**75**-**78**) and proposed that they could occupy the hydrophobic pocket better in the active site of capsid protein. However, these compounds did not show good activity in either assay. Finally, the quinoline (**79**) group showed good activities to abolish capsid assembly and to inhibit HBV replication. We then isolated the two enantiomers of compound **79** with chiral chromatography (Supplemental information)**.** Both of the enantiomers showed similar activities in Capsid-GFP assay and anti-HBV replication assay (Figure S2). These data indicated that the relatively large hydrophobic groups, such as quinoline in compound **79**, would afford good binding affinity with the hydrophobic pocket in HBV capsid protein. The different activities between compounds **76** and compound **79** indicated that the nitrogen atom of quinoline on compound **79** may have strong interactions, such as hydrogen bonds, with certain amino acid residues in the binding pocket.

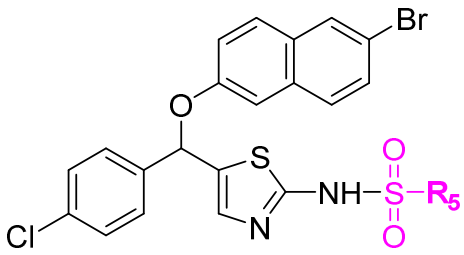

Table 5. The SAR studies of compounds with sulfonamide bonds

Compd. No.	R_5	CGA (%)[a]	CC_{50}	IC_{50}	clogP
69	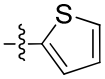	0.44	N	/	8.58
70	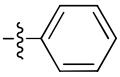	0.63	>50μM	2.32μM	8.51
71	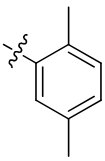	N	>50μM	/	9.13
72	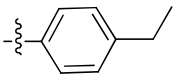	N	>50μM	/	9.08
73	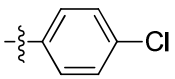	0.50	N	/	9.17
74	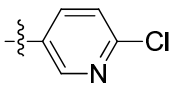	0.30	N	/	8.56
75	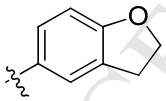	N	>50μM	/	8.45
76	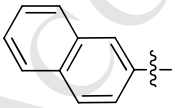	N	>50μM	/	9.67
77	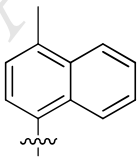	N	>50μM	/	9.98

Compd. No.	R_5	CGA (%)[a]	CC_{50}	IC_{50}	clogP
78	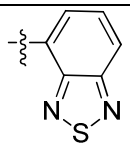	0.50	N	/	8.52
79	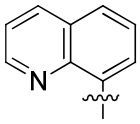	0.63	>50μM	0.18μM	9.06

Section 4. SAR studies at the 4-Chlorobenzene group

In section 2, we observed that the chloride atom on benzene ring was required for the activity. So we used compound **57** as standard to further study whether the substitution groups in this position would increase the activity (Table 6). The compounds with halogen atoms (**80**-**83**) were active in Capsid-GFP assay, but they did not afford better activity in HBV replication assay. Both nitrile and methylsulfonyl groups totally abolished both of the activities. These results, together with the results from section 2, indicated that the chloride group in this position is important for the anti-HBV activity.

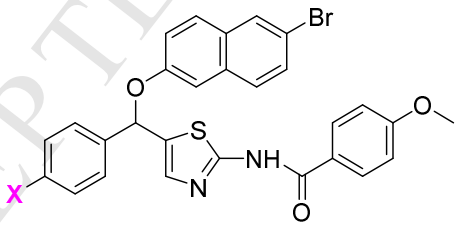

Table 6 The SAR studies at the 4-Chlorobenzene group

Compd. No.	X	CGA (%)[a]	CC_{50}	IC_{50}	clogP
80	Br	0.78	>50μM	/	7.77
81	F	0.76	>50μM	/	7.15
82	-CN	N	N	/	6.89

Compd. No.	X	CGA (%)[a]	CC_{50}	IC_{50}	clogP
83	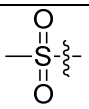	N	N	/	7.50

Section 5. Compound 79 inhibited the HBV capsid assembly

SAR studies afforded compound **79** as the best active compound. Then we performed further studies on how it disrupted the assembly of HBV capsid. We first co-transfected HBc-VN and HBc-VC-expressing plasmids into 293T cells and incubated for 48 h. Then we treated the cells with compound **79** at 0, 0.5, 5, or 50 μM respectively. The MFI (mean fluorescent intensity) of Envision showed that the GFP protein level was inhibited by compound **79** in a dose-dependent manner (Figure 2A). Second, we confirmed that the interactions of HBV capsid protein was interrupted by compound **79** with co-immunoprecipitation assay. The HA-tagged-HBc-VN-expressing plasmid was co-transfected with HA-tagged-HBc-VC-expressing plasmid into 293T cells. Treatment with compound **79** (50 μM, 100 μM) obviously disrupted the dimerization of HBV capsid protein (Figure 2B, C). These results showed that compound **79** inhibited the HBV by disrupting the HBV capsid interactions. To further identify whether treatment of compound **79** had effect on capsid morphology, recombinant HBV capsid protein (HBV capsid protein 1-149, Cp149) was expressed in E.coli and purified, and then subjected to negative staining and examined with electronic microscopy (EM) [15, 26, 32]. After the treatment with compound **79**, almost all capsids did not display a normal morphology (Figure 2D). These results showed that **79** inhibits the aggregation of HBVcAg and consequently disrupts the formation of HBV capsid.

Section 6. The binding model of compound 79 with HBV capsid proteins.

To further elucidate the working mechanism of compound **79**, we performed the molecular docking studies of compound **79** with the crystal structure of HBV capsid protein which included HAP ligand NVR-010-001-E2 (PDB: 5E0I). Frist, the optimized conformation of compound **79** was prepared. Then, the crystal structure of HBV capsid protein was also prepared by removing ligand and unrelated water molecules. We did not specify the HAP ligand site for compound **79** but instead we selected the whole protein for docking studies. The top 5 poses of compound **79** were just in the same binding pocket as the ligand (NVR-010-001-E2). Moreover, compound **79** and NVR-010-001-E2 showed quite similar binding models (Figure 3A). The bromonaphthalene group of **79** had strong hydrophobic or aromatic interactions with the hydrophobic pocket composed by Phe23, Phe24, Trp102, Tyr118, Leu140 of chain B, and Ala132 of chain C (Figure 3A). This was the largest hydrophobic pocket and it was the thiazole group of NVR-010-001-E2 that had bound in this pocket. The quinoline group of compound **79** bound with Thr109 and Val120 of Chain C and it was the similar position that 2-Bromo-4-Fluorophenyl of NVR-010-001-E2 had bound in (Figure 3A). The 4-cholorophenyl group of compound **79** had hydrophobic interactions with Val124 and Trp125 of Chain C (Figure 3B) and the chloride atom pointed to the solvent environment. Compound **79** had three important hydrophobic/aromatic interactions that were also important hydrophobic interactions for HAP inhibitor NVR-010-001-E2. Besides hydrophobic interactions, the nitrogen atoms of the thiazole group and the quinoline group of compound **79** may form hydrogen bound with Ser121 (Figure 3C). The hydrogen bonds between quinoline and Ser121 afforded support on the SAR results of section 3 where we found that the naphthalene group (**76**, **77**) or other aromatic groups could not good activity but only quinoline showed best activities.

To verify the possible hydrogen bonds and the hydrophobic interaction between compound **79** and Ser121 and Tyr118 would be important for its activity, we constructed two mutant HBV capsid proteins Ser121A and Tyr118A. The surface plasmon resonance (SPR) experiments showed that the binding affinity of compound **79** with wildtype HBV capsid protein was high (K_D=5.93*10^{-6}, Figure 4A). However, the HBV capsid mutants S121A and Y118A showed low binding affinity with compound **79**

(Figure. 4B and 4C). These results showed that the hydrogen bond and hydrophobic interaction were vital for the binding affinity and activities of compound **79**.

Section 7. Compound 79 inhibits the HBV replication *in vitro* and *in vivo*.

Compound **79** was applied to treat HepG2.2.15 cells (5×10^4) for 7 days, the HBV replication was detected by the quantitation of HBV DNA in the supernatant with real-time PCR. Compound **79** showed potent anti-HBV replication activity in a dose-dependent way (Figure 5A) with the IC_{50} value of 182.9 nM (Figure 5B) in HepG2.2.15 cells.

The *in vivo* efficacy of compound **79** was evaluated in BALB/c transgenic mice which were injected with replication-competent HBV DNA plasmid HBV-1.2mer and they could produce HBV DNA, HBeAg, HBsAg and HBcAg [33]. These mice were randomly divided into two groups and each group included 3 male BALB/c transgenic mice. We injected by tail vein with 30mg/kg compound **79** and DMSO, respectively. After 2 weeks, mice were scarified and the blood samples were collected to determine the antiviral activity. The data displayed here showed that compound **79** had a significant inhibition of HBV DNA level (Figure. 5C) and HBsAg level (Figure. 5D). Alternatively, to confirm the anti-HBV replication activity of compound **79** *in vivo*, the nude mice were subcutaneously inoculated with HepAD38 cells and then treated with or without compound **79** every 3 days. After 4 weeks, the HBV DNA level in the blood in the treated groups significantly lower than control and it showed that compound **79** had potent antiviral activity *in vivo* (Figure. 5E). Meanwhile, the HBVcAg level in the tumor tissue detected by immunofluorescence assay also decreased in the compound **79** treated group (Figure. 5F).

Section 8. Compound 79 did not show obvious toxicity in acute toxicity test.

The DMPK and toxic properties were the major concerns for the HBV capsid inhibitors [7, 9]. Compound **79** was tested in 5 male Balb/c mice with intraperitoneal injection in the dose of 0 mg/kg,

500 mg/kg, and 1000 mg/kg, respectively. These mice did not show significant change of body weight two weeks after the injections (Figure 6A). In the 14th day, the blood samples and the tissues of heart, liver, lung, spleen, and kidney were examined and no significant abnormity was found. The hepatic and renal functions including the levels of AST, ALT, BUN, and CRE were normal (Figure 6B-D). The histological sections of these organs were also normal (Figure 6E). These preliminary studies on the toxic properties of compound **79** showed that compound **79** could be a good start point to design new HBV capsid inhibitors for lead discoveries.

Discussion and Conclusion

In this report, we developed a cell-based HTS system and screened a commercial library, resulting one of the hit compounds with aminothiazole structure that could block HBV capsid assembly and inhibit HBV replication. In the light of the known working mechanism and structure biology data of active HAP compounds (NVR-010–001-E2 and GLS4), we proposed that our hit compound may have a similar binding model with HAP compounds. Based on this hypothesis, we predicted that the activity of the hit compound may be promoted if it possessed three hydrophobic groups to bind in the binding pocket composed by two HBV capsid proteins, as HAP compounds did. Among the compounds that we deigned and synthesized according to this hypothesis, compound **79** exhibited potent activity to block HBV capsid assembly in the Capsid-GFP assay and it led to the abnormal size and shape of HBV capsid. Compound **79** also inhibited HBV replication both *in vitro* and *in vivo* with no obvious acute toxicity. To elucidate the working mechanism of our effective compounds, we performed docking studies and it showed that compound **79** had similar binding model with ligand NVR-010–001-E2 and the third hydrophobic groups (bromo napthalene) showed strong hydrophobic interactions with pocket composed by Thr128, Tyr118 etc. The quinoline group had hydrophobic interaction with Val120 of Chain C and Thr109 of Chain B. Moreover, the docking studies showed that the nitrogen atoms of aminothiazole and quinoline groups were close to amino acid Ser121 and they could form hydrogen bonds. To acquire

294 better understand of the hydrogen bond interactions, we tested the binding affinity of compound **79** with
295 WT HBV capsid protein and S121A mutant with SPR. Compound **79** showed high binding affinity with
296 WT capsid protein but did not bind with the mutant S121A.

297 Since the HBV capsid assembly process has been proved to be a novel anti-HBV target, both
298 academia and industry have developed HBV capsid inhibitor with different scaffolds. The HAP structure
299 has afforded some promising lead compounds or NCEs in clinical trials. However, the working
300 mechanism of HAP compounds required that the active compounds must have three relatively large
301 hydrophobic/aromatic substitution groups, thus bringing problems in their DMPK properties. Recently,
302 the optimization of HAP structure has focused on the 6-C of dihydropyrimidine by installing various
303 hydrophilic groups to afford better water solubility [7, 9]. The molecular docking data also suggested
304 that this position may point to the solvent environment. Therefore, it could be useful to install
305 hydrophilic groups to acquire both high anti-HBV replication activity and good water solubility. In
306 addition, our work showed that compound **79** probably has a key hydrogen bond with Ser121, which has
307 not been identified before. This hydrogen bond, together with other possible water participated
308 hydrogen bonds, could afford strong binding affinity and also shed light on the design of new HBV
309 capsid inhibitors to bind efficiently to Ser121.

310 In conclusion, our work has identified 2-aminothiazole based HBV capsid inhibitors with potent
311 anti-HBV replication activity. They may bind with HBV capsid protein by hydrophobic interactions and
312 a hydrogen bond with Ser121. These active compounds, especially compound **79**, could be a good start
313 to develop new anti-HBV lead compounds or could be used as chemical tools to study the roles of HBV
314 capsid in viral life cycle.

315 **Experimental methods**

316 **General methods for chemistry.** All starting materials were commercially available and used without

317 further purification. All reactions were carried out with the use of standard techniques under an inert
318 atmosphere (Ar or N_2). NMR spectra were generated on a Bruker 500 or 400MHz instrument and
319 obtained as $CDCl_3$ or DMSO-*d*6 solutions (reported in ppm), using $CDCl_3$ as the reference standard
320 (7.26 ppm) or DMSO-d6 (2.50 ppm). Mass spectral data (ESI) were gathered on Thermofisher LCQ or
321 QE Mass spectrometry. HPLC (Agilent Prostar 218 or 1200) was employed for purity determination.

322 **Synthesis of derivatives of the hit compound**

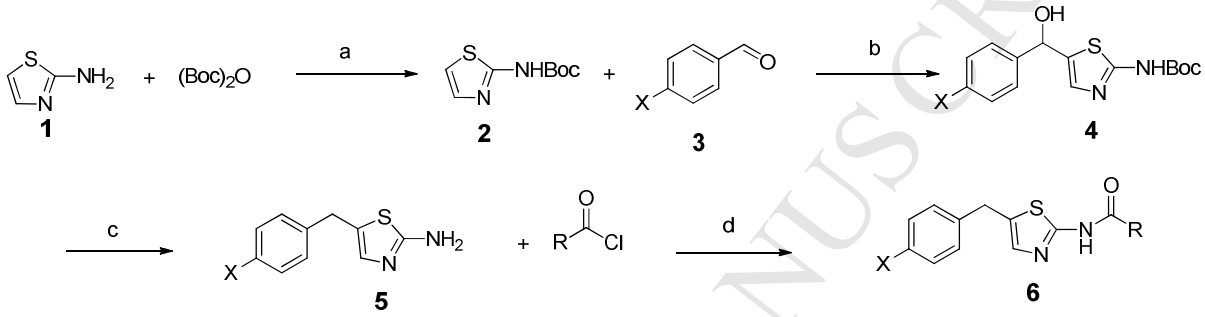

323

324 A suspension of 1, 3-Thiazol-2-amine (**1**) (1g, 9.98 mmol), $(Boc)_2O$ (1.45g, 6.65 mmol) in anhydrous
325 THF was stirred at room temperature for 16h. Upon completion, the reaction mixture was diluted with
326 EtOAc and washed with brine. The organic layer was evaporated to dryness under reduced pressure.
327 The crude product was purified by flash column chromatography on a silica column using
328 c-hexane/acetone (6:1) as the eluent to get while powder compound **2**.

329 *n*-BuLi (1.5 mL 2.5 M in THF, 4 equiv) was added drop wise to compound **2** (1 mmol) in THF (5
330 mL) at -78□ for 1 h and then benzaldehyde derivatives (**3**) (1.2 mmol) were added at -78□ with stirring
331 3-4h. After completion, the reaction system was quenched by adding 1M HCl, extracted with EtOAc
332 and washed with brine. The organic phase was concentrated, and the residue was purified by flash
333 column chromatography on a silica column using c-hexane/acetone (0-50%) to get compound **4.**

334 A mixture of compound **4** (1 equiv), triethylsilane (8 equiv) and TFA (14 equiv) in DCM (10 mL)
335 was stirred overnight at room temperature. After removal of the solvent, the residue was dissolved with

DCM and washed with a saturated solution of aqueous $NaHCO_3$ The organic layer was collected and purified using cyclohexane/acetone (0-30%) to get compound **5**

To a solution of compound **5** in pyridine (3 mL was added acyl chloride derivatives, the reaction mixture was stirred at room temperature for 2h. After concentration, the residue was dissolved in EtOAc, acidified with 1N HCl and washed with brine The organic phase was purified by flash column chromatography on a silica column using cyclohexane/acetone (15%-25%) to get compound **6**

General Procedures for the Synthesis of 24-41, 49-83 analogues for SAR studies

To a solution of compound **4** (0.08 mmol) in 5 mL DCM was added $SOCl_2$ (1 mL). The mixture was refluxed overnight at 80 □. Then the reaction mixture was concentrated in vacuo to get compound **7**. It was used for the next reaction directly.

To a solution of compound **7** in DCM was added compound **8** (0.12 mmol) and K_2CO_3 (0.24 mmol) The resulting mixture was refluxed at 80 □ for 3h before it was quenched with 5 mL of brine The organic layer was collected and purified by flash column chromatography on a silica column using cyclohexane/acetone (0-50%) to get compound **9**.

A mixture of compound **9** (1 equiv) and TFA (14 equiv) in DCM (10 mL) was stirred overnight at room temperature. Then the solvent was evaporated. The residue was washed with a saturated solution of aqueous $NaHCO_3$ mand extracted with DCM The organic layer was collected and purified using cyclohexane/acetone (0-30%) to get compound **10**.

To a solution of compound **10** in pyridine was added acyl chloride or sulfuryl chloride derivatives (**11**), the reaction mixture was stirred at room temperature for 2h. After completion, the reaction system was quenched by adding 1M HCl, extracted with EtOAc and washed with brine. The residue was purified by flash column chromatography on a silica column using cyclohexane/acetone (15%-25%) to

get compound **12**

General procedures for the synthesis of 42-48 analogues for SAR studies.

A mixture of compound **10**, Cs_2CO_3 and halogen substituted alkanes in DMF was stirred overnight at room temperature .The resulting mixture was diluted with EtOAc and washed with brine. The organic layer was collected and purified by flash column chromatography on a silica column using cyclohexane/acetone (0-25%) to get compound **13.**

***N*-(5-(4-fluorobenzyl) thiazol-2-yl) cyclohexanecarboxamide (14)**

^{1}H NMR (500 MHz, $CDCl_3$) δ 7.21 – 7.16 (m, 2H), 7.06 (s, 1H), 7.00 (ddd, *J* = 8.7, 4.5, 2.6 Hz, 2H), 4.03 (s, 2H), 2.48 – 2.39 (m, 1H), 2.34 (tt, *J* = 11.2, 3.6 Hz, 2H), 1.95 (d, *J* = 13.3 Hz, 6H), 1.84 – 1.73 (m, 6H), 1.72 – 1.62 (m, 3H), 1.52 (dtd, *J* = 24.2, 12.4, 3.1 Hz, 7H), 1.39 – 1.17 (m, 11H). ESI-MS m/z: 319.42 $[M+H]^+$.

^{13}C NMR (101 MHz, DMSO) δ 175.79 (s), 163.94 (s), 161.53 (s), 158.95 (s), 138.38 (s), 136.36 (s), 132.69 (s), 131.99 (d, J = 8.0 Hz), 117.43 – 117.22 (m), 117.04 (d, J = 21.2 Hz), 45.09 (s), 32.87 (s), 30.60 (s), 26.97 (d, J = 23.4 Hz), 26.73 – 26.48 (m).

***N*-(5-(4-fluorobenzyl) thiazol-2-yl) benzamide (15)**

^{1}H NMR (500 MHz, $CDCl_3$) δ 8.24 (dt, *J* = 8.7, 1.7 Hz, 1H), 8.17 – 8.13 (m, 2H), 7.66 – 7.62 (m, 1H), 7.59 – 7.52 (m, 3H), 7.50 – 7.45 (m, 1H), 7.24 – 7.19 (m, 3H), 7.09 (s, 1H), 7.07 – 7.01 (m, 3H), 4.18 (s, 1H), 4.08 (s, 2H), 2.17 (s, 1H), 1.26 (s, 1H). ESI-MS m/z: 313.36 $[M+H]^+$.

^{13}C NMR (101 MHz, DMSO) δ 166.85 (s), 163.98 (s), 161.57 (s), 159.66 (s), 138.28 (s), 135.28 (d, J = 203.1 Hz), 134.08 (s), 133.28 (s), 132.07 (d, J = 8.0 Hz), 130.36 (s), 129.91 (s), 117.09 (d, J = 21.2 Hz), 116.94 – 116.70 (m), 32.90 (s).

***N*-(5-(4-fluorobenzyl) thiazol-2-yl)-4-methylbenzamide (16)**

^{1}H NMR (500 MHz, $CDCl_3$) δ 7.91 (d, *J* = 8.2 Hz, 2H), 7.28 (d, *J* = 8.0 Hz, 3H), 7.22 – 7.17 (m, 2H), 7.04 – 6.98 (m, 2H), 6.92 (s, 1H), 4.05 (s, 2H), 2.44 (s, 3H). ESI-MS m/z: 327.39 $[M+H]^+$.

^{13}C NMR (101 MHz, DMSO) δ 166.66 (s), 163.97 (s), 161.57 (s), 159.71 (s), 144.52 (s), 138.29 (s), 136.34 (s), 133.18 (s), 132.06 (d, J = 8.0 Hz), 131.23 (s), 130.91 (s), 129.94 (s), 117.22 (s), 117.08 (d, J

384 = 21.2 Hz), 32.89 (s), 22.89 (s).

385 **4-Bromo-*N*-(5-(4-fluorobenzyl) thiazol-2-yl) benzamide (17)**

386 ^{1}H NMR (500 MHz, $CDCl_3$) δ 8.12 – 8.07 (m, 1H), 7.93 – 7.88 (m, 2H), 7.66 – 7.61 (m, 2H), 7.60 (dd,
387 *J* = 6.1, 3.6 Hz, 1H), 7.22 – 7.17 (m, 2H), 7.07 – 7.01 (m, 2H), 6.90 (s, 1H), 4.18 (s, 1H), 4.06 (s, 2H),
388 1.26 (s, 1H). ESI-MS m/z: 392.26 $[M+H]^+$.

389 ^{13}C NMR (101 MHz, DMSO) δ 166.25 (s), 163.98 (s), 161.58 (s), 159.76 (s), 138.22 (s), 133.40 (s),
390 132.06 (d, J = 10.4 Hz), 128.16 (s), 117.20 (s), 116.99 (s), 32.91 (s).

391 **2,4-Dichloro-*N*-(5-(4-fluorobenzyl) thiazol-2-yl) benzamide (18)**

392 ^{1}H NMR (500 MHz, $CDCl_3$) δ 7.66 (d, *J* = 8.3 Hz, 1H), 7.49 (d, *J* = 1.9 Hz, 1H), 7.36 (dd, *J* = 8.3, 2.0
393 Hz, 1H), 7.20 – 7.15 (m, 2H), 7.03 (ddd, *J* = 8.7, 5.4, 2.1 Hz, 2H), 6.51 (s, 1H), 4.01 (s, 2H). ESI-MS
394 m/z: 382.25 $[M+H]^+$.

395 ^{13}C NMR (101 MHz, DMSO) δ 165.66 (s), 164.00 (s), 161.59 (s), 158.56 (s), 138.26 (s), 137.44 (s),
396 136.50 (s), 135.22 (s), 133.85 (s), 133.40 (s), 132.60 (s), 132.06 (d, J = 8.0 Hz), 131.15 (s), 129.25 (s),
397 117.23 (s), 117.02 (s), 32.90 (s).

398 ***N*-(5-(4-chlorobenzyl) thiazol-2-yl)-2,4-difluorobenzamide (19)**

399 ^{1}H NMR (400 MHz, $CDCl_3$) δ 8.17 (dd, *J* = 15.3, 8.8 Hz, 1H), 7.29 (d, *J* = 8.3 Hz, 2H), 7.18 (d, *J* = 8.3
400 Hz, 3H), 7.10 – 7.02 (m, 1H), 6.99 – 6.90 (m, 1H), 4.07 (s, 2H), 1.26 (s, 3H). ESI-MS m/z:365.80
401 $[M+H]^+$.

402 ^{13}C NMR (101 MHz, DMSO) δ 167.87 (d, J = 12.2 Hz), 165.97 (d, J = 2.9 Hz), 165.24 (dd, J = 23.1,
403 12.6 Hz), 162.54 (d, J = 13.0 Hz), 136.37 (s), 135.81 (d, J = 9.5 Hz), 132.04 (d, J = 7.9 Hz), 117.93 (d, J
404 = 6.8 Hz), 117.20 (s), 116.99 (s), 113.73 (dd, J = 21.6, 3.3 Hz), 107.41 (s), 107.15 (s), 106.89 (s), 32.88
405 (s).

406 **N^1, N^6-bis(5-(4-fluorobenzyl) thiazol-2-yl) adipamide (20)**

407 ^{1}H NMR (500 MHz, DMSO-*d6*) δ 7.27 (dd, *J* = 8.6, 5.6 Hz, 2H), 7.19 (s, 1H), 7.13 – 7.08 (m, 2H), 4.04
408 (s, 6H), 3.10 (dd, *J* = 3.2, 1.6 Hz, 1H), 2.36 (d, *J* = 5.6 Hz, 3H), 1.53 (s, 3H). ESI-MS m/z: 527.20
409 $[M+H]^+$.

410 ^{13}C NMR (101 MHz, DMSO) δ 172.71 (s), 163.92 (s), 161.52 (s), 158.77 (s), 138.34 (s), 136.37 (s),

132.72 (s), 132.01 (d, J = 8.0 Hz), 117.04 (d, J = 21.2 Hz), 36.36 (s), 32.86 (s), 26.11 (s).

***N*-(5-(4-chlorobenzyl) thiazol-2-yl) thiophene-2-carboxamide (21)**

^{1}H NMR (400 MHz, DMSO-*d6*) δ 12.55 (s, 1H), 8.16 (s, 1H), 7.91 (d, *J* = 4.9 Hz, 1H), 7.38 (d, J = 8.4 Hz, 2H), 7.34 – 7.28 (m, 3H), 7.24 – 7.19 (m, 1H), 4.11 (s, 2H), 2.08 (s, 1H). ESI-MS m/z:335.84 $[M+H]^{+}$.

^{13}C NMR (101 MHz, DMSO) δ 141.05 (s), 135.12 (s), 132.96 (s), 132.51 (s), 132.11 (s), 130.33 (s), 33.02 (s).

***N*-(5-(4-bromobenzyl) thiazol-2-yl) thiophene-2-carboxamide (22)**

^{1}H NMR (400 MHz, DMSO-*d6*) δ 12.55 (s, 1H), 8.16 (s, 1H), 7.91 (d, *J* = 4.9 Hz, 1H), 7.51 (d, *J* = 8.3 Hz, 2H), 7.31 (s, 1H), 7.28 – 7.19 (m, 3H), 4.09 (s, 2H), 2.08 (s, 1H), 1.23 (s, 1H). ESI-MS m/z: 380.29 $[M+H]^{+}$.

^{13}C NMR (101 MHz, DMSO) δ 141.46 (s), 134.99 (s), 133.24 (s), 132.45 (s), 130.23 (s), 121.39 (s), 119.73 (s), 33.08 (s).

***N*-(5-(4-bromobenzyl) thiazol-2-yl)-2-naphthamide (23)**

^{1}H NMR (500 MHz, CDCl3) δ 11.99 (s, 1H), 8.49 (s, 1H), 8.02 (dd, J = 8.6, 1.7 Hz, 1H), 7.94 (dd, J = 8.4, 3.3 Hz, 2H), 7.89 (d, J = 8.1 Hz, 1H), 7.65 (dd, J = 11.1, 4.0 Hz, 1H), 7.57 (t, J = 7.1 Hz, 1H), 7.38 (d, J = 8.4 Hz, 2H), 7.04 (d, J = 8.3 Hz, 2H), 6.76 (s, 1H), 3.95 (s, 2H). ESI-MS m/z:424.33 $[M+H]^{+}$.

^{13}C NMR (101 MHz, DMSO) δ 166.96 (s), 159.90 (s), 141.60 (s), 136.48 (s), 133.84 (s), 133.44 – 132.31 (m), 131.08 (t, J = 24.6 Hz), 130.86 – 130.59 (m), 130.41 (s), 130.05 (d, J = 13.8 Hz), 129.51 (s), 128.79 (s), 126.14 (s), 121.40 (s), 33.09 (s).

***tert*-Butyl (5-((4-chlorophenyl) (4-isopropyl-2-methylphenoxy) methyl) thiazol-2-yl) carbamate (24)**

^{1}H NMR (500 MHz, Chloroform-*d*) δ 11.53 (s, 1H), 7.43 (d, *J* = 8.4 Hz, 2H), 7.34 (d, *J* = 8.4 Hz, 2H), 7.07 – 7.01 (m, 2H), 6.73 (d, *J* = 7.5 Hz, 1H), 6.60 (s, 1H), 6.32 (s, 1H), 2.74 (dt, *J* = 13.7, 6.9 Hz, 1H), 2.26 (s, 3H), 1.59 (s, 4H), 1.47 (s, 9H), 1.34 (d, *J* = 2.6 Hz, 1H), 1.26 (s, 1H), 1.15 – 1.10 (m, 6H). ESI-MS m/z: 474.03 $[M+H]^{+}$.

^{13}C NMR (101 MHz, DMSO) δ 148.90 (s), 138.22 (s), 134.21 (s), 132.19 (s), 130.54 (d, *J* = 9.3 Hz),

130.02 (s), 129.65 (d, *J* = 22.3 Hz), 125.82 (s), 120.60 (s), 113.87 (s), 86.52 (s), 83.05 (s), 75.18 (s), 35.06 (s), 29.69 (s), 29.22 (s), 25.61 (s), 17.63 (s).

tert-Butyl (5-((4-bromophenoxy) (4-chlorophenyl) methyl) thiazol-2-yl) carbamate (25)

^{1}H NMR (400 MHz, $CDCl_3$) δ 11.32 (d, *J* = 17.4 Hz, 1H), 7.40 (d, *J* = 8.5 Hz, 2H), 7.36 (s, 1H), 7.33 (t, *J* = 1.8 Hz, 2H), 7.31 (d, *J* = 2.2 Hz, 1H), 6.98 (s, 1H), 6.82 – 6.77 (m, 2H), 6.26 (s, 1H), 1.47 (s, 9H). ESI-MS m/z: 496.82 $[M+H]^+$.

^{13}C NMR (101 MHz, DMSO) δ 162.48 (s), 158.60 (s), 157.76 (s), 154.61 (s), 141.13 (s), 138.61 (s), 134.77 – 134.64 (m), 134.64 – 133.56 (m), 132.74 (s), 130.64 (d, *J* = 9.3 Hz), 129.97 (d, *J* = 17.5 Hz), 129.55 (s), 120.34 (d, *J* = 13.6 Hz), 119.38 (s), 114.85 (s), 111.73 (s), 83.11 (s), 75.91 (s), 29.79 (s), 29.43 (d, *J* = 47.8 Hz).

tert-Butyl (5-((3-chloro-4-fluorophenoxy) (4-chlorophenyl) methyl) thiazol-2-yl) carbamate (26)

^{1}H NMR (500 MHz, $CDCl_3$) δ 7.29 (d, *J* = 8.5 Hz, 2H), 7.12 (d, *J* = 8.4 Hz, 2H), 7.05 (d, *J* = 8.0 Hz, 1H), 6.84 (d, *J* = 11.3 Hz, 1H), 6.74 (d, *J* = 1.0 Hz, 1H), 5.82 (s, 1H), 1.44 (s, 9H). ESI-MS m/z: 470.36 $[M+H]^+$.

^{13}C NMR (101 MHz, CD_3CN) δ 169.81 (s), 154.21 (s), 143.28 (s), 138.71 (s), 132.71 (d, *J* = 12.2 Hz), 132.06 (d, *J* = 15.3 Hz), 130.74 (s), 130.34 (s), 130.06 (s), 129.49 (s), 129.25 (s), 127.49 (s), 121.96 (s), 120.84 (s), 117.31 (s), 62.82 (s), 40.89 (s), 31.25 (s), 15.19 (s).

tert-Butyl (5-((4-chlorophenyl) (3-cyanophenoxy) methyl) thiazol-2-yl) carbamate (27)

^{1}H NMR (500 MHz, Chloroform-*d*) δ 11.40 (s, 1H), 7.39 (q, *J* = 8.4 Hz, 5H), 7.33 (d, *J* = 7.6 Hz, 1H), 7.24 (s, 1H), 7.16 (d, *J* = 7.4 Hz, 2H), 6.99 (s, 1H), 6.32 (s, 1H), 2.17 (d, *J* = 0.9 Hz, 2H), 1.47 (s, 9H), 1.42 (s, 3H), 1.34 (s, 2H), 1.25 (s, 2H). ESI-MS m/z: 442.93 $[M+H]^+$.

^{13}C NMR (101 MHz, DMSO) δ 163.45 (s), 158.38 (s), 157.17 (s), 154.64 (s), 153.65 (s), 140.79 (s), 136.05 (s), 132.10 – 129.83 (m), 129.56 (s), 121.33 (s), 118.76 (s), 118.24 (s), 102.84 (s), 65.10 (s), 63.06 (s), 62.29 (s), 29.69 (s), 29.18 (s), 16.30 (d, *J* = 9.9 Hz), 15.83 (s).

tert-Butyl (5-((4-chlorophenyl) (4-(2-methoxyethyl) phenoxy) methyl) thiazol-2-yl) carbamate (28)

^{1}H NMR (500 MHz, $CDCl_3$) δ 7.41 (d, *J* = 8.5 Hz, 2H), 7.34 (d, *J* = 8.4 Hz, 2H), 7.07 (d, *J* = 8.5 Hz, 2H), 6.98 (s, 1H), 6.83 (d, *J* = 8.6 Hz, 2H), 6.26 (s, 1H), 3.54 (t, *J* = 7.0 Hz, 2H), 3.33 (s, 3H), 2.79 (t, *J*

= 7.0 Hz, 2H), 1.47 (s, 9H), 1.43 (s, 5H), 1.34 (s, 2H), 1.26 (s, 3H). ESI-MS m/z: 476 $[M+H]^+$.

^{13}C NMR (101 MHz, DMSO) δ 162.27 (s), 156.84 (s), 131.58 (s), 130.53 (s), 129.89 (s), 117.82 (s), 83.07 (s), 75.64 (s), 74.67 (s), 59.58 (s), 36.25 (s), 29.68 (s).

***tert*-Butyl (5-((3-bromo-5-methylphenoxy) (4-chlorophenyl) methyl) thiazol-2-yl) carbamate (29)**

^1H NMR (400 MHz, $CDCl_3$) δ 11.51 (s, 1H), 7.39 (s, 2H), 7.36 (s, 2H), 6.99 (s, 1H), 6.93 (s, 1H), 6.87 (s, 1H), 6.67 (s, 1H), 6.27 (s, 1H), 2.25 (s, 3H), 1.48 (s, 9H). ESI-MS m/z: 510.84 $[M+H]^+$.

^{13}C NMR (101 MHz, DMSO) δ 162.47 (s), 160.22 (s), 159.22 (s), 154.61 (s), 143.08 (d, *J* = 27.2 Hz), 141.14 (s), 138.55 (s), 134.50 (s), 132.76 (s), 130.60 (s), 129.85 (s), 129.56 (s), 126.79 (s), 124.14 (s), 123.44 (d, *J* = 13.0 Hz), 118.19 (s), 118.17 – 117.04 (m), 117.04 – 116.77 (m), 83.11 (s), 75.65 (s), 29.67 (s), 29.20 (s), 22.52 (s).

***tert*-Butyl (5-((4-(benzyloxy) phenoxy) (4-chlorophenyl) methyl) thiazol-2-yl) carbamate (30)**

^1H NMR (500 MHz, Chloroform-*d*) δ 11.35 (s, 1H), 7.42 (s, 1H), 7.41 (s, 2H), 7.38 (d, *J* = 3.7 Hz, 2H), 7.37 (s, 1H), 7.35 (s, 1H), 7.32 (d, *J* = 10.6 Hz, 2H), 6.96 (s, 1H), 6.83 (s, 4H), 6.18 (s, 1H), 4.97 (s, 2H), 1.58 (s, 4H), 1.47 (s, 9H), 1.34 (s, 1H), 1.26 (s, 1H). ESI-MS m/z: 524.04 $[M+H]^+$.

^{13}C NMR (101 MHz, DMSO) δ 162.32 (s), 154.96 (s), 154.77 (d, *J* = 32.1 Hz), 152.52 (s), 141.73 (s), 139.07 (s), 138.27 (s), 134.30 (s), 133.45 (s), 130.48 (s), 130.20 (s), 129.94 (s), 129.52 (d, *J* = 9.6 Hz), 119.35 (s), 117.39 (s), 83.05 (s), 76.42 (s), 71.45 (s), 29.68 (s).

***tert*-Butyl (5-(((6-bromonaphthalen-2-yl) oxy) (4-chlorophenyl) methyl) thiazol-2-yl) carbamate (31)**

^1H NMR (500 MHz, MeOD) δ 7.94 (d, *J* = 2.1 Hz, 1H), 7.76 (d, *J* = 9.0 Hz, 1H), 7.67 (d, *J* = 8.9 Hz, 1H), 7.36 (dd, *J* = 9.2, 1.8 Hz, 1H), 7.25 (d, *J* = 2.4 Hz, 1H), 7.23 (t, *J* = 3.7 Hz, 3H), 7.19 (d, *J* = 9.0 Hz, 1H), 7.06 (s, 1H), 6.61 (s, 1H), 2.15 (s, 1H), 1.47 (s, 9H). FTMS-c ESI m/z: 545.01319 $[M-H]^-$.

^{13}C NMR (101 MHz, CD_3CN) δ 162.23 (s), 158.11 (s), 154.33 (s), 154.00 (s), 142.83 (s), 136.97 (s), 133.83 (s), 133.62 (s), 133.46 – 132.72 (m), 132.65 (s), 132.11 (d, *J* = 9.4 Hz), 130.90 (s), 130.25 (dd, *J* = 28.2, 18.3 Hz), 129.59 (s), 127.36 (s), 121.64 (s), 120.84 (s), 117.34 (s), 83.00 (s), 62.84 (s), 40.66 (s), 28.69 (s), 15.20 (s).

***tert*-Butyl (5-((4-benzylphenoxy) (4-chlorophenyl) methyl) thiazol-2-yl) carbamate (32)**

^{1}H NMR (400 MHz, $CDCl_3$) δ 11.33 (s, 1H), 7.41 (d, *J* = 8.4 Hz, 2H), 7.33 (d, *J* = 8.4 Hz, 2H), 7.29 – 7.23 (m, 4H), 7.19 (d, *J* = 7.1 Hz, 1H), 7.14 (d, *J* = 7.9 Hz, 2H), 7.03 (d, *J* = 8.4 Hz, 2H), 6.98 (s, 1H), 6.83 (d, *J* = 8.5 Hz, 2H), 6.26 (s, 1H), 3.88 (s, 2H), 1.47 (s, 9H). ESI-MS m/z: 508.04 $[M+H]^+$.

^{13}C NMR (101 MHz, DMSO) δ 162.31 (s), 156.81 (s), 154.60 (s), 143.28 (s), 141.62 (s), 138.24 (s), 136.12 (s), 134.32 (s), 133.35 (s), 131.45 (s), 130.52 (s), 130.32 (d, *J* = 22.4 Hz), 129.86 (s), 127.70 (s), 119.83 (s), 117.99 (s), 83.06 (s), 75.70 (s), 29.66 (s).

_N_-(5-(((6-bromonaphthalen-2-yl)oxy)(4-chlorophenyl)methyl)thiazol-2-yl)thiophene-2-carboxamide (33)

^{1}H NMR (400 MHz, $CDCl_3$) δ 8.05 (s, 1H), 7.87 – 7.82 (m, 1H), 7.78 (d, *J* = 9.2 Hz, 2H), 7.67 – 7.63 (m, 1H), 7.53 – 7.48 (m, 1H), 7.37 (d, *J* = 8.9 Hz, 1H), 7.13 (dd, *J* = 9.4, 4.3 Hz, 5H), 6.86 (s, 1H), 6.32 (s, 1H), 4.84 (s, 2H), 1.43 (s, 7H). ESI-MS m/z:555.89 $[M+H]^+$.

^{13}C NMR (101 MHz, DMSO) δ 170.87 (s), 161.05 (s), 148.10 (s), 143.28 (s), 139.95 (s), 137.15 (s), 136.84 (s), 135.16 (s), 133.15 (s), 132.49 (s), 132.18 (s), 131.54 (s), 130.71 (s), 130.12 (s), 129.95 (d, *J* = 25.0 Hz), 128.68 (s), 126.20 (s), 125.73 (s), 120.88 (s).

_N_-(5-(((4-bromobenzyl)oxy)(phenyl)methyl)thiazol-2-yl)thiophene-2-carboxamide (34)

^{1}H NMR (500 MHz, $CDCl_3$) δ 7.88 – 7.82 (m, 1H), 7.50 – 7.45 (m, 3H), 7.39 (ddd, *J* = 8.2, 5.5, 3.2 Hz, 3H), 7.34 (ddd, *J* = 10.0, 5.6, 2.9 Hz, 1H), 7.24 (s, 1H), 7.11 – 7.07 (m, 1H), 6.76 (d, *J* = 1.0 Hz, 1H), 5.81 (s, 1H), 5.28 (s, 2H), 1.35 (d, *J* = 19.3 Hz, 1H), 1.27 (d, *J* = 15.1 Hz, 2H). ESI-MS m/z: 486.42 $[M+H]^+$.

^{13}C NMR (101 MHz, DMSO) δ 169.41 (s), 167.83 (s), 145.05 (s), 144.56 (s), 137.60 (s), 133.46 (s), 133.11 – 132.92 (m), 132.69 (d, J = 27.0 Hz), 132.34 (s), 130.20 (s), 129.91 (s), 129.44 (s), 127.93 (s), 125.04 (s), 123.08 (s), 70.51 (s), 52.11 (s).

_N_-(5-(((4-chlorobenzyl)oxy)(phenyl)methyl)thiazol-2-yl)thiophene-2-carboxamide(35)

^{1}H NMR (500 MHz, $CDCl_3$) δ 7.97 – 7.86 (m, 1H), 7.50 – 7.47 (m, 1H), 7.47 – 7.42 (m, 1H), 7.40 – 7.36 (m, 2H), 7.36 – 7.30 (m, 3H), 7.29 (s, 1H), 7.28 (d, *J* = 4.8 Hz, 1H), 7.10 (dt, *J* = 4.9, 3.5 Hz, 1H), 6.83 – 6.76 (m, 1H), 6.44 (s, 1H), 6.02 (s, 1H), 5.82 (s, 1H), 5.43 (s, 1H), 5.32 (ddd, *J* = 39.3, 20.1, 10.8 Hz, 2H), 2.17 (s, 1H), 1.26 (s, 1H). ESI-MS m/z: 441.97 $[M+H]^{+\cdot}$

^{13}C NMR (126 MHz, CD_3CN) δ 166.87 (s), 143.14 (s), 142.57 (s), 135.26 (s), 133.41 (s), 131.10 (s),

130.77 (s), 129.96 (s), 128.77 (s), 128.57 (s), 127.98 (d, *J* = 6.1 Hz), 126.23 (s), 123.07 (s), 69.56 (s), 50.67 (s).

_N_-(5-(((4-methylbenzyl)oxy)(phenyl)methyl)thiazol-2-yl)thiophene-2-carboxamide (36)

^{1}H NMR (500 MHz, $CDCl_3$) δ 7.91 – 7.85 (m, 1H), 7.53 – 7.45 (m, 1H), 7.36 (dddd, *J* = 25.5, 12.3, 6.7, 2.1 Hz, 5H), 7.21 (d, *J* = 8.0 Hz, 1H), 7.19 – 7.11 (m, 2H), 7.11 – 7.07 (m, 1H), 6.79 (d, *J* = 0.9 Hz, 1H), 6.46 (d, *J* = 1.0 Hz, 1H), 6.01 (s, 1H), 5.80 (s, 1H), 5.39 – 5.23 (m, 2H), 2.34 (dd, *J* = 8.3, 4.3 Hz, 3H). ESI-MS m/z: 421.55 $[M+H]^{+}$.

^{13}C NMR (126 MHz, CD_3CN) δ 168.37 (s), 166.75 (s), 143.27 (s), 142.63 (s), 138.07 (s), 133.37 (s), 131.01 (s), 130.69 (s), 129.38 (s), 128.55 (s), 128.24 (s), 127.95 (d, *J* = 6.1 Hz), 126.20 (s), 123.16 (s), 69.56 (s), 51.17 (s), 20.16 (s).

_N_-(5-(((4-methoxybenzyl)oxy)(phenyl)methyl)thiazol-2-yl)thiophene-2-carboxamide (37)

^{1}H NMR (500 MHz, $CDCl_3$) δ 7.89 (dt, *J* = 6.8, 1.9 Hz, 1H), 7.47 (ddd, *J* = 4.9, 3.0, 1.2 Hz, 1H), 7.44 – 7.30 (m, 6H), 7.10 (dd, *J* = 4.9, 3.7 Hz, 1H), 6.86 (dt, *J* = 5.8, 5.3 Hz, 2H), 6.80 – 6.75 (m, 1H), 6.47 (d, *J* = 0.9 Hz, 1H), 5.78 (s, 1H), 5.40 (s, 1H), 5.29 – 5.19 (m, 2H), 3.80 – 3.76 (m, 3H), 2.17 (s, 1H) ESI-MS m/z: 437.55 $[M+H]^{+\cdot}$.

^{13}C NMR (126 MHz, CD_3CN) δ 168.37 (s), 166.66 (s), 159.59 (s), 143.29 (s), 142.63 (s), 131.02 (s), 130.71 (s), 129.88 (s), 128.69 (d, *J* = 33.4 Hz), 128.33 (s), 127.97 (s), 126.99 (s), 126.20 (s), 123.09 (s), 114.09 (s), 69.58 (s), 54.94 (s), 50.91 (s).

_N_-(5-(((2,4-difluorobenzyl)oxy)(phenyl)methyl)thiazol-2-yl)thiophene-2-carboxamide (38)

^{1}H NMR (500 MHz, CDCl3) δ 7.91 – 7.86 (m, 3H), 7.66 (ddt, J = 25.3, 18.6, 7.5 Hz, 4H), 7.51 – 7.30 (m, 21H), 7.13 – 7.08 (m, 3H), 6.95 – 6.79 (m, 9H), 6.57 (s, 1H), 5.83 (s, 1H), 5.47 (s, 1H), 5.33 (s, 4H), 5.28 – 5.24 (m, 2H), 2.17 (s, 1H), 1.26 (s, 2H). ESI-MS m/z: 443.50 $[M+H]^{+}$.

^{13}C NMR (101 MHz, CD3CN) δ 169.76 (s), 168.27 (s), 144.41 (s), 143.94 (s), 133.77 (dd, J = 9.9, 5.4 Hz), 132.49 (s), 132.19 (s), 131.87 (s), 129.91 (s), 129.33 (d, J = 3.8 Hz), 127.59 (s), 124.68 (s), 112.99 (s), 112.77 (s), 105.48 (s), 105.22 (s), 104.96 (s), 70.91 (s).

_N_-(5-(((2-bromo-4-fluorobenzyl)oxy)(phenyl)methyl)thiazol-2-yl)thiophene-2-carboxamide (39)

^{1}H NMR (500 MHz, CDCl3) δ 7.90 – 7.84 (m, 1H), 7.59 – 7.54 (m, 1H), 7.47 (qd, J = 9.0, 4.9 Hz, 2H),

7.41 (dd, J = 12.4, 6.9 Hz, 2H), 7.37 – 7.30 (m, 3H), 7.09 (dt, J = 8.6, 2.3 Hz, 1H), 7.05 – 6.96 (m, 1H), 6.95 (s, 1H), 6.88 (s, 1H), 6.63 (s, 1H), 5.82 (s, 1H), 5.50 – 5.28 (m, 3H), 2.17 (s, 1H). ESI-MS m/z: 504.41 $[M+H]^+$.

^{13}C NMR (101 MHz, DMSO) δ 169.46 (s), 167.99 (s), 164.40 (s), 161.93 (s), 145.05 (s), 144.45 (s), 133.48 (d, J = 18.2 Hz), 133.34 – 132.54 (m), 132.54 – 132.27 (m), 130.22 (s), 130.02 (d, J = 31.7 Hz), 129.43 (s), 127.94 (s), 125.10 (s), 124.59 (d, J = 10.0 Hz), 122.43 – 122.01 (m), 121.85 (d, J = 24.8 Hz), 117.16 (s), 116.95 (s), 70.45 (s), 52.46 (s).

_N_-(5-(((2-bromo-5-methoxybenzyl)oxy)(phenyl)methyl)thiazol-2-yl)thiophene-2-carboxamide (40)

^{1}H NMR (500 MHz, CDCl3) δ 7.89 (dd, J = 6.6, 3.7 Hz, 1H), 7.49 – 7.44 (m, 2H), 7.41 (ddd, J = 10.2, 8.0, 2.0 Hz, 2H), 7.37 (dd, J = 9.6, 4.8 Hz, 1H), 7.34 – 7.30 (m, 1H), 7.12 – 7.07 (m, 1H), 7.06 (d, J = 3.0 Hz, 1H), 7.01 (d, J = 2.9 Hz, 1H), 6.97 (d, J = 10.3 Hz, 1H), 6.75 (tdd, J = 11.6, 8.1, 3.8 Hz, 1H), 6.04 (s, 1H), 5.83 (s, 1H), 5.56 – 5.40 (m, 2H), 5.39 (s, 1H), 5.32 (s, 1H), 3.67 (t, J = 8.8 Hz, 3H), 2.17 (s, 1H), 1.26 (s, 1H). ESI-MS m/z: 516.44 $[M+H]^+$

^{13}C NMR (101 MHz, DMSO) δ 169.46 (s), 168.00 (s), 160.68 (s), 145.11 (s), 144.47 (s), 138.00 (s), 135.48 (s), 133.58 (s), 132.61 (d, J = 9.0 Hz), 130.16 (s), 129.85 (s), 129.42 (s), 127.88 (s), 125.00 (s), 117.55 (s), 116.83 (s), 114.40 (s), 70.42 (s), 57.21 (s), 52.91 (s).

_N_-(5-((naphthalen-2-ylmethoxy)(phenyl)methyl)thiazol-2-yl)thiophene-2-carboxamide (41)

^{1}H NMR (500 MHz, CDCl3) δ 7.91 (tdd, J = 4.8, 3.8, 1.2 Hz, 2H), 7.86 – 7.76 (m, 7H), 7.55 – 7.45 (m, 8H), 7.44 – 7.29 (m, 9H), 7.14 – 7.08 (m, 2H), 6.84 (s, 1H), 6.53 (s, 1H), 6.01 (s, 1H), 5.80 (s, 1H), 5.52 (d, J = 2.8 Hz, 2H), 2.17 (s, 2H), 1.26 (s, 2H). ESI-MS m/z: 457.58 $[M+H]^+$

^{13}C NMR (126 MHz, CD_3CN) δ 168.42 (s), 166.94 (s), 143.23 (s), 142.63 (s), 133.86 (s), 133.22 (s), 132.90 (s), 131.05 (s), 130.74 (s), 128.57 (d, *J* = 5.4 Hz), 127.95 (d, *J* = 5.1 Hz), 127.71 (d, *J* = 15.0 Hz), 127.30 (s), 126.59 (s), 126.47 (d, *J* = 20.9 Hz), 126.22 (s), 125.87 (s), 123.24 (s), 69.58 (s), 51.57 (s).

5-(((6-Bromonaphthalen-2-yl) oxy) (4-chlorophenyl) methyl)-*N*-(2-ethylhexyl) thiazol-2-amine (42)

^{1}H NMR (300 MHz, DMSO-*d6*) δ 8.16 (d, *J* = 2.1 Hz, 1H), 7.92 (d, *J* = 9.2 Hz, 1H), 7.52 (t, *J* = 9.8 Hz, 2H), 7.29 (t, *J* = 7.3 Hz, 2H), 7.07 (d, *J* = 8.4 Hz, 2H), 6.79 (d, *J* = 17.0 Hz, 3H), 6.48 (s, 1H), 5.76 (s, 1H), 3.99 – 3.89 (m, 1H), 3.82 (s, 1H), 2.08 (s, 1H), 1.39 (s, 4H), 1.27 – 1.08 (m, 8H), 0.88 – 0.70 (m,

7H). ESI-MS m/z: 558.99 $[M+H]^+$.

^{13}C NMR (101 MHz, CD3CN) δ 169.85 (s), 156.18 (s), 143.81 (s), 138.81 (s), 132.63 (s), 132.35 (s), 132.03 (d, J = 13.2 Hz), 130.60 (s), 130.30 (d, J = 9.1 Hz), 129.49 (s), 128.88 (s), 127.42 (s), 124.90 (d, J = 5.8 Hz), 117.79 (s), 117.42 (d, J = 8.7 Hz), 73.03 (s), 40.90 (d, J = 33.9 Hz), 40.64 (s), 31.45 (d, J = 8.6 Hz), 30.10 (s), 24.77 (d, J = 10.0 Hz), 24.12 (d, J = 3.1 Hz), 14.77 (s), 11.77 (d, J = 7.3 Hz).

5-(((6-Bromonaphthalen-2-yl) oxy) (4-chlorophenyl) methyl)-*N*-(cyclohexylmethyl) thiazol-2-amine (43)

^1H NMR (300 MHz, DMSO-*d6*) δ 8.17 (d, *J* = 2.1 Hz, 1H), 7.90 (d, *J* = 9.2 Hz, 1H), 7.56 – 7.46 (m, 2H), 7.31 (d, *J* = 8.6 Hz, 2H), 7.06 (d, *J* = 8.4 Hz, 2H), 6.90 (s, 1H), 6.77 (s, 2H), 6.48 (s, 1H), 2.08 (s, 1H), 1.60 (s, 4H), 1.39 (s, 3H), 1.27 (dd, *J* = 16.5, 13.7 Hz, 6H), 1.12 (d, *J* = 11.3 Hz, 3H), 0.84 (d, *J* = 6.7 Hz, 3H). ESI-MS m/z: 542.99 $[M+H]^+$.

^{13}C NMR (101 MHz, CD3CN) δ 169.87 (s), 139.03 (s), 132.40 (s), 131.97 (s), 130.71 (s), 130.23 (d, J = 5.4 Hz), 129.42 (s), 128.84 (s), 127.15 (s), 125.03 (s), 117.45 (s), 75.93 (s), 41.22 (s), 39.01 (s), 30.82 (d, J = 8.8 Hz), 27.52 (s), 26.92 (s).

5-(((6-Bromonaphthalen-2-yl) oxy) (4-chlorophenyl) methyl)-N-(2-methoxyethyl) thiazol-2-amine (44)

^1H NMR (300 MHz, DMSO-*d6*) δ 8.17 (d, *J* = 2.2 Hz, 1H), 7.91 (d, *J* = 9.1 Hz, 2H), 7.55 – 7.48 (m, 2H), 7.32 (d, *J* = 8.6 Hz, 2H), 7.13 (d, *J* = 8.3 Hz, 2H), 6.79 (d, *J* = 13.2 Hz, 3H), 6.51 (s, 1H), 4.25 – 4.15 (m, 1H), 4.06 (s, 1H), 3.43 (d, *J* = 7.3 Hz, 2H), 3.21 (s, 3H), 2.08 (s, 1H), 1.39 (s, 3H). ESI-MS m/z: 504.93 $[M+H]^+$.

^{13}C NMR (101 MHz, DMSO) δ 170.55 (s), 155.90 (s), 144.51 (s), 139.51 (s), 132.52 (s), 132.25 (s), 130.75 (t, J = 15.3 Hz), 129.84 (s), 128.19 (s), 126.81 (s), 125.99 (s), 118.58 (s), 118.19 (s), 72.14 (s), 70.18 (s), 60.01 (s).

5-(((6-Bromonaphthalen-2-yl) oxy) (4-chlorophenyl) methyl)-*N*-(3-methoxypropyl) thiazol-2-amine (45)

^1H NMR (300 MHz, DMSO-*d6*) δ 8.18 (d, *J* = 2.1 Hz, 1H), 7.92 (d, *J* = 9.1 Hz, 1H), 7.58 – 7.46 (m, 2H), 7.31 (d, *J* = 8.6 Hz, 2H), 7.07 (d, *J* = 8.4 Hz, 2H), 6.91 (s, 1H), 6.77 (s, 2H), 6.48 (s, 1H), 4.09 (dt, *J* = 11.1, 5.7 Hz, 1H), 3.96 (s, 1H), 3.14 (s, 4H), 2.09 (s, 1H), 1.72 (dd, *J* = 12.3, 6.1 Hz, 2H), 1.40 (s,

603 10H). ESI-MS m/z: 518.94 $[M+H]^+$.

604 ^{13}C NMR (126 MHz, CD_3CN) δ 168.45 (s), 154.43 (s), 142.77 (s), 137.75 (s), 131.17 (s), 130.99 (s),
605 130.68 (d, *J* = 10.0 Hz), 129.43 (s), 128.91 (s), 128.05 (s), 127.38 (s), 125.72 (s), 123.67 (s), 115.91 (s),
606 68.57 (s), 65.96 (s), 57.71 (s), 39.91 (s), 30.67 (s), 29.84 – 28.75 (m), 28.92 – 28.75 (m).

607 **Ethyl 4-((5-(((6-bromonaphthalen-2-yl) oxy) (4-chlorophenyl) methyl) thiazol-2-yl) amino)**
608 **butanoate (46)**

609 ^1H NMR (500 MHz, DMSO-*d6*) δ 8.17 (d, *J* = 2.1 Hz, 1H), 7.92 (d, *J* = 9.1 Hz, 1H), 7.53 (d, *J* = 9.2 Hz,
610 1H), 7.48 (d, *J* = 9.1 Hz, 1H), 7.29 (d, *J* = 8.5 Hz, 2H), 7.06 (d, *J* = 8.4 Hz, 2H), 6.91 (s, 1H), 6.75 (s,
611 2H), 6.47 (s, 1H), 4.11 – 4.05 (m, 1H), 4.05 – 3.98 (m, 2H), 3.93 (s, 1H), 2.08 (s, 2H), 1.77 (s, 2H), 1.39
612 (s, 5H), 1.17 (t, *J* = 7.1 Hz, 3H). ESI-MS m/z: 560.92 $[M+H]^+$.

613 ^{13}C NMR (126 MHz, CD_3CN) δ 172.91 (s), 168.82 (s), 154.28 (s), 142.68 (s), 137.21 (s), 131.25 (s),
614 130.90 (dd, *J* = 53.2, 20.1 Hz), 130.54 – 130.29 (m), 129.50 (s), 128.86 (d, *J* = 17.9 Hz), 128.08 (s),
615 127.04 (s), 125.67 (s), 123.58 (s), 116.58 (s), 115.83 (s), 67.90 (s), 60.09 (s), 30.12 (s), 24.31 (s), 13.60
616 (s).

617 **Methyl 5-((5-(((6-bromonaphthalen-2-yl) oxy) (4-chlorophenyl) methyl) thiazol-2-yl) amino)**
618 **pentanoate (47)**

619 ^1H NMR (300 MHz, DMSO-*d6*) δ 8.17 (d, *J* = 2.1 Hz, 1H), 7.92 (d, *J* = 9.1 Hz, 1H), 7.52 (dd, *J* = 13.1,
620 5.6 Hz, 2H), 7.29 (d, *J* = 8.5 Hz, 2H), 7.07 (d, *J* = 8.4 Hz, 2H), 6.88 (s, 1H), 6.79 (s, 2H), 6.48 (s, 1H),
621 4.05 (s, 1H), 3.91 (s, 1H), 3.58 (s, 3H), 2.24 (t, *J* = 7.1 Hz, 2H), 2.08 (s, 1H), 1.39 (s, 3H). ESI-MS m/z:
622 560.92 $[M+H]^+$.

623 ^{13}C NMR (101 MHz, DMSO) δ 174.89 (s), 170.71 (s), 155.86 (s), 144.80 (s), 139.62 (s), 132.93 –
624 132.71 (m), 132.34 (d, J = 21.9 Hz), 131.05 (s), 130.52 (d, J = 12.5 Hz), 129.78 (s), 127.78 (s), 126.66
625 (s), 125.40 (s), 117.98 (d, J = 7.5 Hz), 69.96 (s), 53.04 (s), 34.74 (s), 29.89 (s), 22.80 (s).

626 **5-(((6-bromonaphthalen-2-yl) oxy) (4-chlorophenyl) methyl)-*N*-((tetrahydro-2*H*-pyran-4-yl)**
627 **methyl) thiazol-2-amine (48)**

628 ^1H NMR (300 MHz, DMSO-*d6*) δ 8.18 (d, *J* = 2.1 Hz, 1H), 7.92 (d, *J* = 9.1 Hz, 1H), 7.52 (dd, *J* = 14.1,
629 5.6 Hz, 2H), 7.34 – 7.28 (m, 2H), 7.07 (d, *J* = 8.4 Hz, 2H), 6.90 (s, 1H), 6.77 (s, 2H), 6.49 (s, 1H), 3.90
630 (d, *J* = 6.3 Hz, 1H), 3.86 – 3.69 (m, 3H), 3.20 (dd, *J* = 22.7, 11.4 Hz, 2H), 1.51 (d, *J* = 12.6 Hz, 2H),

1.39 (s, 4H), 1.20 (dd, *J* = 24.6, 7.7 Hz, 3H). ESI-MS m/z: 544.96 $[M+H]^+$.

^{13}C NMR (126 MHz, CD_3CN) δ 168.46 (s), 154.50 (s), 140.28 (d, *J* = 639.7 Hz), 137.74 (s), 131.41 – 131.27 (m), 131.02 (s), 130.94 – 130.75 (m), 130.63 (s), 129.43 (s), 128.89 (s), 128.09 (s), 127.41 (s), 125.77 (s), 123.75 (s), 116.54 (s), 116.07 (s), 73.79 (s), 66.97 (s), 39.87 (s), 35.02 (s), 29.43 (d, *J* = 19.3 Hz).

_N_-(5-(((6-bromonaphthalen-2-yl) oxy) (4-chlorophenyl) methyl) thiazol-2-yl) cyclopropanecarboxamide (49)

^1H NMR (500 MHz, DMSO) δ 12.32 (s, 2H), 12.04 (s, 1H), 8.27 (d, *J* = 16.1 Hz, 2H), 7.94 (d, *J* = 9.0 Hz, 1H), 7.67 (d, *J* = 9.0 Hz, 1H), 7.34 (dd, *J* = 11.5, 8.6 Hz, 4H), 7.11 (d, *J* = 8.4 Hz, 2H), 6.67 (s, 1H), 1.39 (s, 4H), 0.90 – 0.73 (m, 11H). ESI-MS m/z: 514.83 $[M+H]^+$.

^{13}C NMR (126 MHz, CD_3CN) δ 172.73 (s), 171.84 (s), 158.28 (s), 141.20 (s), 136.59 (s), 133.46 (s), 132.09 (s), 132.02 – 131.41 (m), 130.88 (s), 130.59 (s), 129.82 (s), 129.55 – 128.88 (m), 128.70 (d, *J* = 12.1 Hz), 128.38 (d, *J* = 7.7 Hz), 126.49 (s), 124.37 (s), 40.25 (s), 13.74 (s), 12.38 (s), 9.09 (d, *J* = 10.2 Hz), 7.97 (s), 7.69 (s).

_N_-(5-(((6-bromonaphthalen-2-yl) oxy) (4-chlorophenyl) methyl) thiazol-2-yl) hexanamide (50)

^1H NMR (300 MHz, Chloroform-*d*) δ 11.43 (s, 1H), 8.02 (d, *J* = 2.0 Hz, 1H), 7.83 (d, *J* = 9.3 Hz, 1H), 7.74 (d, *J* = 8.9 Hz, 1H), 7.48 (dd, *J* = 9.2, 2.0 Hz, 1H), 7.29 – 7.18 (m, 4H), 7.13 (d, *J* = 8.3 Hz, 3H), 6.37 (s, 1H), 2.37 (t, *J* = 7.5 Hz, 3H), 2.17 (dt, *J* = 16.2, 7.5 Hz, 1H), 1.61 (dp, *J* = 22.6, 7.5 Hz, 7H), 1.40 – 1.14 (m, 11H), 0.86 (q, *J* = 7.0 Hz, 7H). ESI-MS m/z: 544.90 $[M+H]^+$.

^{13}C NMR (101 MHz, DMSO) δ 172.91 (d, J = 19.5 Hz), 159.89 (s), 148.66 (s), 143.26 (s), 138.57 (s), 134.99 (s), 132.83 (d, J = 11.8 Hz), 132.48 (s), 132.17 (s), 131.54 (s), 130.95 (s), 130.65 (s), 130.15 (s), 128.53 (s), 126.27 (s), 120.73 (s), 36.54 (s), 34.74 (s), 32.44 (d, J = 15.6 Hz), 26.18 (s), 25.36 (s), 23.63 (s), 15.58 (s).

_N_-(5-(((6-bromonaphthalen-2-yl)oxy)(4-chlorophenyl)methyl)thiazol-2-yl)pivalamide (51)

^1H NMR (500 MHz, DMSO) δ 11.63 (s, 1H), 10.24 (s, 1H), 8.09 (d, J = 2.1 Hz, 1H), 7.79 (t, J = 14.5 Hz, 1H), 7.46 (d, J = 9.0 Hz, 1H), 7.32 (t, J = 6.0 Hz, 3H), 7.24 (d, J = 8.9 Hz, 1H), 7.17 (d, J = 8.5 Hz, 2H), 6.60 (s, 1H), 1.39 (s, 4H), 1.18 (s, 9H). ESI-MS m/z: 530.88 $[M+H]^+$

^{13}C NMR (126 MHz, CD_3CN) δ 169.75 (s), 157.76 (s), 152.90 (s), 141.69 (s), 136.11 (s), 132.86 (s),

132.14 (s), 131.73 (d, *J* = 9.8 Hz), 131.50 (s), 131.26 (s), 130.74 (d, *J* = 9.0 Hz), 129.44 (s), 128.87 (dd, *J* = 36.1, 24.0 Hz), 128.18 (s), 126.00 (s), 48.49 (s), 28.85 (s).

_N_-(5-(((6-bromonaphthalen-2-yl) oxy) (4-chlorophenyl) methyl) thiazol-2-yl)-2-ethylbutanamide (52)

^{1}H NMR (500 MHz, DMSO) δ 8.25 (d, *J* = 2.1 Hz, 1H), 8.12 – 8.07 (m, 1H), 7.90 (d, *J* = 9.0 Hz, 1H), 7.61 (dd, *J* = 9.1, 2.0 Hz, 1H), 7.31 (dd, *J* = 8.7, 3.7 Hz, 3H), 7.11 (d, *J* = 8.5 Hz, 2H), 6.83 (d, *J* = 2.1 Hz, 3H), 6.40 (s, 1H), 3.33 (s, 19H), 1.39 (s, 8H), 1.23 (s, 1H), 1.09 (t, *J* = 7.0 Hz, 4H), 1.03 – 0.95 (m, 5H). ESI-MS m/z:546.00 $[M+H]^{+}$.

^{13}C NMR (126 MHz, CD_3CN) δ 168.67 (s), 152.93 (s), 147.94 (s), 141.42 (s), 137.52 (s), 133.25 (s), 131.63 (s), 130.68 (d, *J* = 26.4 Hz), 130.57 – 130.03 (m), 129.49 (s), 129.11 (d, *J* = 17.6 Hz), 128.12 (d, *J* = 18.8 Hz), 126.66 (s), 124.69 (s), 41.94 (s), 41.65 (s), 40.45 (s), 13.59 (s), 12.58 (s).

_N_-(5-(((6-bromonaphthalen-2-yl) oxy) (4-chlorophenyl) methyl) thiazol-2-yl) tetrahydrofuran-2-carboxamide (53)

^{1}H NMR (400 MHz, DMSO-d_6) δ 8.06 (d, *J* = 2.1 Hz, 1H), 7.89 (s, 1H), 7.75 (d, *J* = 8.9 Hz, 1H), 7.44 (dd, *J* = 9.2, 1.7 Hz, 1H), 7.34 – 7.27 (m, 3H), 7.22 (d, *J* = 8.9 Hz, 1H), 7.14 (d, *J* = 8.5 Hz, 2H), 6.58 (s, 1H), 4.45 (ddd, *J* = 7.1, 5.0, 1.8 Hz, 1H), 4.27 (dd, *J* = 8.4, 4.8 Hz, 0H), 4.01 (q, *J* = 7.1 Hz, 1H), 3.89 (qd, *J* = 6.9, 4.6 Hz, 1H), 3.82 – 3.70 (m, 2H), 2.18 – 2.07 (m, 1H), 1.96 (s, 1H), 1.91 – 1.74 (m, 4H). ESI-MS m/z:544.86 $[M+H]^{+}$.

^{13}C NMR (101 MHz, DMSO) δ 173.22 (s), 155.15 (s), 138.19 (s), 134.63 (s), 132.27 (s), 131.06 (s), 130.83 (s), 130.46 (s), 129.90 (s), 127.44 (s), 121.56 (s), 117.12 (s), 78.63 (s), 77.73 (s), 70.72 (s), 70.08 (s), 31.71 (s), 26.94 (s).

_N_-(5-(((6-bromonaphthalen-2-yl) oxy) (4-chlorophenyl) methyl) thiazol-2-yl) tetrahydro-2*H*-pyran-4-carboxamide (54)

^{1}H NMR (400 MHz, DMSO-*d6*) δ8.11 (d, *J* = 2.0 Hz, 1H), 8.00 (d, *J* = 8.5 Hz, 1H), 7.92 (s, 1H), 7.80 (d, *J* = 8.9 Hz, 1H), 7.74 (d, *J* = 8.3 Hz, 1H), 7.57 (t, *J* = 7.6 Hz, 1H), 7.53 – 7.41 (m, 2H), 7.40 – 7.32 (m, 3H), 7.27 (d, *J* = 8.9 Hz, 1H), 7.19 (d, *J* = 8.4 Hz, 2H), 6.62 (s, 1H), 3.96 – 3.79 (m, 3H), 2.78 – 2.65 (m, 1H), 2.28 (t, *J* = 6.6 Hz, 1H), 2.02 (s, 1H), 1.84 – 1.51 (m, 7H), 1.26 (s, 1H), 1.20 (dd, *J* = 13.0, 5.9 Hz, 1H). ESI-MS m/z: 559 $[M+H]^{+}$.

^{13}C NMR (101 MHz, DMSO) δ 174.53 (s), 159.58 (s), 155.14 (s), 143.82 (s), 138.08 (s), 134.11 (s),

132.92 (s), 132.32 (d, *J* = 11.1 Hz), 131.80 (s), 131.04 (s), 130.79 (s), 130.42 (s), 129.89 (s), 127.51 (s), 121.91 (s), 121.54 (s), 121.02 (s), 117.10 (s), 68.02 (s), 30.32 (d, *J* = 9.9 Hz), 28.26 (s).

_N_-(5-(((6-bromonaphthalen-2-yl)oxy)(4-chlorophenyl)methyl)thiazol-2-yl)benzamide (55)

^{1}H NMR (500 MHz, MeOD) δ 8.03 – 8.00 (m, 1H), 7.96 – 7.93 (m, 3H), 7.80 (d, *J* = 8.9 Hz, 1H), 7.69 (d, *J* = 8.9 Hz, 1H), 7.58 (d, *J* = 7.4 Hz, 1H), 7.49 (t, *J* = 7.7 Hz, 2H), 7.47 – 7.43 (m, 1H), 7.37 (dd, *J* = 9.2, 1.9 Hz, 1H), 7.27 – 7.23 (m, 5H), 7.21 (d, *J* = 8.9 Hz, 1H), 6.68 (s, 1H), 1.45 (s, 9H). ESI-MS m/z: 549.87 $[M+H]^{+}$.

^{13}C NMR (101 MHz, CD_3CN) δ 166.79 (s), 160.35 (s), 154.28 (s), 142.68 (s), 137.37 (s), 134.84 (s), 134.26 (s), 134.26 – 133.61 (m), 132.98 (s), 132.65 (s), 132.12 (d, *J* = 8.1 Hz), 130.92 (s), 130.56 (s), 130.31 (s), 129.88 (d, *J* = 10.9 Hz), 129.59 (s), 129.20 (s), 127.32 (s), 121.73 (s), 120.87 (s), 117.40 (s), 40.67 (s).

_N_-(5-(((6-bromonaphthalen-2-yl) oxy) (4-chlorophenyl) methyl) thiazol-2-yl)-4-methylbenzamide (56)

^{1}H NMR (500 MHz, DMSO) δ 12.40 (s, 1H), 10.28 (s, 1H), 8.09 (d, *J* = 2.1 Hz, 1H), 7.92 (d, *J* = 8.2 Hz, 3H), 7.77 (d, *J* = 8.9 Hz, 1H), 7.61 (dd, *J* = 12.2, 7.3 Hz, 8H), 7.57 – 7.49 (m, 5H), 7.47 (d, *J* = 8.6 Hz, 1H), 7.36 (s, 1H), 7.31 (dd, *J* = 11.2, 8.4 Hz, 4H), 7.24 (d, *J* = 9.0 Hz, 1H), 7.19 (d, *J* = 8.5 Hz, 2H), 6.63 (s, 1H), 2.35 (s, 3H). ESI-MS m/z: 562.67 $[M-H]^{+}$.

^{13}C NMR (101 MHz, CD_3CN) δ 166.36 (s), 159.98 (s), 154.54 (s), 144.88 (s), 142.91 (s), 137.48 (s), 134.88 (s), 134.44 (s), 133.85 – 133.13 (m), 133.13 – 132.58 (m), 132.06 (s), 130.97 (s), 130.93 – 130.22 (m), 130.09 (d, J = 12.0 Hz), 129.55 (s), 129.26 (s), 127.30 (s), 121.76 (s), 120.96 (s), 117.25 (s), 21.97 (s).

_N_-(5-(((6-bromonaphthalen-2-yl) oxy) (4-chlorophenyl) methyl) thiazol-2-yl)-4-methoxybenzamide (57)

^{1}H NMR (500 MHz, DMSO-*d6*) δ 8.08 (d, *J* = 1.7 Hz, 1H), 8.02 (d, *J* = 8.8 Hz, 3H), 7.92 (s, 1H), 7.77 (d, *J* = 8.9 Hz, 1H), 7.45 (d, *J* = 8.3 Hz, 3H), 7.36 (s, 1H), 7.27 (s, 1H), 7.24 (d, J = 9.0 Hz, 1H), 7.21 (d, *J* = 7.5 Hz, 1H), 7.13 (d, *J* = 8.3 Hz, 2H), 7.02 (d, *J* = 8.8 Hz, 3H), 6.60 (s, 1H), 3.81 (s, 4H). ESI-MS m/z: 579.89 $[M+H]^{+}$.

^{13}C NMR (101 MHz, DMSO) δ 166.27 (s), 164.56 (s), 160.68 (s), 158.07 (s), 157.55 (s), 141.35 (s), 134.96 (s), 134.03 (d, *J* = 21.5 Hz), 133.61 (d, *J* = 10.4 Hz), 133.36 – 133.02 (m), 132.05 (s), 131.61 (s),

130.87 (s), 130.73 – 130.72 (m), 130.42 (d, *J* = 33.5 Hz), 129.82 (s), 129.44 (s), 129.02 (s), 128.56 (s), 128.13 (s), 125.83 (s), 115.71 (s), 57.34 (s), 49.29 (s), 28.18 (s), 15.72 (s), 15.25 (s).

_N_-(5-(((6-bromonaphthalen-2-yl) oxy) (4-chlorophenyl) methyl) thiazol-2-yl)-4-fluorobenzamide (58)

^{1}H NMR (500 MHz, Methanol-d_4) δ 8.09 – 8.05 (m, 1H), 8.03 (dd, *J* = 8.8, 5.3 Hz, 2H), 7.96 (d, *J* = 2.0 Hz, 1H), 7.81 (d, *J* = 8.8 Hz, 1H), 7.69 (d, *J* = 8.9 Hz, 1H), 7.41 – 7.36 (m, 1H), 7.25 (s, 5H), 7.23 (d, *J* = 8.8 Hz, 2H), 7.21 – 7.17 (m, 1H), 6.68 (s, 1H). ESI-MS m/z: 568.86 $[M+H]^+$.

^{13}C NMR (101 MHz, CD_3CN) δ 163.91 (s), 152.53 (s), 142.75 (s), 141.56 (s), 139.27 (s), 135.04 (s), 133.01 (s), 132.23 (d, *J* = 12.3 Hz), 131.46 (s), 130.57 (s), 129.88 (s), 129.63 (s), 127.76 (s), 125.57 (d, *J* = 15.5 Hz), 120.91 (s), 42.08 (s).

4-bromo-N-(5-(((6-bromonaphthalen-2-yl) oxy) (4-chlorophenyl) methyl) thiazol-2-yl) benzamide (59)

^{1}H NMR (500 MHz, Methanol-d_4) δ 7.95 (d, *J* = 2.1 Hz, 1H), 7.87 (d, *J* = 8.6 Hz, 2H), 7.80 (d, *J* = 9.2 Hz, 1H), 7.68 (t, *J* = 8.3 Hz, 3H), 7.37 (dd, *J* = 9.2, 2.2 Hz, 1H), 7.25 (s, 5H), 7.22 (s, 1H), 7.20 (s, 1H), 6.68 (s, 1H). ESI-MS m/z: 629.76 $[M+H]^+$.

^{13}C NMR (101 MHz, CD_3CN) δ 165.79 (s), 159.96 (s), 154.24 (s), 142.71 (s), 137.36 (s), 135.11 (s), 133.05 (d, *J* = 13.9 Hz), 132.64 (s), 132.12 (s), 131.12 (s), 130.87 (s), 130.59 (s), 130.35 (s), 129.60 (s), 128.14 (s), 127.27 (s), 121.79 (s), 120.85 (s), 117.42 (s), 40.69 (s).

_N_-(5-(((6-bromonaphthalen-2-yl) oxy) (4-chlorophenyl) methyl) thiazol-2-yl)-2,4-difluorobenzamide (60)

^{1}H NMR (500 MHz, Methanol-d_4) δ 7.96 (d, *J* = 2.1 Hz, 1H), 7.86 (dd, *J* = 8.6, 6.5 Hz, 1H), 7.83 – 7.78 (m, 1H), 7.69 (d, *J* = 8.9 Hz, 1H), 7.38 (dd, *J* = 9.2, 1.7 Hz, 1H), 7.28 – 7.23 (m, 5H), 7.21 (d, *J* = 8.9 Hz, 1H), 7.16 – 7.11 (m, 1H), 7.11 – 7.08 (m, 1H), 6.68 (s, 1H). ESI-MS m/z: 586.85 $[M+H]^+$.

^{13}C NMR (101 MHz, CD_3CN) δ 162.19 (s), 158.95 (s), 154.22 (s), 142.71 (s), 137.60 (s), 135.45 (s), 134.19 (d, *J* = 13.6 Hz), 133.00 (s), 132.62 (s), 132.14 (d, *J* = 5.9 Hz), 130.73 (d, *J* = 24.4 Hz), 130.59 – 130.48 (m), 130.36 (s), 129.59 (s), 127.26 (s), 121.76 (s), 120.84 (s), 117.43 (s), 113.64 (d, *J* = 21.7 Hz),

113.51 – 113.33 (m), 106.58 – 106.30 (m), 106.29 (s), 106.02 (t, *J* = 26.7 Hz), 40.68 (s).

2-Bromo-*N*-(5-(((6-bromonaphthalen-2-yl) oxy) (4-chlorophenyl) methyl) thiazol-2-yl)-4-fluorobenzamide (61)

^{1}H NMR (400 MHz, DMSO-*d6*) δ 8.13 (d, *J* = 2.1 Hz, 1H), 8.02 (s, 1H), 7.82 (d, *J* = 8.9 Hz, 1H), 7.70 (dd, *J* = 8.7, 2.5 Hz, 1H), 7.67 (s, 1H), 7.57 – 7.49 (m, 1H), 7.45 (s, 1H), 7.40 – 7.35 (m, 3H), 7.29 (d, *J* = 8.9 Hz, 1H), 7.22 (d, *J* = 8.5 Hz, 2H), 6.68 (s, 1H). FTMS-cESI m/z: 644.88861 $[M-H]^{-}$.

^{13}C NMR (126 MHz, CD_3CN) δ 164.68 (s), 164.10 (s), 162.09 (s), 158.21 (s), 152.84 (s), 141.06 (s), 135.45 (s), 134.18 (s), 132.92 (s), 131.71 (s), 131.40 – 130.95 (m), 130.81 (s), 129.77 – 129.58 (m), 129.39 (d, *J* = 23.8 Hz), 129.09 (s), 128.26 (s), 125.80 (s), 120.60 (s), 120.26 (dd, *J* = 20.9, 10.8 Hz), 119.43 (s), 116.09 (s), 115.86 – 115.17 (m), 114.98 (d, *J* = 21.8 Hz).

***N*-(5-(((6-bromonaphthalen-2-yl) oxy) (4-chlorophenyl) methyl) thiazol-2-yl)-2,4,5-trifluorobenzamide (62)**

^{1}H NMR (400 MHz, DMSO-d_6) δ 10.33 (s, 1H), 8.07 (d, *J* = 2.1 Hz, 1H), 7.94 (s, 0H), 7.85 – 7.78 (m, 1H), 7.77 (d, *J* = 8.8 Hz, 1H), 7.66 (td, *J* = 10.2, 6.5 Hz, 1H), 7.47 (d, *J* = 9.1 Hz, 1H), 7.38 (s, 1H), 7.31 (d, *J* = 8.5 Hz, 2H), 7.23 (d, *J* = 8.9 Hz, 1H), 7.17 (d, *J* = 8.5 Hz, 3H), 6.61 (s, 1H). ESI-MS m/z: 604.84 $[M+H]^{+}$.

^{13}C NMR (126 MHz, CD_3CN) δ 159.83 (s), 157.42 (s), 152.87 (s), 141.35 (s), 136.25 (s), 134.29 (s), 131.62 (s), 131.24 (s), 130.75 (s), 129.64 – 129.54 (m), 129.36 (d, *J* = 24.0 Hz), 129.02 (s), 128.23 (s), 125.87 (s), 120.35 (s), 119.44 (s), 118.92 (d, *J* = 21.2 Hz), 118.82 – 118.63 (m), 116.06 (s), 107.24 – 106.78 (m), 106.64 (s), 106.63 – 106.45 (m).

***N*-(5-(((6-bromonaphthalen-2-yl) oxy) (4-chlorophenyl) methyl) thiazol-2-yl)-3-cyanobenzamide (63)**

^{1}H NMR (500 MHz, DMSO-*d6*) δ 8.49 (s, 1H), 8.32 (d, *J* = 8.1 Hz, 1H), 8.14 (d, *J* = 2.1 Hz, 1H), 8.10 (d, *J* = 7.7 Hz, 1H), 8.00 (d, *J* = 8.3 Hz, 1H), 7.83 (d, *J* = 8.9 Hz, 1H), 7.77 (t, *J* = 7.9 Hz, 1H), 7.53 (d, *J* = 8.3 Hz, 1H), 7.46 (s, 1H), 7.38 (d, *J* = 8.5 Hz, 2H), 7.29 (d, *J* = 8.9 Hz, 1H), 7.23 (d, *J* = 8.5 Hz, 3H), 6.68 (s, 1H). ESI-MS m/z: 576 $[M+H]^{+}$.

^{13}C NMR (126 MHz, CD_3CN) δ 163.73 (s), 158.49 (s), 152.86 (s), 141.34 (s), 135.74 (d, *J* = 12.5 Hz), 133.88 (d, *J* = 7.1 Hz), 132.24 (s), 131.83 (s), 131.62 (s), 131.26 (s), 130.74 (s), 129.73 (s), 129.50 (s), 129.13 (d, *J* = 31.3 Hz), 128.99 – 128.73 (m), 128.25 (s), 125.94 (s), 120.36 (s), 119.45 (s), 116.07 (s),

112.57 (s).

_N_-(5-(((6-bromonaphthalen-2-yl)oxy)(4-chlorophenyl)methyl)thiazol-2-yl)-3,5-dimethylisoxazole-4-carboxamide (64)

^{1}H NMR (500 MHz, DMSO) δ 13.86 (s, 1H), 10.39 (s, 1H), 8.10 (d, J = 2.1 Hz, 1H), 7.80 (d, J = 8.9 Hz, 1H), 7.54 – 7.47 (m, 2H), 7.32 (d, J = 8.5 Hz, 2H), 7.23 (d, J = 8.9 Hz, 1H), 7.18 (d, J = 8.5 Hz, 2H), 6.56 (s, 1H), 6.30 (dd, J = 17.3, 1.5 Hz, 1H), 6.20 – 6.13 (m, 1H), 5.92 (dd, J = 10.3, 1.5 Hz, 1H), 4.01 (q, J = 7.1 Hz, 2H), 1.97 (s, 3H), 1.16 (t, J = 7.1 Hz, 3H). ESI-MS m/z:569.87 $[M+H]^{+}$.

^{13}C NMR (101 MHz, DMSO) δ 172.95 (s), 155.19 (s), 132.36 (d, *J* = 14.0 Hz), 131.06 (s), 130.52 (s), 129.92 (s), 121.60 (s), 117.14 (s), 61.58 (s), 15.92 (s), 14.27 (s), 13.14 (s), 12.44 (s).

_N_-(5-(((6-bromonaphthalen-2-yl)oxy)(4-chlorophenyl)methyl)thiazol-2-yl)-6-chloronicotinamide (65)

^{1}H NMR (500 MHz, MeOD) δ 8.94 (d, J = 2.4 Hz, 1H), 8.31 (dd, J = 8.4, 2.5 Hz, 1H), 7.94 (d, J = 2.1 Hz, 1H), 7.80 (d, J = 9.0 Hz, 1H), 7.68 (d, J = 8.9 Hz, 1H), 7.56 (d, J = 8.4 Hz, 1H), 7.37 (dd, J = 9.2, 1.8 Hz, 1H), 7.25 (s, 4H), 7.22 (d, J = 5.8 Hz, 2H), 7.19 (d, J = 5.0 Hz, 1H), 7.14 (d, J = 7.5 Hz, 1H), 7.10 (t, J = 7.3 Hz, 1H), 6.65 (s, 1H), 2.31 (s, 1H), 2.15 (s, 1H). ESI-MS m/z:586.30 $[M+H]^{+\cdot}$

^{13}C NMR (101 MHz, DMSO) δ 155.22 (s), 151.58 (s), 143.58 (s), 141.14 (s), 133.00 (s), 132.39 (d, *J* = 18.0 Hz), 131.79 (s), 131.46 – 130.33 (m), 129.94 (s), 127.39 (s), 126.07 (s), 121.60 (s), 117.15 (s).

***(2S,3R,4R,5S)*-6-((5-(((6-bromonaphthalen-2-yl) oxy) (4-chlorophenyl) methyl) thiazol-2-yl) carbamoyl) tetrahydro-2*H*-pyran-2,3,4,5-tetrayl tetraacetate (66)**

^{1}H NMR (300 MHz, Chloroform-*d*) δ 8.12 (s, 1H), 8.01 (d, *J* = 2.1 Hz, 1H), 7.87 (d, *J* = 9.2 Hz, 1H), 7.74 (d, *J* = 8.9 Hz, 1H), 7.49 (dd, *J* = 9.2, 2.1 Hz, 1H), 7.26 (d, *J* = 4.5 Hz, 5H), 7.21 (d, *J* = 2.1 Hz, 1H), 7.15 (d, *J* = 8.3 Hz, 2H), 7.09 (d, *J* = 0.8 Hz, 1H), 6.30 (s, 1H), 5.77 (d, *J* = 7.8 Hz, 1H), 5.36 – 5.10 (m, 4H), 4.23 – 4.07 (m, 2H), 3.75 (s, 3H), 3.04 (d, *J* = 7.6 Hz, 6H), 2.14 – 2.10 (m, 5H), 2.06 – 2.01 (m, 12H), 1.44 (d, *J* = 7.3 Hz, 1H), 1.37 (s, 2H), 1.30 – 1.23 (m, 8H). ESI-MS m/z:791.03 $[M+H]^{+}$.

^{13}C NMR (126 MHz, CD_3CN) δ 169.73 (s), 169.32 (d, *J* = 8.6 Hz), 168.90 (s), 164.33 (s), 152.81 (s), 141.39 (s), 136.48 (d, *J* = 16.3 Hz), 134.33 (s), 131.60 (s), 131.24 (s), 130.74 (s), 129.79 – 129.02 (m), 129.00 (s), 128.31 (d, *J* = 22.6 Hz), 127.70 (s), 125.85 (s), 119.45 (s), 116.09 (s), 110.00 (s), 91.09 (s), 72.83 (d, *J* = 8.3 Hz), 71.29 (s), 69.65 (d, *J* = 25.6 Hz), 68.63 (d, *J* = 7.9 Hz), 39.28 (s), 27.32 (s), 19.91

(d, *J* = 21.9 Hz).

***N*-(5-((4-chlorophenyl)(naphthalen-1-ylamino)methyl)thiazol-2-yl)-4-methoxybenzamide (67)**

^{1}H NMR (400 MHz, DMSO) δ 12.32 (s, 1H), 8.10 (d, *J* = 7.9 Hz, 1H), 8.03 (d, *J* = 8.8 Hz, 2H), 7.95 (d, *J* = 8.3 Hz, 1H), 7.41 – 7.33 (m, 4H), 7.26 (d, *J* = 8.4 Hz, 2H), 7.03 (d, *J* = 8.8 Hz, 2H), 6.98 (s, 1H), 6.85 (d, *J* = 7.9 Hz, 1H), 6.63 (d, *J* = 7.9 Hz, 1H), 6.38 (s, 1H), 5.72 (s, 2H), 3.82 (s, 3H), 2.08 (s, 1H), 1.39 (s, 3H), 1.23 (s, 1H). FTMS-cESI m/z: 498.10519 $[M-H]^-$.

^{13}C NMR (101 MHz, CD_3CN) δ 165.92 (s), 164.58 (s), 159.99 (s), 144.85 (s), 144.06 (s), 137.44 (s), 137.12 (s), 133.31 (d, *J* = 9.1 Hz), 131.75 (s), 131.27 (s), 129.83 (s), 129.05 (s), 128.73 (s), 127.52 (s), 125.91 (s), 125.68 (s), 125.63 – 125.45 (m), 125.28 (d, *J* = 21.1 Hz), 123.58 (s), 115.23 (s), 109.19 (s), 56.69 (s).

***N*-(5-((4-chlorophenyl)(naphthalen-2-ylthio)methyl)thiazol-2-yl)-4-methoxybenzamide (68)**

^{1}H NMR (400 MHz, DMSO) δ 12.37 (s, 1H), 8.04 (d, *J* = 8.7 Hz, 2H), 7.93 (s, 1H), 7.83 (t, *J* = 8.4 Hz, 2H), 7.80 – 7.76 (m, 1H), 7.59 (d, *J* = 8.4 Hz, 2H), 7.52 (d, *J* = 8.8 Hz, 1H), 7.49 – 7.46 (m, 2H), 7.42 (d, *J* = 8.4 Hz, 2H), 7.35 (s, 1H), 7.04 (d, *J* = 8.8 Hz, 2H), 6.36 (s, 1H), 3.82 (s, 3H), 1.39 (s, 3H). ESI-MS m/z: 517.06 $[M+H]^+$.

^{13}C NMR (101 MHz, DMSO) δ 164.56 (s), 141.35 (s), 134.96 (s), 134.03 (d, *J* = 21.5 Hz), 133.61 (d, *J* = 10.4 Hz), 133.36 – 133.02 (m), 132.05 (s), 131.61 (s), 130.87 (s), 130.73 – 130.72 (m), 130.42 (d, *J* = 33.5 Hz), 129.82 (s), 129.44 (s), 129.02 (s), 128.56 (s), 128.13 (s), 115.71 (s), 57.34 (s).

***N*-(5-(((6-bromonaphthalen-2-yl)oxy)(4-chlorophenyl)methyl)thiazol-2-yl)thiophene-2-sulfonamide (69)**

^{1}H NMR (500 MHz, MeOD) δ 7.98 (dd, *J* = 5.2, 1.5 Hz, 2H), 7.94 (dd, *J* = 3.9, 1.4 Hz, 1H), 7.88 (d, *J* = 9.2 Hz, 1H), 7.73 (d, *J* = 8.9 Hz, 1H), 7.68 (dd, *J* = 5.0, 1.3 Hz, 1H), 7.49 (dd, *J* = 3.7, 1.3 Hz, 1H), 7.46 (dd, *J* = 9.2, 2.0 Hz, 1H), 7.32 (d, *J* = 1.2 Hz, 1H), 7.29 (d, *J* = 5.8 Hz, 4H), 7.19 (d, *J* = 8.9 Hz, 1H), 7.10 (dd, *J* = 4.9, 4.0 Hz, 1H), 7.03 (dd, *J* = 5.0, 3.8 Hz, 1H), 6.34 (s, 1H), 2.16 (s, 6H), 1.45 (s, 1H), 1.34 (s, 1H), 1.30 (s, 3H), 1.28 (s, 2H). ESI-MS m/z: 591.95 $[M+H]^+$

^{13}C NMR (101 MHz, CD_3CN) δ 166.03 (s), 154.53 (s), 142.75 (s), 140.13 (s), 139.60 (d, *J* = 5.1 Hz), 135.37 (s), 133.91 (s), 133.69 (s), 133.27 (s), 132.71 (s), 132.31 (t, *J* = 35.9 Hz), 131.66 – 130.70 (m), 129.87 (s), 129.49 (s), 128.69 (s), 127.58 (s), 126.39 (s), 121.94 (s), 120.92 (s).

_N_-(5-(((6-bromonaphthalen-2-yl) oxy) (4-chlorophenyl) methyl) thiazol-2-yl) benzenesulfonamide (70)

^{1}H NMR (500 MHz, MeOD) δ 8.00 (d, J = 2.1 Hz, 1H), 7.91 (dd, *J* = 8.5, 1.0 Hz, 2H), 7.74 (d, *J* = 8.9 Hz, 1H), 7.65 (t, *J* = 7.5 Hz, 1H), 7.59 – 7.54 (m, 3H), 7.47 – 7.46 (m, 1H), 7.45 (s, 1H), 7.43 (d, *J* = 2.9 Hz, 1H), 7.41 (s, 1H), 7.34 (d, *J* = 1.3 Hz, 1H), 7.31 (s, 3H), 7.24 – 7.18 (m, 3H), 7.15 (d, *J* = 7.4 Hz, 2H), 7.11 (t, *J* = 7.2 Hz, 1H), 6.35 (s, 1H), 4.58 (s, 1H), 2.16 (s, 8H). FTMS-c ESI m/z: 584.95402[M-H] $^{-}$.

^{13}C NMR (101 MHz, DMSO) δ 154.01 (s), 136.23 (s), 133.33 (s), 131.59 (s), 130.97 (s), 130.33 – 129.17 (m), 128.76 (s), 128.03 (s), 126.41 – 125.83 (m), 125.19 (s), 121.10 (s), 120.23 (s), 116.15 (s).

_N_-(5-(((6-bromonaphthalen-2-yl)oxy)(4-chlorophenyl)methyl)thiazol-2-yl)-2,5-dimethyl-benzenesulfonamide(71)

^{1}H NMR (500 MHz, MeOD) δ 8.01 (d, *J* = 2.1 Hz, 1H), 7.91 (d, *J* = 9.2 Hz, 1H), 7.75 (d, *J* = 8.9 Hz, 1H), 7.72 (s, 1H), 7.59 (s, 1H), 7.49 (dd, *J* = 9.2, 2.0 Hz, 1H), 7.34 (dd, *J* = 6.7, 1.9 Hz, 5H), 7.26 (d, *J* = 7.5 Hz, 2H), 7.21 (d, *J* = 8.9 Hz, 1H), 7.16 (d, *J* = 7.8 Hz, 1H), 7.07 (d, *J* = 7.7 Hz, 1H), 6.38 (s, 1H), 2.32 (d, *J* = 7.2 Hz, 6H), 2.07 (d, *J* = 15.7 Hz, 6H), 1.46 (s, 13H). ESI-MS m/z: 613.97 [M+H] $^{+}$.

^{13}C NMR (101 MHz, CD_3CN) δ 164.54 (s), 154.60 (s), 138.05 (s), 137.49 (s), 137.29 (s), 136.47 (s), 135.52 (s), 134.80 (d, *J* = 18.6 Hz), 133.79 (dd, *J* = 21.9, 14.8 Hz), 132.74 (s), 132.22 (s), 132.00 (s), 131.07 (d, *J* = 11.5 Hz), 129.93 (s), 129.41 (s), 127.19 (s), 126.38 (s), 121.71 (s), 120.94 (s), 21.14 (d, *J* = 17.5 Hz), 20.12 (s), 19.85 (s).

_N_-(5-(((6-bromonaphthalen-2-yl)oxy)(4-chlorophenyl)methyl)thiazol-2-yl)-4-ethylbenzene-sulfonamide (72)

1H NMR (500 MHz, MeOD) δ 7.98 (d, J = 2.1 Hz, 1H), 7.89 – 7.83 (m, 1H), 7.81 (d, J = 8.4 Hz, 2H), 7.72 (d, J = 8.9 Hz, 1H), 7.48 (d, J = 8.3 Hz, 2H), 7.45 (dd, J = 9.1, 2.0 Hz, 1H), 7.31 – 7.28 (m, 5H), 7.25 (dd, J = 8.1, 6.7 Hz, 4H), 7.18 (d, J = 8.9 Hz, 1H), 6.33 (s, 1H), 1.29 (dd, J = 5.4, 2.5 Hz, 2H), 1.23 (dd, J = 7.6, 3.8 Hz, 4H). ESI-MS m/z: 613.99 [M+H] $^{+}$.

^{13}C NMR (101 MHz, CD_3CN) δ 165.30 (s), 154.50 (s), 151.23 (s), 140.11 (s), 139.44 (s), 133.72 (d, *J* = 11.0 Hz), 132.70 (s), 132.13 (d, *J* = 18.8 Hz), 131.00 (dd, *J* = 17.9, 12.5 Hz), 130.00 (s), 129.74 (d, *J* = 23.1 Hz), 127.66 (s), 126.94 (s), 126.51 (s), 121.78 (s), 120.91 (s), 29.77 (d, *J* = 16.3 Hz), 15.86 (s), 15.57 (s).

_N_-(5-(((6-bromonaphthalen-2-yl)oxy)(4-chlorophenyl)methyl)thiazol-2-yl)-4-chloro-benzenesulfonamide(73)

^{1}H NMR (500 MHz, MeOD) δ 8.00 (d, *J* = 2.1 Hz, 1H), 7.91 (d, *J* = 9.1 Hz, 1H), 7.87 – 7.83 (m, 2H), 7.75 (d, *J* = 8.9 Hz, 1H), 7.54 – 7.51 (m, 2H), 7.50 (dd, *J* = 9.2, 2.0 Hz, 1H), 7.46 – 7.40 (m, 4H), 7.35 (d, *J* = 1.2 Hz, 1H), 7.31 (s, 4H), 7.21 (s, 1H), 7.15 (d, *J* = 7.5 Hz, 1H), 6.36 (s, 1H), 2.32 (s, 1H), 2.15 (s, 1H). ESI-MS m/z:629.36 $[M+H]^{+}$.

^{13}C NMR (101 MHz, CD_3CN) δ 166.00 (s), 154.52 (s), 143.04 (s), 140.96 (s), 140.08 (d, *J* = 7.6 Hz), 135.23 (s), 133.69 (s), 132.73 (s), 132.26 (d, *J* = 6.5 Hz), 132.02 (s), 131.11 (d, *J* = 12.3 Hz), 130.78 – 130.77 (m), 130.60 (d, *J* = 23.4 Hz), 129.87 (s), 129.04 (s), 127.44 (s), 126.46 (s), 121.62 (s), 120.95 (s), 41.76 (s).

_N_-(5-(((6-bromonaphthalen-2-yl) oxy) (4-chlorophenyl) methyl) thiazol-2-yl)-6-chloropyridine-3-sulfonamide (74)

^{1}H NMR (400 MHz, DMSO-d_6) δ 8.70 (d, *J* = 2.5 Hz, 1H), 8.12 (d, *J* = 2.5 Hz, 1H), 8.10 (d, *J* = 2.3 Hz, 1H), 8.03 (s, 1H), 7.79 (d, *J* = 8.9 Hz, 1H), 7.64 (d, *J* = 8.4 Hz, 1H), 7.55 – 7.47 (m, 1H), 7.31 (d, *J* = 8.5 Hz, 2H), 7.22 (d, *J* = 8.9 Hz, 1H), 7.19 – 7.10 (m, 3H), 6.40 (s, 1H), 1.97 (s, 2H). ESI-MS m/z: 622.35 $[M+H]^{+}$.

^{13}C NMR (126 MHz, CD_3CN) δ 147.17 (s), 136.98 (s), 130.80 (s), 129.54 (s), 128.36 (s), 127.42 (s), 124.59 (s), 121.59 (s).

_N_-(5-(((6-bromonaphthalen-2-yl)oxy)(4-chlorophenyl)methyl)thiazol-2-yl)-2,3-dihydrobenzofuran-5-sulfonamide (75)

^{1}H NMR (500 MHz, DMSO) δ 10.49 (s, 1H), 8.23 – 8.09 (m, 1H), 7.86 – 7.76 (m, 1H), 7.74 – 7.51 (m, 2H), 7.42 – 7.11 (m, 3H), 6.80 (dd, *J* = 28.0, 8.3 Hz, 1H), 6.45 (s, 1H), 4.02 (q, *J* = 7.1 Hz, 1H), 3.18 – 3.07 (m, 2H). ESI-MS m/z: 627.96 $[M+H]^{+}$.

^{13}C NMR (101 MHz, DMSO) δ 167.47 (s), 165.10 (s), 155.42 (s), 134.02 (s), 133.63 (s), 133.29 (s), 132.95 (s), 132.35 (s), 131.52 (s), 130.78 (d, *J* = 61.3 Hz), 130.14 (s), 128.98 (s), 128.34 (s), 127.12 (s), 126.51 (s), 124.96 (s), 122.46 (s), 121.61 (s), 119.34 (s), 117.50 (s), 111.14 (s), 110.51 (s), 74.80 (s), 74.11 (s), 30.05 (d, *J* = 27.5 Hz), 29.91 – 29.81 (m).

_N_-(5-(((6-bromonaphthalen-2-yl)oxy)(4-chlorophenyl)methyl)thiazol-2-yl)naphthalene-2-sulfonam

ide (76)

^{1}H NMR (500 MHz, MeOD) δ 8.51 (s, 1H), 7.97 (d, *J* = 2.1 Hz, 1H), 7.96 (s, 1H), 7.90 (d, *J* = 9.2 Hz, 1H), 7.74 – 7.68 (m, 3H), 7.66 (d, *J* = 8.8 Hz, 3H), 7.63 – 7.57 (m, 2H), 7.56 – 7.50 (m, 2H), 7.46 (dd, *J* = 9.2, 1.9 Hz, 1H), 7.41 (d, *J* = 1.4 Hz, 1H), 7.40 – 7.36 (m, 1H), 7.34 – 7.28 (m, 4H), 7.27 (d, *J* = 8.7 Hz, 1H), 7.19 (d, *J* = 8.9 Hz, 1H), 7.04 (dd, *J* = 8.6, 1.8 Hz, 1H), 6.38 (s, 1H), 2.15 (s, 2H), 1.30 (s, 2H). ESI-MS m/z: 635.98 $[M+H]^{+}$

^{13}C NMR (101 MHz, CD_3CN) δ 165.86 (s), 154.57 (s), 140.08 (s), 138.78 (s), 136.82 (s), 135.79 (s), 133.67 (s), 133.35 (s), 132.93 – 132.27 (m), 132.23 (s), 132.03 (s), 131.65 (s), 131.32 – 130.41 (m), 130.43 – 130.41 (m), 130.43 – 129.60 (m), 129.24 (s), 128.91 (d, *J* = 16.7 Hz), 127.89 (s), 127.33 (s), 126.56 (s), 123.56 (s), 122.41 (s), 121.80 (s), 120.91 (s).

***N*-(5-(((6-bromonaphthalen-2-yl) oxy) (4-chlorophenyl) methyl) thiazol-2-yl)-4-methylnaphthalene-1-sulfonamide (77)**

^{1}H NMR (400 MHz, DMSO-d_6) δ 10.50 (s, 1H), 8.27 (d, *J* = 11.0 Hz, 1H), 8.20 – 8.09 (m, 3H), 8.03 (d, *J* = 8.6 Hz, 1H), 7.96 (s, 1H), 7.83 (d, *J* = 8.2 Hz, 3H), 7.73 (d, *J* = 7.5 Hz, 1H), 7.61 (t, *J* = 8.0 Hz, 2H), 7.58 – 7.53 (m, 1H), 7.50 – 7.44 (m, 1H), 7.36 (dd, *J* = 12.5, 8.1 Hz, 3H), 7.23 (d, *J* = 8.9 Hz, 1H), 7.17 (t, *J* = 7.1 Hz, 3H), 6.58 (d, *J* = 7.5 Hz, 2H), 4.01 (q, *J* = 7.1 Hz, 2H), 2.73 (s, 3H), 1.16 (t, *J* = 7.1 Hz, 4H). ESI-MS m/z: 651.00 $[M+H]^{+}$.

^{13}C NMR (101 MHz, DMSO) δ 164.54 (s), 155.41 (s), 146.63 (s), 143.00 (s), 141.90 (s), 135.97 (s), 135.40 (s), 134.26 (s), 133.86 (s), 133.36 (s), 132.88 (s), 132.42 (s), 131.62 (s), 131.21 (s), 130.65 (s), 130.12 (s), 128.96 (d, *J* = 14.2 Hz), 128.67 (s), 128.34 (s), 127.83 (s), 126.74 (d, *J* = 16.2 Hz), 126.40 (s), 125.92 (s), 123.87 (s), 123.32 (s), 121.60 (s), 119.29 (s), 117.52 (s), 21.62 (s), 21.41 (s).

***N*-(5-(((6-bromonaphthalen-2-yl)oxy)(4-chlorophenyl)methyl)thiazol-2-yl)benzo[c][1,2,5]thiadiazole-4-sulfonamide (78)**

^{1}H NMR (500 MHz, DMSO) δ 10.49 (s, 1H), 8.39 (t, *J* = 17.7 Hz, 1H), 8.27 (d, *J* = 8.8 Hz, 1H), 8.19 (d, *J* = 2.1 Hz, 1H), 8.08 (dd, *J* = 22.5, 7.1 Hz, 3H), 7.85 (d, *J* = 8.9 Hz, 1H), 7.82 – 7.69 (m, 2H), 7.66 (dd, *J* = 9.2, 2.0 Hz, 1H), 7.47 (d, *J* = 8.5 Hz, 2H), 7.24 (dd, *J* = 8.5, 6.1 Hz, 3H), 6.99 (dd, *J* = 8.7, 7.3 Hz, 1H), 6.69 (s, 1H). ESI-MS m/z: 643.98 $[M+H]^{+}$.

^{13}C NMR (126 MHz, CD_3CN) δ 154.96 (s), 154.05 (s), 153.30 (s), 147.77 (s), 139.23 (s), 136.26 (s), 132.33 (d, *J* = 27.1 Hz), 131.53 (s), 130.87 (d, *J* = 35.3 Hz), 129.80 (d, *J* = 27.4 Hz), 129.53 (s), 129.53

(s), 129.53 (s), 128.52 (s), 128.12 (s), 126.74 (s), 126.12 (s), 125.93 (s), 125.31 (d, *J* = 25.5 Hz), 121.29 (s), 119.58 (s).

_N_-(5-(((6-bromonaphthalen-2-yl) oxy) (4-chlorophenyl) methyl) thiazol-2-yl) quinoline-8-sulfonamide (79)

^{1}H NMR (400 MHz, DMSO-*d6*) δ 10.43 (s, 1H), 8.58 (s, 1H), 8.34 (d, *J* = 8.3 Hz, 1H), 8.19 (d, *J* = 2.0 Hz, 1H), 8.16 (dd, *J* = 8.4, 1.4 Hz, 1H), 8.13 (d, *J* = 6.5 Hz, 1H), 8.07 (t, *J* = 6.7 Hz, 2H), 8.03 (d, *J* = 8.5 Hz, 1H), 7.96 (s, 1H), 7.86 (d, *J* = 8.9 Hz, 1H), 7.67 (dd, *J* = 9.2, 1.6 Hz, 1H), 7.61 (t, *J* = 7.8 Hz, 1H), 7.52 (dd, *J* = 8.3, 4.2 Hz, 1H), 7.48 (d, *J* = 8.5 Hz, 2H), 7.45 (d, J = 8.5 Hz, 1H), 7.32 (d, *J* = 8.4 Hz, 2H), 7.26 (d, *J* = 8.9 Hz, 1H), 7.18 (s, 1H), 6.99 (dd, *J* = 8.3, 4.1 Hz, 1H), 6.76 (t, *J* = 7.8 Hz, 1H), 6.66 (s, 1H), 2.07 (s, 6H). FTMS-cESI m/z: 633.94895 $[M-H]^-$.

^{13}C NMR (101 MHz, DMSO) δ 167.67 (s), 155.53 (s), 153.21 (s), 150.83 (s), 143.77 (s), 142.40 (s), 139.13 (s), 137.87 – 137.04 (m), 134.99 (s), 133.50 (s), 132.77 (s), 132.35 (d, *J* = 11.1 Hz), 131.99 – 131.08 (m), 131.18 (s), 131.40 – 130.50 (m), 130.06 (s), 129.51 (s), 129.02 (s), 126.93 (s), 125.34 (s), 124.69 (s), 124.11 (d, *J* = 15.5 Hz), 121.66 (s), 119.86 (s), 117.41 (s), 32.51 (s).

_N_-(5-(((6-bromonaphthalen-2-yl)oxy)(4-bromophenyl)methyl)thiazol-2-yl)-4-methoxy-benzamide(80)

^{1}H NMR (500 MHz, DMSO) δ 8.08 (d, *J* = 1.7 Hz, 1H), 8.02 (d, *J* = 8.8 Hz, 3H), 7.92 (s, 1H), 7.77 (d, *J* = 8.9 Hz, 1H), 7.45 (d, *J* = 8.3 Hz, 3H), 7.36 (s, 1H), 7.28 (d, *J* = 8.5 Hz, 1H), 7.24 (d, *J* = 9.0 Hz, 1H), 7.21 (d, *J* = 7.5 Hz, 1H), 7.13 (d, *J* = 8.3 Hz, 2H), 7.02 (d, *J* = 8.8 Hz, 3H), 6.60 (s, 1H), 3.81 (s, 4H). ESI-MS m/z: 624.34 $[M+H]^+$.

^{13}C NMR (126 MHz, CD_3CN) δ 164.48 (s), 163.21 (s), 158.71 (s), 152.87 (s), 142.04 (s), 136.20 (s), 133.12 (s), 131.19 (s), 130.72 (s), 129.89 (d, *J* = 6.3 Hz), 129.18 (s), 128.94 (s), 128.35 (s), 127.85 (s), 125.99 (s), 124.47 (s), 120.44 (s), 119.52 (d, *J* = 19.3 Hz), 116.03 (s), 113.86 (s), 55.34 (s).

_N_-(5-(((6-bromonaphthalen-2-yl)oxy)(4-fluorophenyl)methyl)thiazol-2-yl)-4-methoxy-benzamide(8 1)

^{1}H NMR (500 MHz, DMSO) δ 8.08 (d, *J* = 2.1 Hz, 1H), 8.02 (d, *J* = 8.9 Hz, 2H), 7.99 – 7.86 (m, 1H), 7.78 (t, *J* = 9.5 Hz, 1H), 7.45 (d, *J* = 8.5 Hz, 1H), 7.30 (s, 1H), 7.27 – 7.20 (m, 3H), 7.09 (t, *J* = 8.8 Hz, 2H), 7.02 (d, *J* = 8.9 Hz, 2H), 6.62 (s, 1H), 3.81 (s, 3H). ESI-MS m/z: 563.44 $[M+H]^+$.

^{13}C NMR (126 MHz, CD_3CN) δ 130.69 (s), 129.88 (s), 129.61 (s), 128.96 (d, *J* = 29.6 Hz), 114.85 (d, *J*

945 = 21.3 Hz), 113.88 (s), 55.33 (s), 39.12 (s), 30.67 (s), 29.50 (s).

946 ***N*-(5-(((6-bromonaphthalen-2-yl)oxy)(4-cyanophenyl)methyl)thiazol-2-yl)-4-methoxy-benzamide(8**
947 **2)**

948 ^{1}H NMR (500 MHz, DMSO) δ 10.32 (s, 1H), 8.10 (d, *J* = 2.1 Hz, 1H), 8.03 (d, *J* = 8.9 Hz, 3H), 7.76
949 (dd, *J* = 31.5, 8.7 Hz, 3H), 7.55 – 7.40 (m, 2H), 7.32 (d, *J* = 8.2 Hz, 1H), 7.23 (d, *J* = 8.9 Hz, 1H), 7.03
950 (d, *J* = 8.9 Hz, 2H), 6.71 (s, 1H), 3.82 (s, 3H). ESI-MS m/z: 570.46 $[M+H]^{+}$

951 ^{13}C NMR (126 MHz, CD_3CN) δ 132.12 (s), 130.78 (s), 129.95 (s), 129.46 (s), 128.52 (s), 119.49 (s),
952 113.92 (s), 55.35 (s).

953 ***N*-(5-(((7-bromonaphthalen-2-yl)oxy)(4-(methylsulfonyl)phenyl)methyl)thiazol-2-yl)-4-methoxybe**
954 **nzamide (83)**

955 ^{1}H NMR (500 MHz, DMSO) δ 12.35 (s, 1H), 10.33 (s, 1H), 8.11 (d, *J* = 2.0 Hz, 1H), 8.03 (d, *J* = 8.9 Hz,
956 2H), 7.83 (d, *J* = 8.5 Hz, 2H), 7.80 (d, *J* = 8.9 Hz, 1H), 7.52 (s, 1H), 7.45 (s, 1H), 7.41 (d, *J* = 8.3 Hz,
957 2H), 7.24 (d, *J* = 8.9 Hz, 1H), 7.03 (d, *J* = 8.9 Hz, 2H), 6.73 (s, 1H), 3.82 (s, 3H), 3.16 (s, 3H), 2.07 (s,
958 1H). ESI-MS m/z: 623.54 $[M+H]^{+}$

959 ^{13}C NMR (101 MHz, CD_3CN) δ 165.85 (s), 164.69 (s), 160.70 (s), 154.24 (s), 150.44 (s), 140.29 (s),
960 137.13 (s), 133.68 (s), 132.28 (t, *J* = 25.7 Hz), 132.04 – 131.51 (m), 131.51 – 131.43 (m), 131.43 –
961 130.48 (m), 130.49 – 130.31 (m), 128.64 (dd, *J* = 187.0, 116.2 Hz), 126.93 (s), 126.93 (s), 125.62 (s),
962 121.49 (s), 120.91 (s), 115.28 (s), 56.72 (s), 44.94 (s).

963 **Plasmid construction.** Plasmids of two nonfluorescent fragments of VFP (N1-154aa and C155-239aa)
964 were constructed into pcDNA 3.1 vector. Then they were fused these two fragments with HBV capsid
965 protein, which were HBVcAg-VFP-N1-154 (HBc-VN) and HBVcAg-VFP-C155-239 (HBc-VC).

966 **High throughput screening (HTS) of HBV capsid assembly inhibitors.** The HBc-VN and HBc-VC
967 plasmids were co-transfected into 293T cells and the cells were treated with a commercial drug-like
968 chemical library composed of 40155 compounds at 50 μM concentration with TECAN EVO150. After
969 48 h, the wells containing GFP-positive cells were detected by an Envision system (Perkin Elmer). After
970 the active compounds were confirmed by the same system, they were further tested for their potential

anti-HBV replication activity by an anti-HBV-1replication assay. HepG2.2.15 cells (5×10^6) were seeded into a 96-well-plate. After cells attached, the active compounds were added into each well. Then, the HBV replication was monitored by the detection of HBV DNA copies in supernatant after 4 days. The amount of HBV DNA was quantified by qPCR.

Protein purification. The plasmid pET32a harboring His-tagged HBVcAg or Cp149 genes were transformed into E. Coli BL21 competent cells (Novagen) respectively. After the expression of proteins was induced by 1 mM isopropylthio-β-d-galactoside, the bacterial cells were lysed by sonication. The insoluble fraction was pelleted at 10,000 × g for 10 min, and the supernatant was applied to a Ni-conjugated agarose bead column (GE). After washing, the bound His fusion proteins were eluted with 500 μM imidazole. Then the proteins were suspended in PBS buffer and the concentration was measured by the Bradford method. The samples were then aliquoted and frozen at −80 ^{o}C.

Electro microscopy. HBV capsid protein (Cp149, 10 μM) in 50 mM pH 7.5 HEPES buffer was incubated for 1 h with different concentrations of compounds prior to assembly. Assembly was initiated by adding 1 M NaCl solution to 50 mM. The assembly reactions were allowed to equilibrate for 60h at 23 □. The supernatants were determined by transmission electron microscopy. Samples were adsorbed to freshly glow-discharged grids and stained with 2% uranyl acetate. Grids were carbon-coated collodion on a 300-mesh copper substrate. Samples were visualized on a JEOL JEM-100CX II transmission electron microscope [15, 26, 32].

SPR The recombinant HBV capsid 149-His protein was immobilized on a CM5 Sensor Chip (carboxymethylated dextran covalently attached to a gold surface) with an amine coupling kit from GE Healthcare. The recombinant HBV capsid149-His protein was pre-incubated with different concentration of compound **79** in a PBS buffer (10 mM) with 1% DMSO. The signals were recorded with a BiacoreT100 instrument with the standard protocol.

HBV replication assay in cells HepG2.2.15 cells (5×10^4) were seeded into 96-well plate and then treated with or without different concertation of **79**. After 7 days, the HBV replication was detected by the quantitation of HBV DNA in the supernatant after by real-time PCR with a commercial kit based on real time quantitative PCR from Daan Gene.

HBV replication assay in mice The *in vivo* efficacy of compound **79** was evaluated in BALB/c transgenic mice which were injected with replication-competent HBV DNA plasmid HBV-1.2mer. These transgenic mice were purchased from Vitalstar Company and could produce HBV DNA, HBeAg, HBsAg and HBcAg [33]. These mice were randomly divided into two groups and each group was 3 male BALB/c transgenic mice. The compound 79 at 30mg/kg and DMSO were injected by tail vein manner respectively. After 2 weeks, mice were scarified and the blood samples were collected to determine the antiviral activity. Alternatively, to further characterize compound **79** *in vivo*, another HBV mouse model was applied to assess compound **79**. The nude mice were subcutaneously inoculated with HepAD38 cells and then treated with or without compound **79** every 3 days. After 4 weeks, mice were scarified. The blood samples yielded similar results and show the potent antiviral activity. Meanwhile, the immunofluorescence assay of HBVcAg in the tumor tissue was also decreased in the compound **79** treated group.

Molecular docking modeling. The docking studies were prepared with Ligandscout (4.1) with MMFF 94 energy minimization. The HBV capsid protein (PDB: 5E0I) were prepared with ligandscout (4.1) by removing the ligand and unnecessary water molecules. Then the whole protein was selected for docking and the prepared molecules were inserted. The docking was carried out by AutoDock Vina 1.1(Exhaustiveness =20, Max. Energy difference= 3).

Acute toxicity test Compounds were tested in 5 male Balb/c mice with intraperitoneal injection at the dose of 0 mg/kg, 500 mg/kg, and 1000 mg/kg, respectively. On the 14^{th} day, the tissues of heart, liver, lung, spleen and kidney were examined. The hepatic and renal functions including the levels of AST,

ALT, BUN, and CRE were examined.

Supporting Information. This material is available free of charge via the Internet at http://pubs.acs.org.

ACKNOWLEDGMENTS

This work was supported by the grants from National Natural Science Foundation of China (21572281, 21877132), Scientific Plan of Guangzhou City (201704030087), Scientific Plan of Guangdong Province (2017A020211003) to C.B; supported by the Introduction of Innovative R&D Team Program of Guangdong Province (2009010058), the National Special Research Program of China for Important Infectious Diseases (2018ZX10302103 and 2017ZX10202102), the Important Key Program of Natural Science Foundation of China (81730060), the International Collaboration Program of Natural Science Foundation of China and US NIH (81561128007), and the Joint-innovation Program in Healthcare for Special Scientific Research Projects of Guangzhou (201803040002) to H.Z; also supported by National Natural Science Foundation of China (No.31500740), Natural Science Foundation of Guangdong (2015A030310442), the Science and Technology Planning Project of Guangzhou (201704020226), Pearl River S&T Nova Program of Guangzhou (201806010118) to T.P.

Figure 1. The cell-based HTS system for HBV capsid inhibitors. **(A)** The design of HTS for HBV capsid inhibitor. **(B)** The flow chart of multiple screening and the hit compound in this study. **(C)** Effect of the hit compound on the cell viability. Hit compound did not show obvious toxicity in 293T cells at 500 μM. **(D)** The IC_{50} of hit compound was 6.153μM in HepG2.2.15 cells. Error bars represent the average of three independent experiments.

Figure 2. Compound **79** inhibits HBV capsid assembly. **(A)** The MFI analysis for the effect of compound **79** on the intensity of VFP fluorescence. HBc-VN and HBc-VC were co-transfected into HEK293T cells and then the cells were treated with DMSO or multiple concentrations (0.5, 5, or 50 μM) of compound **79** respectively. After 48 h, the fluorescence was detected by microplate reader and

representative fluorescence microscope images were shown. Compound **79** effectively inhibited the fluorescence concentration-dependently. **(B)** HEK293T cells were transfected with HBc-VN-HA or HBc-VC-FALG and then were treated with DMSO, 50 μM and 100 μM compound **79** respectively. After 48 h, cells were harvested for western blot with primary antibodies of HA, FLAG and GAPDH. **(C)** HEK293T cells were co-transfected with HBc-VN-HA and HBc-VC-FALG and then were treated with DMSO and compound **79** respectively. After 48 h, cells were harvested for co-IP assay with anti-HA beads. **(D)** Transmission electron micrographs of assembly of 10 μM Cp149 in assembly reactions (50 mM NaCl). Normal HBV capsid assembly was observed in DMSO treated group. Non-capsid particles were observed when treated with compound **79** (0.2 μM and 4 μM). Non-particle oligomers were induced by compound **79** (10 μM and 50 μM). Compound GLS4 (50μM) abolished HBV capsid assembly as positive control. Lamivudine (50μM) did not induce any abnormalities in HBV capsid assembly.

Figure 3. The molecular docking studies of compound **79**. **(A)** Compound **79** (yellow) bound in the interface of two subunits (B, cyan and C, magenta) of HBV capsid, the similar pocket in which the NVR-010–001-E2 (green) bound (left). The analysis of docking results showed the hydrophobic interactions and hydrogen bonds of compound **79** with HBV capsid protein. **(B)** Molecular modeling showed that the bromo-naphtalene group of compound **79** had hydrophobic/aromatic interactions with F23, F24, W102 and Y118 of Chian B (left). The quinoline group had hydrophobic interactions with Val120 of Chain C and Thr109 of Chain B (middle). The Chloro-benzene group had hydrophobic interaction with W125 of Chain C (right). **(C)**. The S121 was close to the nitrogen atoms of thiazole and quinoline groups of compound **79** and they could form hydrogen bonds.

Figure 4. The surface plasmon resonance (SPR) studies of compound **79** with wildtype and mutant HBV capsid proteins. **(A)** The binding affinity of compound **79** and wild type HBV capsid (HBVcAg) was $K_D = 5.93*10^{-6}$ M. **(B)** Compound **79** did not bind with mutant HBV capsid protein

(HBVcAg-S121A). **(C)** Compound **79** did not bind with mutant HBV capsid protein (HBVcAg-Y118A).

Figure 5. Compound **79** inhibits the HBV replication *in vitro* and *in vivo*. **(A)** HepG2.2.15 cell were seeded into 96-well plate and then the cells were treated with DMSO or multiple concentrations (0.5, 5, or 50 μM) of compound **79** and GLS4 respectively. After 7 days, the HBV replication was detected by the quantitation of HBV DNA in the supernatant by real-time PCR. Both Compound **79** and GLS4 inhibited HBV replication effectively in a concentration dependent manner. **(B)** The quantitative experiments showed the IC_{50} value of compound **79** in HepG2.2.15 cell was 182.9 nM. **(C-D)** HBV transgenic mice were detected HBV DNA copies at day 0 by extracting the eyeball blood samples and then randomly divided into two groups. These mice were treated with 30 mg/kg compound **79** or DMSO every 2 days. After 2 weeks, mice were scarified and the blood samples were collected to determine the antiviral activity. The HBV DNA copies were determined by real-time PCR **(C)** and the HBsAg were detected by HBsAg ELISA kit **(D)**. **(E-F)** Xenografts were established using HepAD38 cell line in female NOD-SCID mice. Two groups were randomly assigned and injected with DMSO or 30 mg/kg compound **79** by orthotopic injection every 3 days (n = 3). After 4 weeks, mice were scarified and the liver samples were collected to determine the HBV DNA levels by real-time PCR **(E)**. Representative immunofluorescent staining of tumor tissues with HBVcAg antibody and DAPI **(F).**

Figure 6. Compound **79** showed low acute toxicities. (A) The measurement of weight of male Balb/c mice after intraperitoneally injected with compound **79** (0.5g/Kg or 1g/Kg). (B-D) Compound **79** did not cause obvious toxicities on the hepatic and renal function of mice (BUN: Blood urea nitrogen, CRE: Creatine, AST: Aspartate Transaminase, ALT: Alanine transaminase). (E) The vital organs from the mice treated with various doses of compounds **79** were histologically sectioned and HE stained and compound **79** did not cause obvious damage on these organs.

Corresponding Author Information

1089 *C.B.: phone, 086-20-87332588; e-mail, baichuan@mail.sysu.edu.cn.

1090 *H.Z.: phone, 086-20-87332588; e-mail, zhangh92@mail.sysu.edu.cn.

1091

References

[1] W.H. Organization, GLOBAL HEPATITIS REPORT, 2017, (2017)
[2] S.J. Hadziyannis, Update on Hepatitis B Virus Infection: Focus on Treatment, Journal of clinical and translational hepatology, 2 (2014) 285-291 http://doi.org/10.14218/JCTH.2014.00026.
[3] C.R. You, S.W. Lee, J.W. Jang, S.K. Yoon, Update on hepatitis B virus infection, World J Gastroenterol, 20 (2014) 13293-13305 http://doi.org/10.3748/wjg.v20.i37.13293.
[4] J. Chang, F. Guo, X. Zhao, J.T. Guo, Therapeutic strategies for a functional cure of chronic hepatitis B virus infection, Acta Pharm Sin B, 4 (2014) 248-257 http://doi.org/10.1016/j.apsb.2014.05.002.
[5] G. Baltayiannis, P. Karayiannis, Treatment options beyond IFNalpha and NUCs for chronic HBV infection: expectations for tomorrow, J Viral Hepat, 21 (2014) 753-761 http://doi.org/10.1111/jvh.12307.
[6] R. Orlando, M. Foggia, A.E. Maraolo, S. Mascolo, G. Palmiero, O. Tambaro, G. Tosone, Prevention of hepatitis B virus infection: from the past to the future, Eur J Clin Microbiol Infect Dis, 34 (2015) 1059-1070 http://doi.org/10.1007/s10096-015-2341-x.
[7] Z. Qiu, X. Lin, M. Zhou, Y. Liu, W. Zhu, W. Chen, W. Zhang, L. Guo, H. Liu, G. Wu, M. Huang, M. Jiang, Z. Xu, Z. Zhou, N. Qin, S. Ren, H. Qiu, S. Zhong, Y. Zhang, Y. Zhang, X. Wu, L. Shi, F. Shen, Y. Mao, X. Zhou, W. Yang, J.Z. Wu, G. Yang, A.V. Mayweg, H.C. Shen, G. Tang, Design and Synthesis of Orally Bioavailable 4-Methyl Heteroaryldihydropyrimidine Based Hepatitis B Virus (HBV) Capsid Inhibitors, J Med Chem, 59 (2016) 7651-7666 http://doi.org/10.1021/acs.jmedchem.6b00879.
[8] A. Zlotnick, S. Mukhopadhyay, Virus assembly, allostery and antivirals, Trends Microbiol, 19 (2011) 14-23 http://doi.org/10.1016/j.tim.2010.11.003.
[9] Z. Qiu, X. Lin, W. Zhang, M. Zhou, L. Guo, B. Kocer, G. Wu, Z. Zhang, H. Liu, H. Shi, B. Kou, T. Hu, Y. Hu, M. Huang, S.F. Yan, Z. Xu, Z. Zhou, N. Qin, Y.F. Wang, S. Ren, H. Qiu, Y. Zhang, Y. Zhang, X. Wu, K. Sun, S. Zhong, J. Xie, G. Ottaviani, Y. Zhou, L. Zhu, X. Tian, L. Shi, F. Shen, Y. Mao, X. Zhou, L. Gao, J.A.T. Young, J.Z. Wu, G. Yang, A.V. Mayweg, H.C. Shen, G. Tang, W. Zhu, Discovery and Pre-Clinical Characterization of Third-Generation 4-H Heteroaryldihydropyrimidine (HAP) Analogues as Hepatitis B Virus (HBV) Capsid Inhibitors, J Med Chem, 60 (2017) 3352-3371 http://doi.org/10.1021/acs.jmedchem.7b00083.
[10] K. Deres, C.H. Schroder, A. Paessens, S. Goldmann, H.J. Hacker, O. Weber, T. Kramer, U. Niewohner, U. Pleiss, J. Stoltefuss, E. Graef, D. Koletzki, R.N. Masantschek, A. Reimann, R. Jaeger, R. Gross, B. Beckermann, K.H. Schlemmer, D. Haebich, H. Rubsamen-Waigmann, Inhibition of hepatitis B virus replication by drug-induced depletion of nucleocapsids, Science, 299 (2003) 893-896 http://doi.org/10.1126/science.1077215.
[11] J. Lucifora, Y. Xia, F. Reisinger, K. Zhang, D. Stadler, X. Cheng, M.F. Sprinzl, H. Koppensteiner, Z. Makowska, T. Volz, C. Remouchamps, W.M. Chou, W.E. Thasler, N. Huser, D. Durantel, T.J. Liang, C. Munk, M.H. Heim, J.L. Browning, E. Dejardin, M. Dandri, M. Schindler, M. Heikenwalder, U. Protzer, Specific and nonhepatotoxic degradation of nuclear hepatitis B virus cccDNA, Science, 343 (2014) 1221-1228 http://doi.org/10.1126/science.1243462.
[12] A. Zlotnick, B. Venkatakrishnan, Z. Tan, E. Lewellyn, W. Turner, S. Francis, Core protein: A pleiotropic keystone in the HBV lifecycle, Antiviral Res, 121 (2015) 82-93 http://doi.org/10.1016/j.antiviral.2015.06.020.
[13] Z. Tan, K. Pionek, N. Unchwaniwala, M.L. Maguire, D.D. Loeb, A. Zlotnick, The interface between hepatitis B virus capsid proteins affects self-assembly, pregenomic RNA packaging, and reverse transcription, J Virol, 89 (2015) 3275-3284 http://doi.org/10.1128/JVI.03545-14.
[14] N. Patel, S.J. White, R.F. Thompson, R. Bingham, E.U. Weiss, D.P. Maskell, A. Zlotnick, E. Dykeman, R. Tuma, R. Twarock, N.A. Ranson, P.G. Stockley, HBV RNA pre-genome encodes specific motifs that mediate interactions with the viral core protein that promote nucleocapsid assembly, Nat Microbiol, 2 (2017) 17098 http://doi.org/10.1038/nmicrobiol.2017.98.
[15] A. Zlotnick, P. Ceres, S. Singh, J.M. Johnson, A small molecule inhibits and misdirects assembly of hepatitis B virus capsids, J Virol, 76 (2002) 4848-4854

http://doi.org/10.1128/Jvi.76.10.4848-4854.2002.
[16] Y.J. Wang, D. Lu, Y.B. Xu, W.Q. Xing, X.K. Tong, G.F. Wang, C.L. Feng, P.L. He, L. Yang, W. Tang, Y.H. Hu, J.P. Zuo, A novel pyridazinone derivative inhibits hepatitis B virus replication by inducing genome-free capsid formation, Antimicrob Agents Chemother, 59 (2015) 7061-7072 http://doi.org/10.1128/AAC.01558-15.
[17] L. Yang, Y.J. Wang, H.J. Chen, L.P. Shi, X.K. Tong, Y.M. Zhang, G.F. Wang, W.L. Wang, C.L. Feng, P.L. He, Y.B. Xu, M.J. Lu, W. Tang, F.J. Nan, J.P. Zuo, Effect of a hepatitis B virus inhibitor, NZ-4, on capsid formation, Antiviral Res, 125 (2016) 25-33 http://doi.org/10.1016/j.antiviral.2015.11.004.
[18] M.R. Campagna, F. Liu, R. Mao, C. Mills, D. Cai, F. Guo, X. Zhao, H. Ye, A. Cuconati, H. Guo, J. Chang, X. Xu, T.M. Block, J.T. Guo, Sulfamoylbenzamide derivatives inhibit the assembly of hepatitis B virus nucleocapsids, J Virol, 87 (2013) 6931-6942 http://doi.org/10.1128/JVI.00582-13.
[19] D. Lu, F. Liu, W. Xing, X. Tong, L. Wang, Y. Wang, L. Zeng, C. Feng, L. Yang, J. Zuo, Y. Hu, Optimization and Synthesis of Pyridazinone Derivatives as Novel Inhibitors of Hepatitis B Virus by Inducing Genome-free Capsid Formation, ACS Infect Dis, 3 (2017) 199-205 http://doi.org/10.1021/acsinfecdis.6b00159.
[20] A.G. Cole, Modulators of HBV capsid assembly as an approach to treating hepatitis B virus infection, Curr Opin Pharmacol, 30 (2016) 131-137 http://doi.org/10.1016/j.coph.2016.08.004.
[21] W.E.t. Delaney, R. Edwards, D. Colledge, T. Shaw, P. Furman, G. Painter, S. Locarnini, Phenylpropenamide derivatives AT-61 and AT-130 inhibit replication of wild-type and lamivudine-resistant strains of hepatitis B virus in vitro, Antimicrob Agents Chemother, 46 (2002) 3057-3060
[22] X.Y. Wang, Z.M. Wei, G.Y. Wu, J.H. Wang, Y.J. Zhang, J. Li, H.H. Zhang, X.W. Xie, X. Wang, Z.H. Wang, L. Wei, Y. Wang, H.S. Chen, In vitro inhibition of HBV replication by a novel compound, GLS4, and its efficacy against adefovir-dipivoxil-resistant HBV mutations, Antivir Ther, 17 (2012) 793-803 http://doi.org/10.3851/IMP2152.
[23] G. Wu, B. Liu, Y. Zhang, J. Li, A. Arzumanyan, M.M. Clayton, R.F. Schinazi, Z. Wang, S. Goldmann, Q. Ren, F. Zhang, M.A. Feitelson, Preclinical characterization of GLS4, an inhibitor of hepatitis B virus core particle assembly, Antimicrob Agents Chemother, 57 (2013) 5344-5354 http://doi.org/10.1128/AAC.01091-13.
[24] K. Klumpp, A.M. Lam, C. Lukacs, R. Vogel, S. Ren, C. Espiritu, R. Baydo, K. Atkins, J. Abendroth, G. Liao, A. Efimov, G. Hartman, O.A. Flores, High-resolution crystal structure of a hepatitis B virus replication inhibitor bound to the viral core protein, Proc Natl Acad Sci U S A, 112 (2015) 15196-15201 http://doi.org/10.1073/pnas.1513803112.
[25] B. Venkatakrishnan, S.P. Katen, S. Francis, S. Chirapu, M.G. Finn, A. Zlotnick, Hepatitis B Virus Capsids Have Diverse Structural Responses to Small-Molecule Ligands Bound to the Heteroaryldihydropyrimidine Pocket, J Virol, 90 (2016) 3994-4004 http://doi.org/10.1128/JVI.03058-15.
[26] S.J. Stray, C.R. Bourne, S. Punna, W.G. Lewis, M.G. Finn, A. Zlotnick, A heteroaryldihydropyrimidine activates and can misdirect hepatitis B virus capsid assembly, P Natl Acad Sci USA, 102 (2005) 8138-8143 http://doi.org/10.1073/pnas.0409732102.
[27] S.J. Stray, J.M. Johnson, B.G. Kopek, A. Zlotnick, An in vitro fluorescence screen to identify antivirals that disrupt hepatitis B virus capsid assembly, Nat Biotechnol, 24 (2006) 358-362 http://doi.org/10.1038/nbt1187.
[28] A. Zlotnick, A. Lee, C.R. Bourne, J.M. Johnson, P.L. Domanico, S.J. Stray, In vitro screening for molecules that affect virus capsid assembly (and other protein association reactions), Nat Protoc, 2 (2007) 490-498 http://doi.org/10.1038/nprot.2007.60.
[29] A. Khalil, J.A. Edwards, C.A. Rappleye, W. Tjarks, Design, synthesis, and biological evaluation of aminothiazole derivatives against the fungal pathogens Histoplasma capsulatum and Cryptococcus neoformans, Bioorg Med Chem, 23 (2015) 532-547 http://doi.org/10.1016/j.bmc.2014.12.006.
[30] E. Kitas, P. Mohr, B. Kuhn, P. Hebeisen, H.P. Wessel, W. Haap, A. Ruf, J. Benz, C. Joseph, W.

1192 Huber, R.A. Sanchez, A. Paehler, A. Benardeau, M. Gubler, B. Schott, E. Tozzo, Sulfonylureido
1193 thiazoles as fructose-1,6-bisphosphatase inhibitors for the treatment of type-2 diabetes, Bioorg Med
1194 Chem Lett, 20 (2010) 594-599 http://doi.org/10.1016/j.bmcl.2009.11.093.
1195 [31] N.K.C. Brennan, Edcon; Kaldor, Stephen W.; Kiryanov, Andre A.; Jennings, Andrew J.; Stafford,
1196 Jeffrey A., Preparation of sulfonamides, particularly N-(thiazol-2-yl)sulfonamides, as inhibitors of
1197 hydroxysteroid dehydrogenases, especially 11β-hydroxysteroid dehydrogenase, WO 2006066109, A2,
1198 (2006)
1199 [32] S.J. Stray, A. Zlotnick, BAY 41-4109 has multiple effects on Hepatitis B virus capsid assembly, J
1200 Mol Recognit, 19 (2006) 542-548 http://doi.org/10.1002/jmr.801.
1201 [33] L.G. Guidotti, B. Matzke, H. Schaller, F.V. Chisari, High-level hepatitis B virus replication in
1202 transgenic mice, J Virol, 69 (1995) 6158-6169

1203

Figure 1.

A

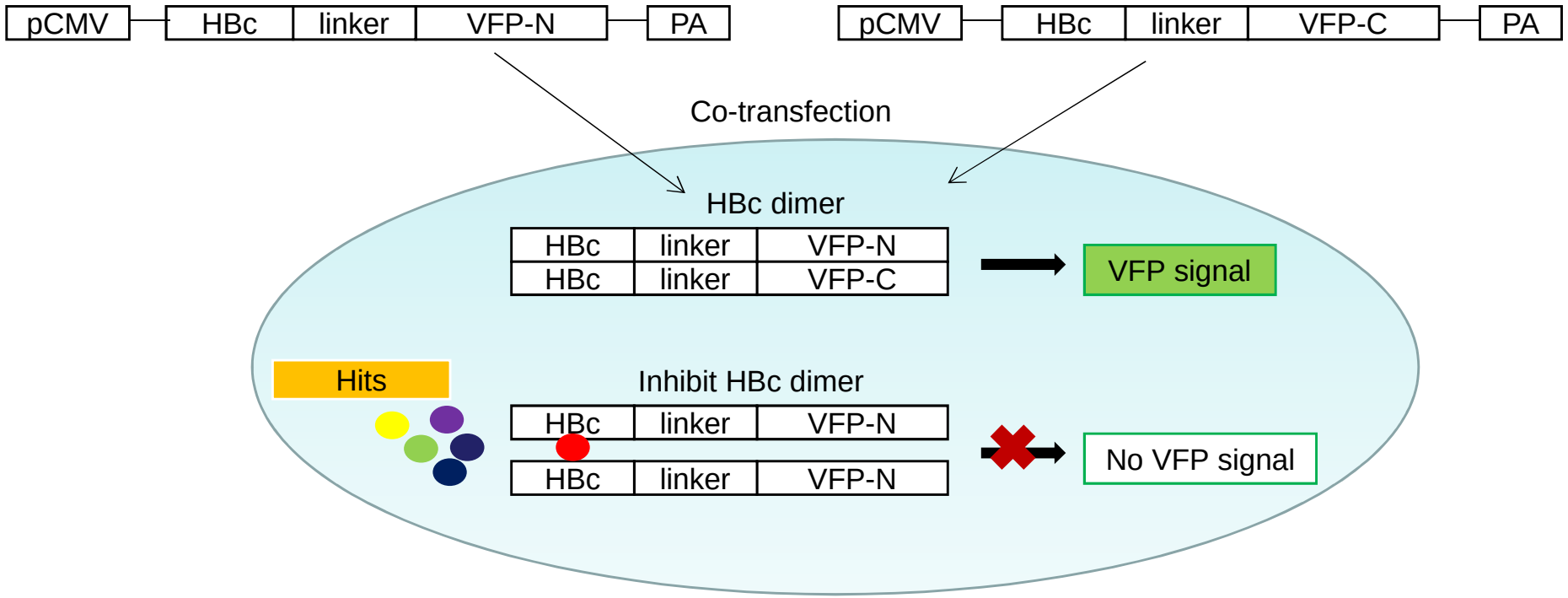
pCMV
HBc
linker
VFP-N
PA
pCMV
HBc
linker
VFP-C
PA
Co-transfection
HBc dimer
HBc
linker
VFP-N
HBc
linker
VFP-C
VFP signal
Hits
Inhibit HBc dimer
HBc
linker
VFP-N
HBc
linker
VFP-N
No VFP signal

Figure 1.

B

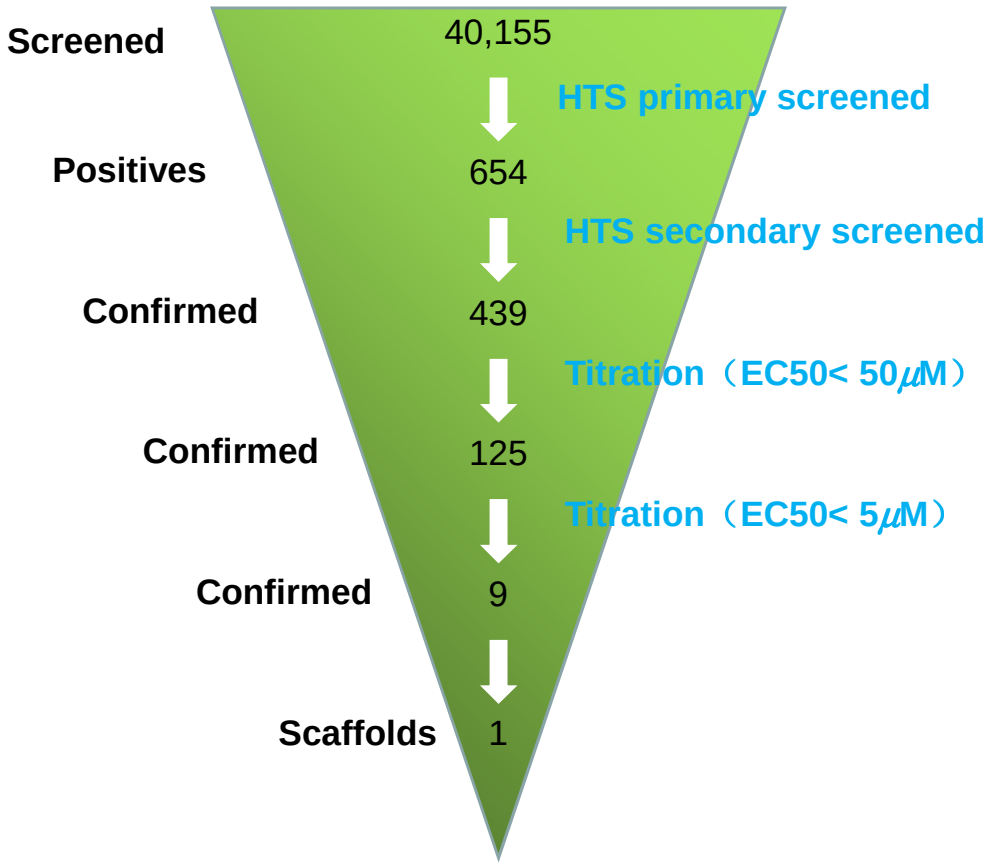

The hit compound in this study

C

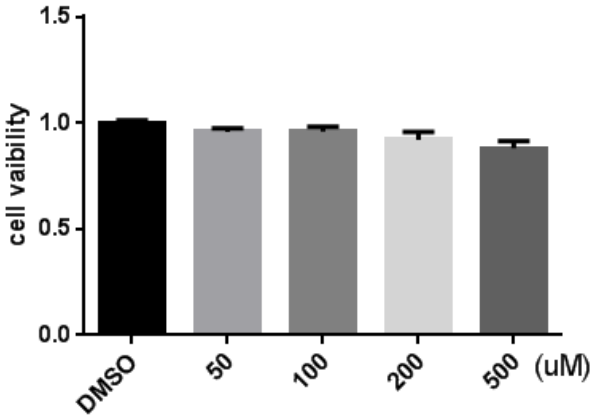

D

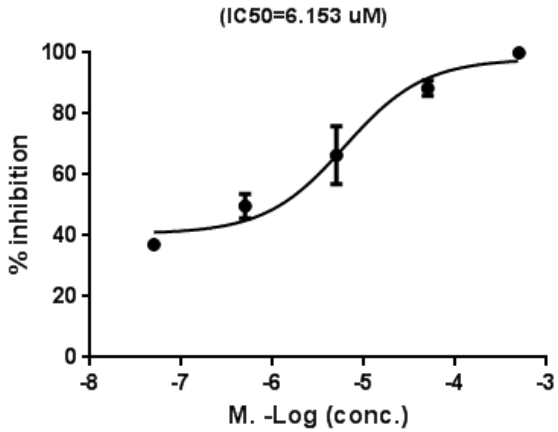

Figure 2.

A

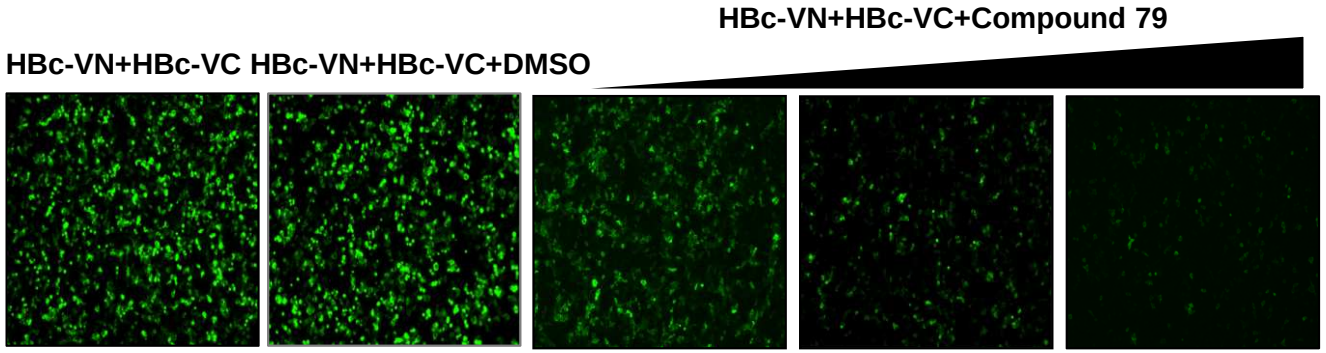
HBc-VN+HBc-VC+Compound 79
HBc-VN+HBc-VC HBc-VN+HBc-VC+DMSO

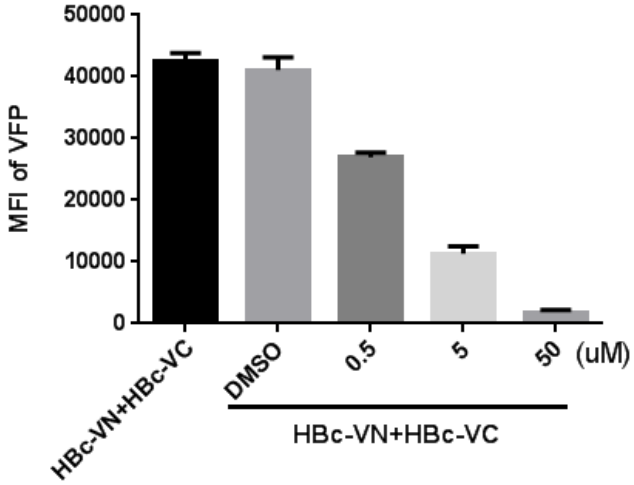
50000
40000
30000
20000
10000
0
MFI of VFP
HBc-VN+HBc-VC
DMSO
0.5
5
50
(uM)
HBc-VN+HBc-VC

B

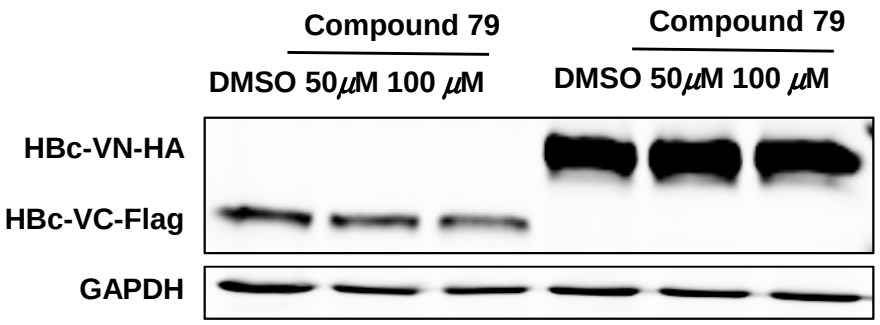
Compound 79
Compound 79
DMSO 50μM 100 μM
DMSO 50μM 100 μM
HBc-VN-HA
HBc-VC-Flag
GAPDH

C

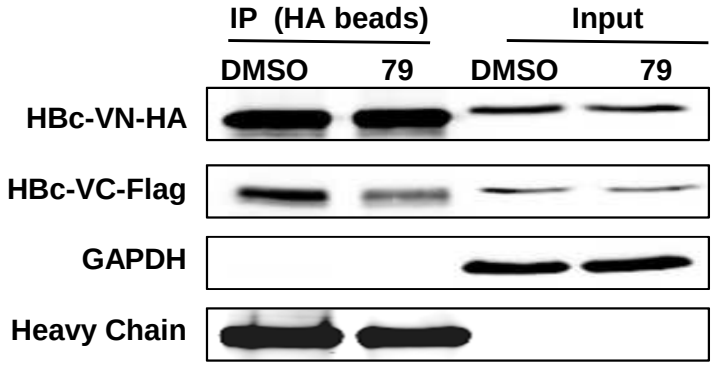
IP (HA beads)
Input
DMSO
79
DMSO
79
HBc-VN-HA
HBc-VC-Flag
GAPDH
Heavy Chain

Figure 2.

D

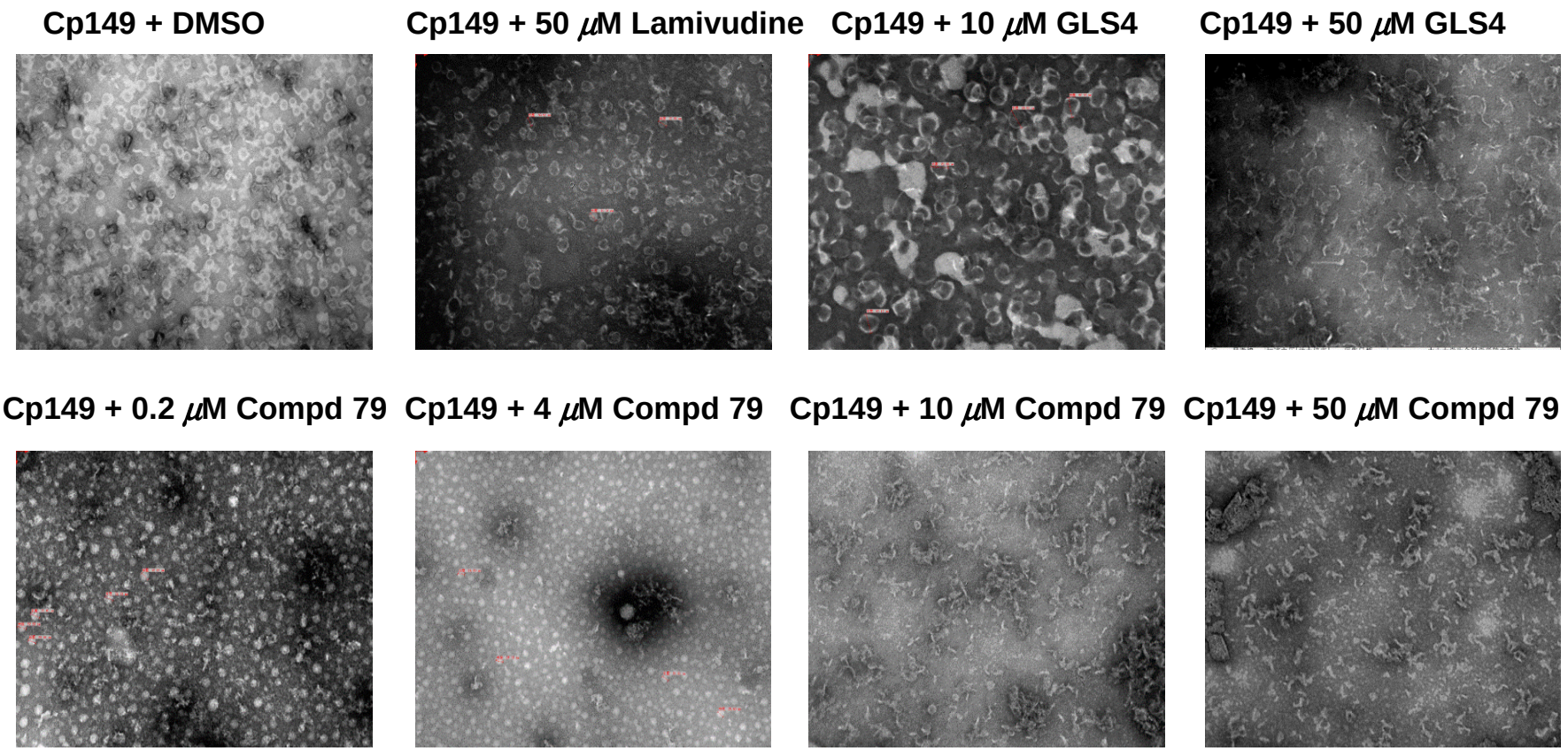
Cp149 + DMSO
Cp149 + 50 μM Lamivudine
Cp149 + 10 μM GLS4
Cp149 + 50 μM GLS4
Cp149 + 0.2 μM Compd 79
Cp149 + 4 μM Compd 79
Cp149 + 10 μM Compd 79
Cp149 + 50 μM Compd 79

Figure 3.

A

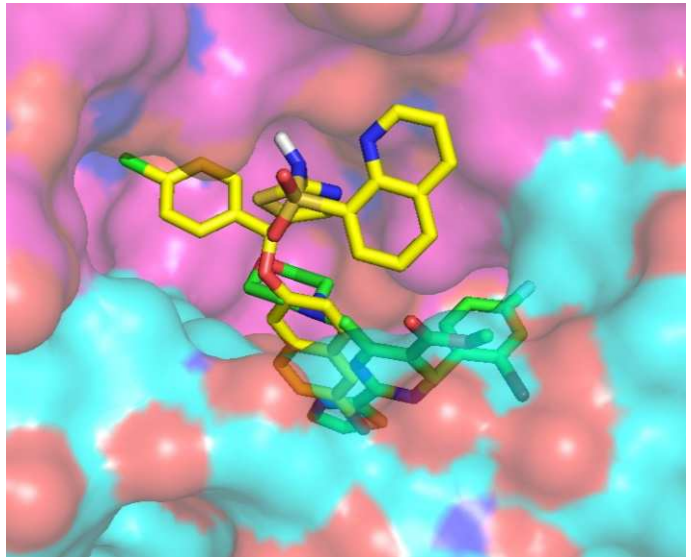

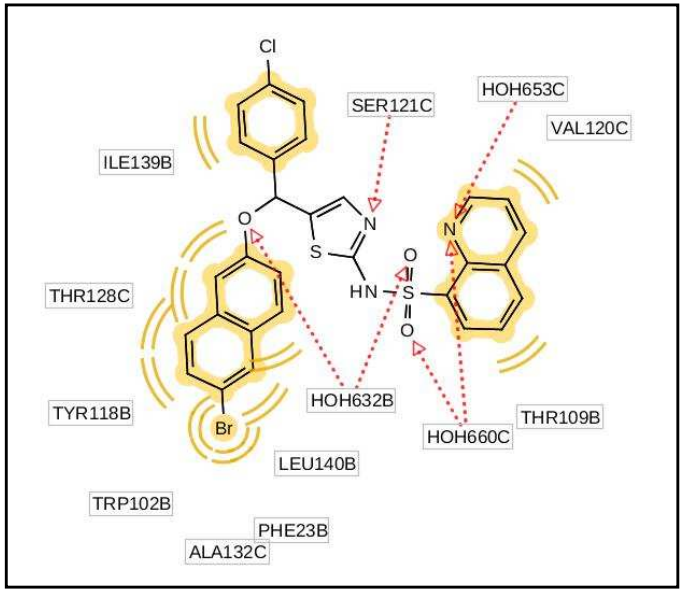
Cl
SER121C
HOH653C
VAL120C
ILE139B
O
N
S
HN
O
S
O
N
THR128C
TYR118B
HOH632B
Br
HOH660C
THR109B
LEU140B
TRP102B
PHE23B
ALA132C

Figure 3.

B

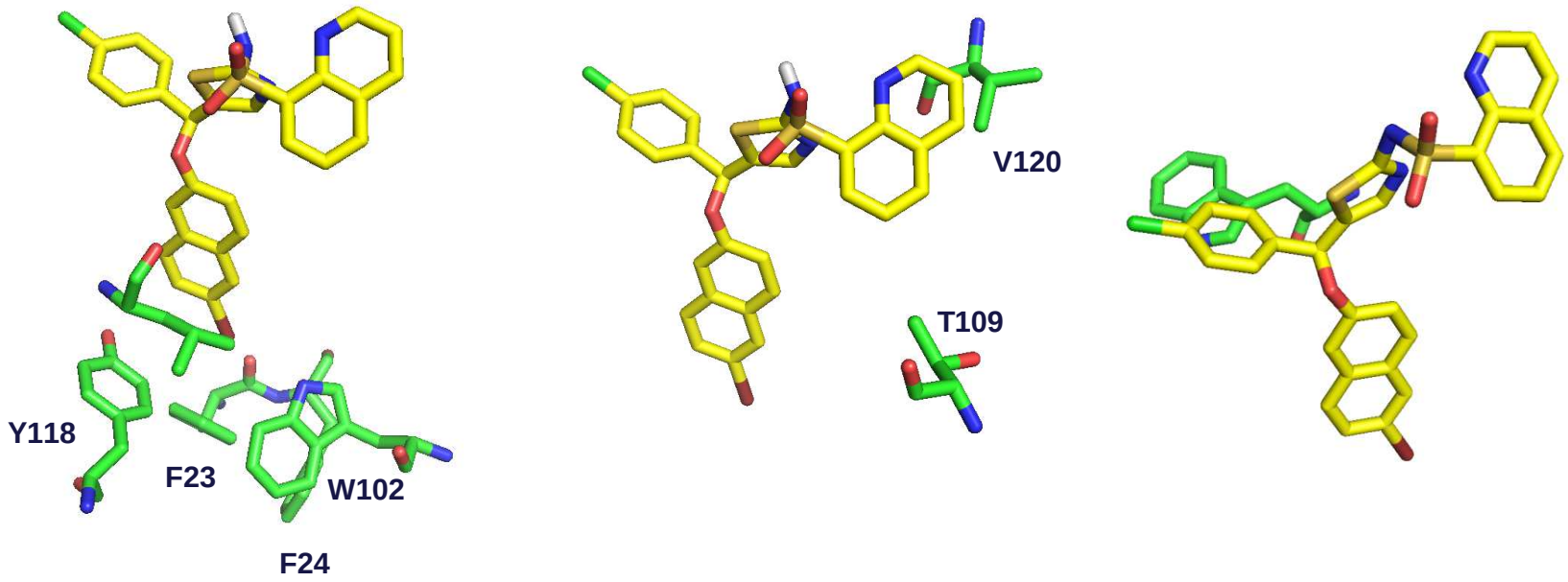

C

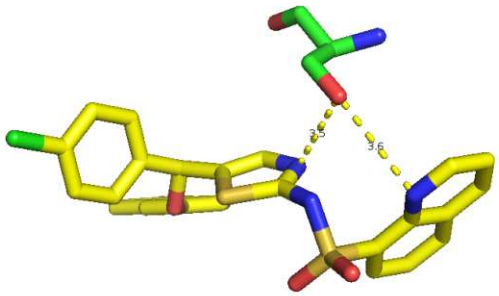

Figure 4.

A

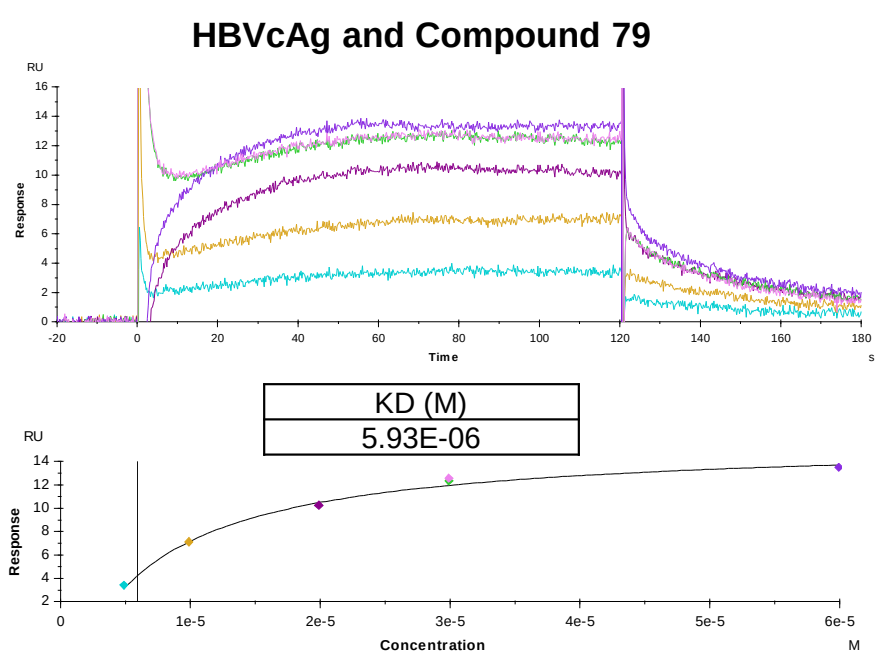
HBVcAg and Compound 79
RU
Response
Time
s
KD (M)
5.93E-06
RU
Response
Concentration
M

B

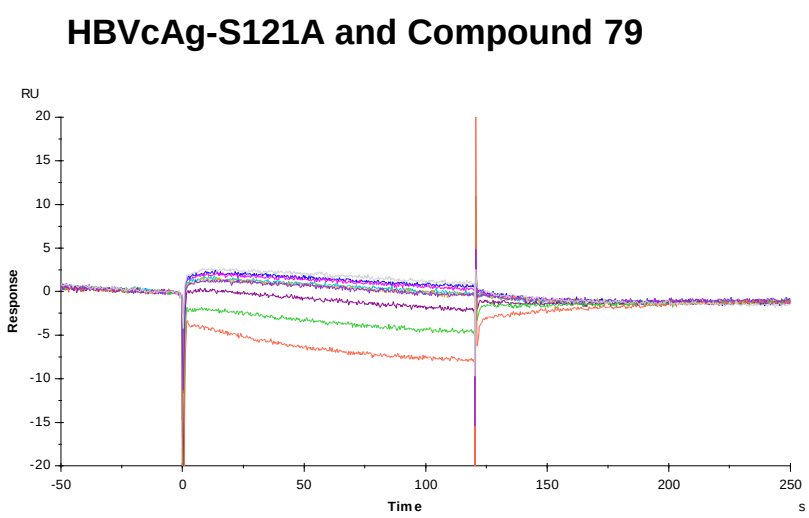
HBVcAg-S121A and Compound 79
RU
Response
Time
s

C

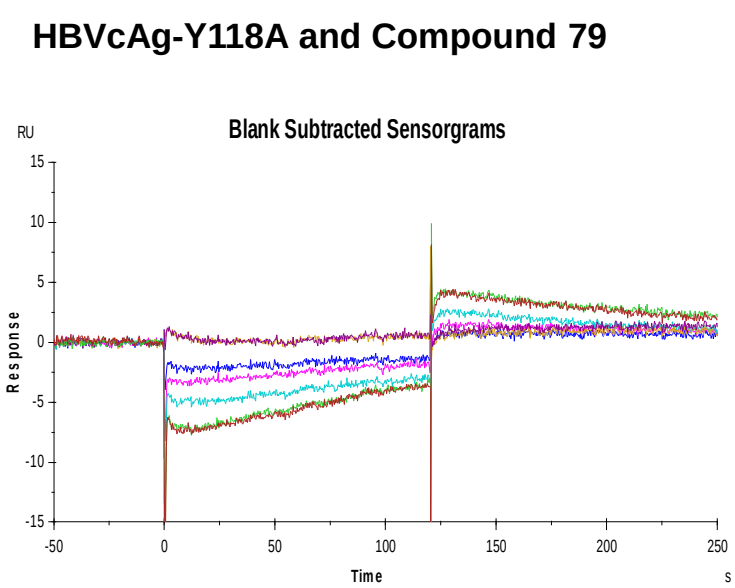
HBVcAg-Y118A and Compound 79
Blank Subtracted Sensorgrams
RU
Response
Time
s

Figure 5.

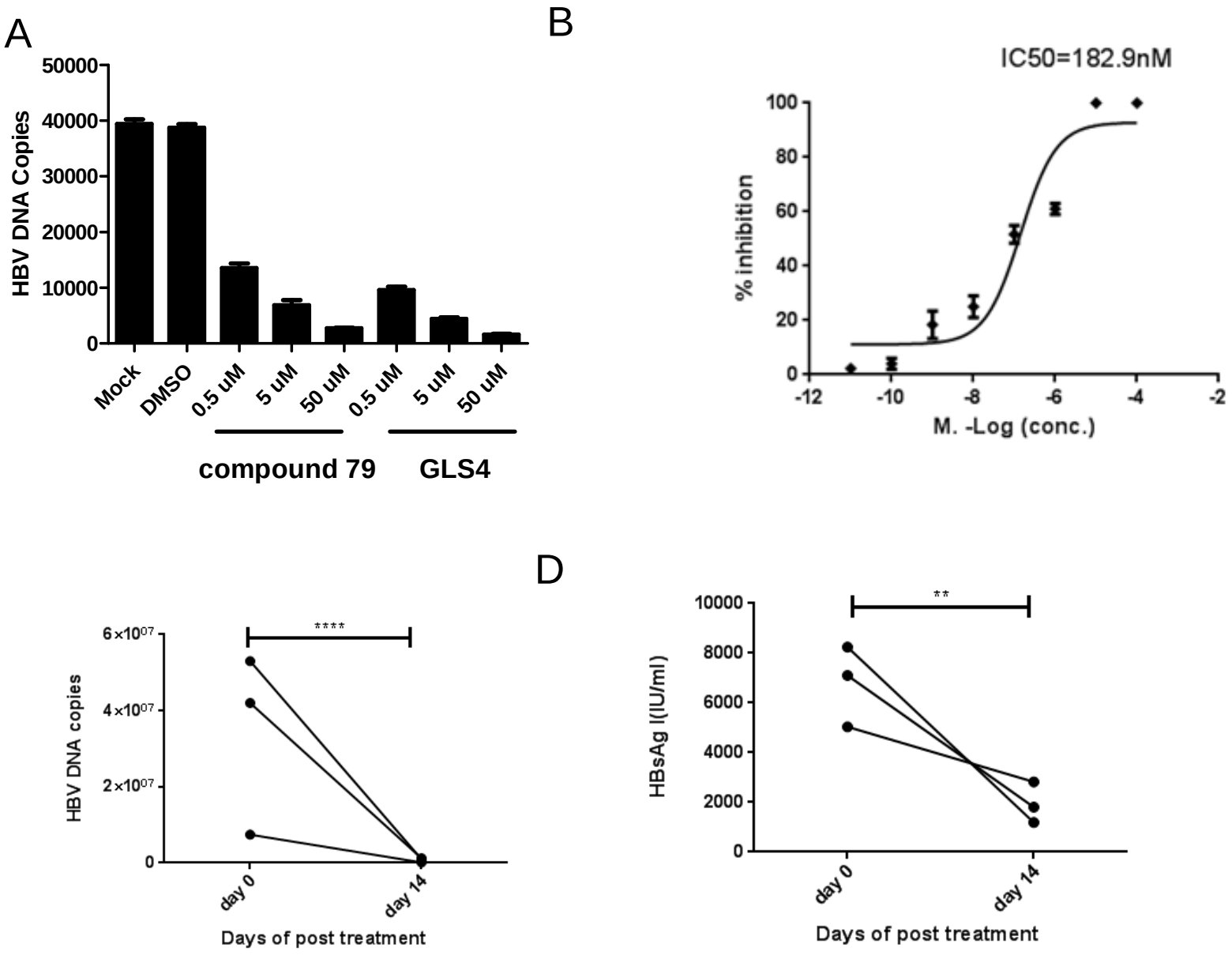
A
HBV DNA Copies
50000
40000
30000
20000
10000
0
Mock
DMSO
0.5 uM
5 uM
50 uM
0.5 uM
5 uM
50 uM
compound 79
GLS4
B
IC50=182.9nM
% inhibition
100
80
60
40
20
0
-12
-10
-8
-6
-4
-2
M. -Log (conc.)
C
HBV DNA copies
6×10^07
4×10^07
2×10^07
0
****
day 0
day 14
Days of post treatment
D
HBsAg I(IU/ml)
10000
8000
6000
4000
2000
0
**
day 0
day 14
Days of post treatment

E

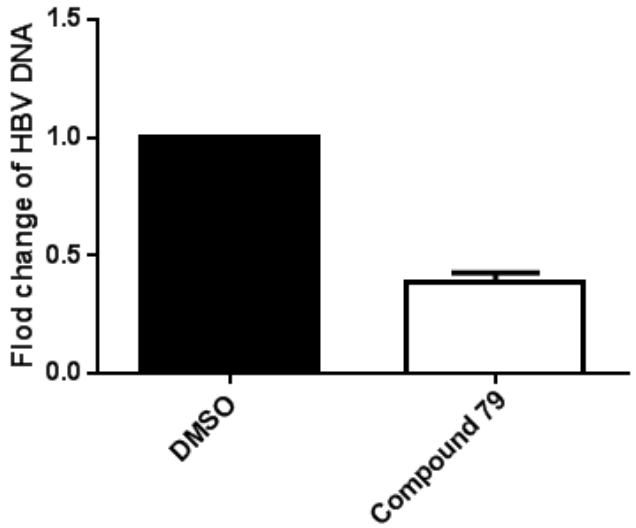
Flod change of HBV DNA
1.5
1.0
0.5
0.0
DMSO
Compound 79

F

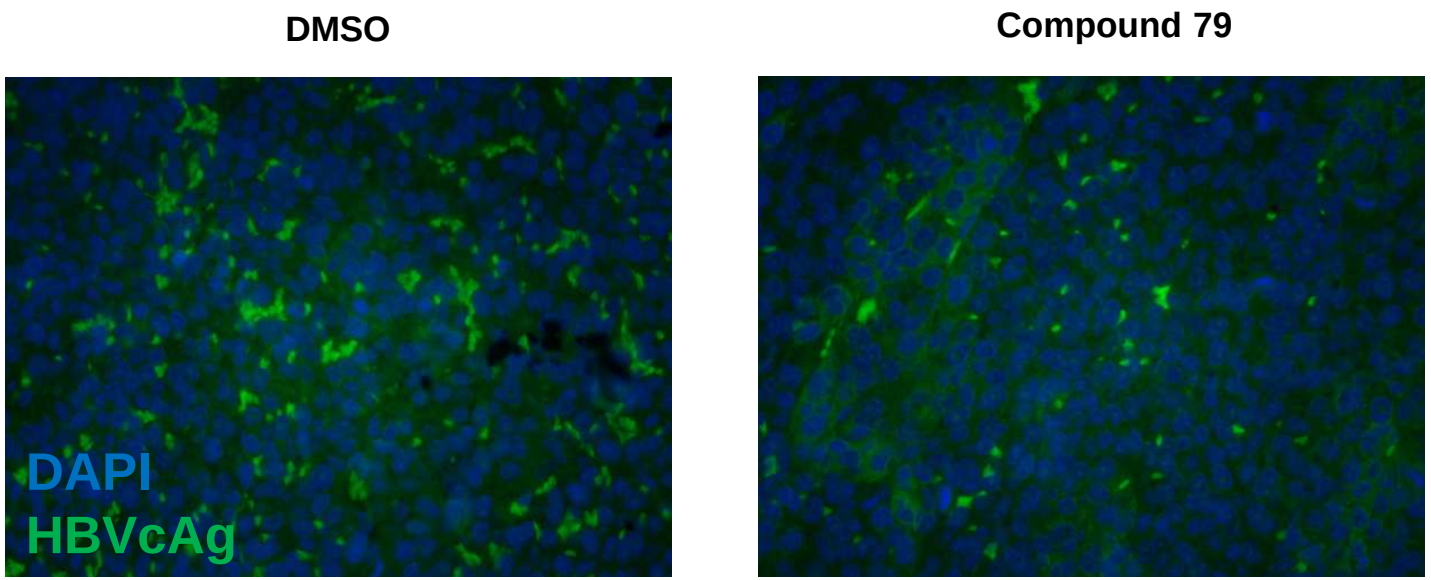
DMSO
Compound 79
DAPI
HBVcAg

Figure 6.

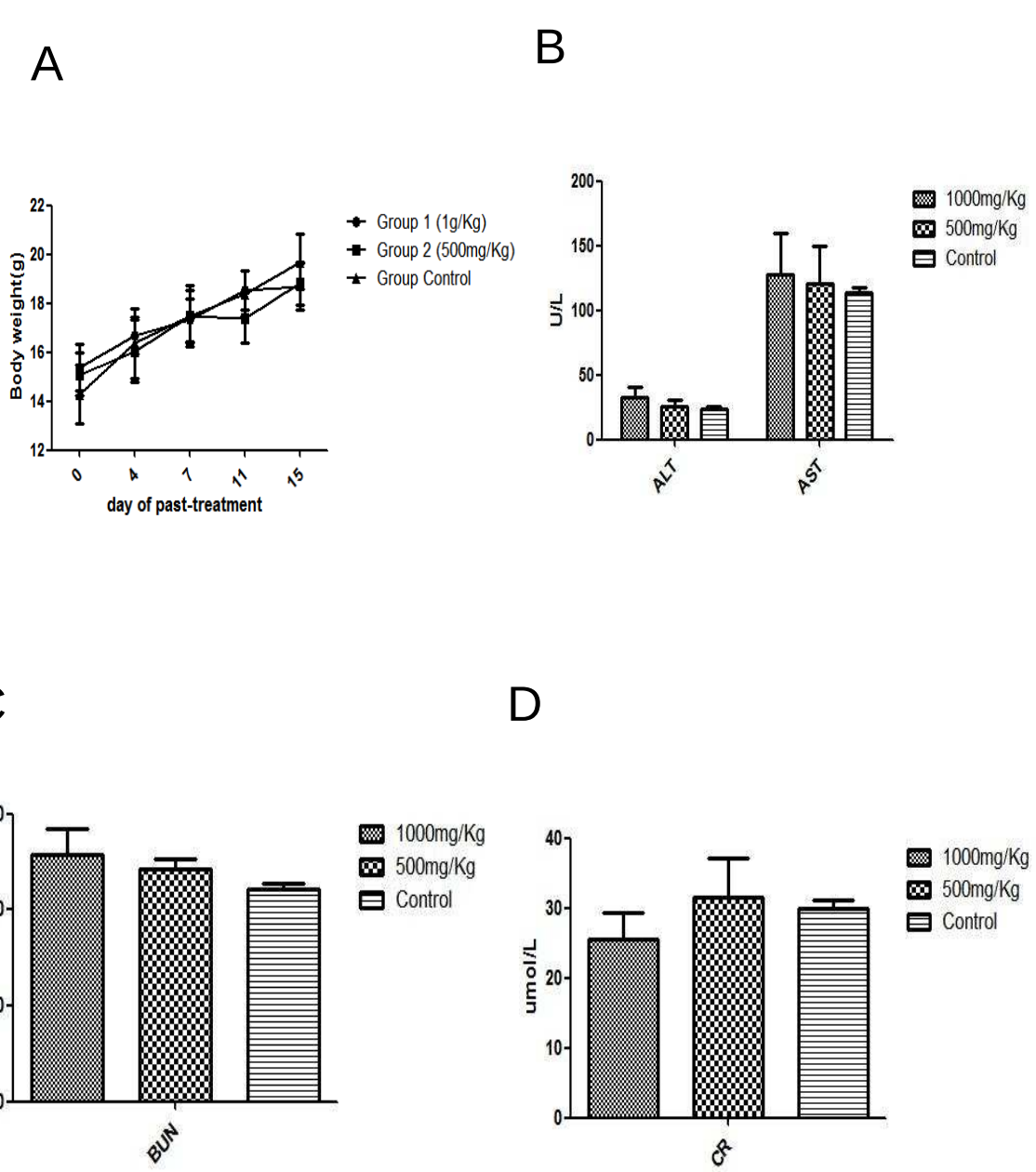
A
Body weight(g)
22
20
18
16
14
12
0
4
7
11
15
day of past-treatment
Group 1 (1g/Kg)
Group 2 (500mg/Kg)
Group Control
B
U/L
200
150
100
50
0
ALT
AST
1000mg/Kg
500mg/Kg
Control
C
mg/dl
30
20
10
0
BUN
1000mg/Kg
500mg/Kg
Control
D
umol/L
40
30
20
10
0
CR
1000mg/Kg
500mg/Kg
Control

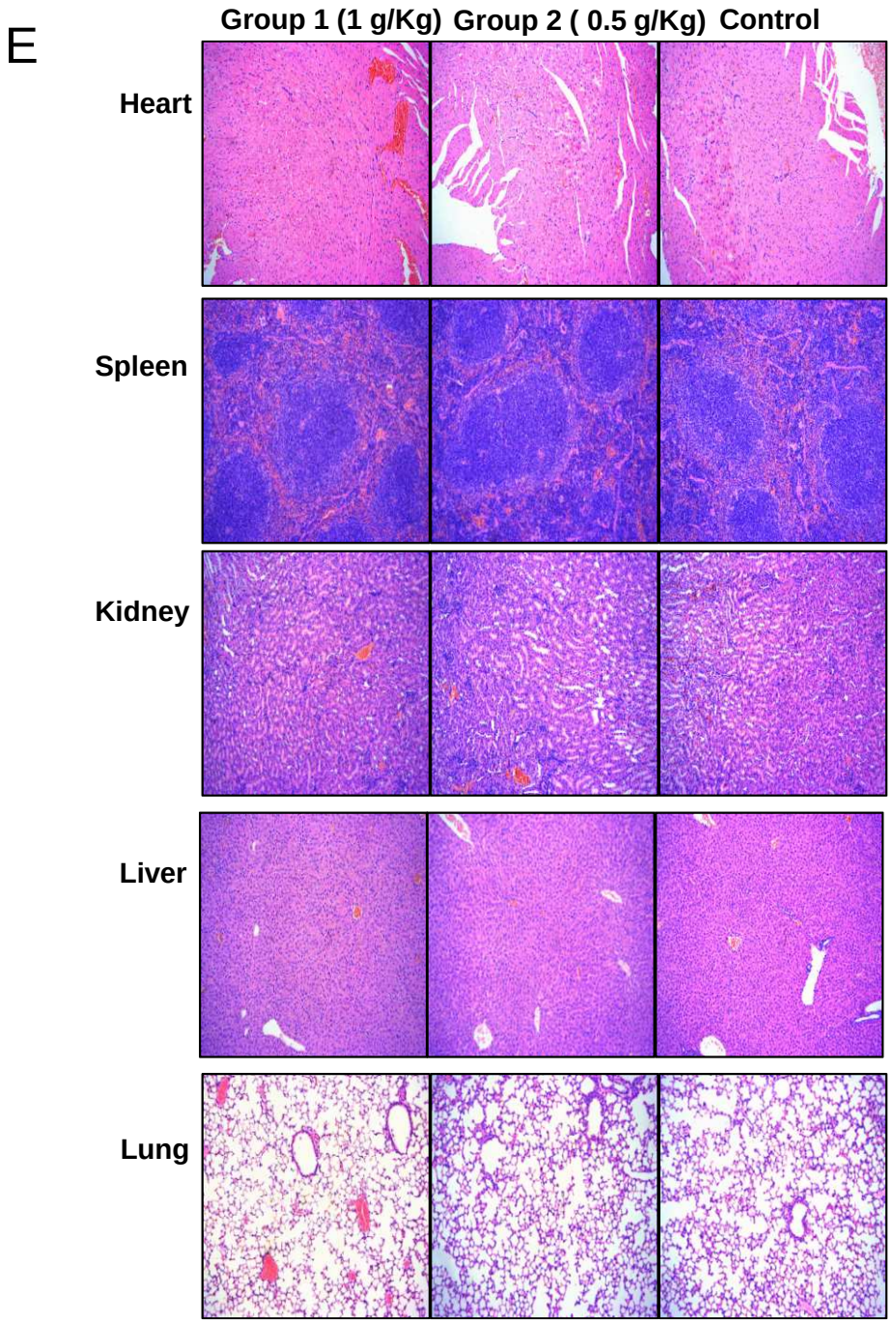
E
Group 1 (1 g/Kg)
Group 2 (0.5 g/Kg)
Control
Heart
Spleen
Kidney
Liver
Lung

Highlights

- A class of Aminothiazole derivatives was explored as potential anti-HBV replication agents through high- throughput screening and structure-activity relationship studies.
- Compound **79** disrupted HBV capsid assembly in vitro.
- Compound **79** inhibited the HBV replication in cells (IC_{50}=0.18 μM) and in animal models.
- Compound **79** showed low toxicity in the acute toxicity assay.